

Antihypertrophic Effect of Hemin in Deoxycorticosterone Acetate-Salt-Induced Hypertensive Rat Model

A Thesis

**Submitted to the College of Graduate Studies and Research
in Partial Fulfillment of the Requirements
for the Degree of
Doctor of Philosophy in Physiology
University of Saskatchewan**

By

Ashok Bhagwan Jadhav

PERMISSION TO USE STATEMENT

In presenting this thesis, I agree that the libraries of the University of Saskatchewan may make it freely available for inspection. I further agree that permission for copying of this thesis in any manner, in whole or in part, for scholarly purposes may be granted by the professor or professors who supervised my thesis work or, in their absence, by the Head of the Department of Physiology or the Dean of Medicine. It is understood that any copying, publication, or use of this thesis or any part for financial gain shall not be allowed without my expressed written permission. It is also understood that due recognition shall be given to me and to the University of Saskatchewan in any scholarly use that may be made of any material of this thesis.

Requests for permission to copy or make other use of material in this thesis should be addressed to:

Head of Department of Physiology
College of Medicine
University of Saskatchewan, 107 Wiggins Rd
Saskatoon, Saskatchewan,
Canada S7N 5E5

Abstract

The application of the synthetic mineralocorticoid, deoxycorticosterone acetate (DOCA)-salt, to unilaterally nephrectomised rats induces severe hypertension due to volume-overload, and mimics human primary aldosteronism. Importantly, DOCA-salt hypertension is characterized by severe cardiac and renal lesions triggered by nuclear factor kappa B (NF- κ B), activating protein (AP-1), and transforming growth factor beta1 (TGF- β ₁) leading to end-stage organ damage. Although DOCA-salt hypertension is a low renin model, local production of angiotensin-II and aldosterone in cardiac and renal tissues stimulate TGF- β ₁, fibronectin and collagen-1 causing fibrosis and hypertrophy. Since TGF- β ₁ gene promoter contains binding sites for NF- κ B and AP-1, cross-talk between TGF- β ₁, NF- κ B and AP-1 can be envisaged. Accordingly, the activation of TGF- β ₁, fibronectin, collagen, NF- κ B and AP-1 may constitute a potent destructive force in hypertension.

Emerging evidence indicates that upregulation of the heme oxygenase (HO) system is cytoprotective with antioxidant, antihypertensive and antihypertrophic effects. Interestingly, the promoter region of HO-1 gene harbors consensus-binding sites for NF- κ B and AP-1; therefore, the HO system may regulate these transcription factors to counteract tissue insults. However, the multifaceted interactions between the HO system, NF- κ B, AP-1, TGF- β ₁, fibronectin and collagen in mineralocorticoid-induced end-stage-organ damage have not been fully characterized. Similarly, the effect of the HO system on tissue angiotensin-II and aldosterone levels in mineralocorticoid-induced hypertension remains unclear. Therefore, the present study was designed to investigate

the antihypertrophic effect of the HO system in cardiac and renal tissue of DOCA-salt hypertensive rats.

In this study, the HO inducer, hemin, lowered blood pressure and attenuated cardiac/renal hypertrophy, whereas the HO inhibitor, chromium mesoporphyrin (CrMP), nullified the effects of hemin and exacerbated cardiac/renal injury the DOCA-salt hypertensive rats. The protective effect of hemin was associated with increased HO-1, HO activity, cyclic guanosine monophosphate (cGMP), superoxide dismutase activity, ferritin and the total antioxidant capacity in the cardiac and renal tissue. In contrast, angiotensin-II, aldosterone, 8-isoprostane, NF- κ B and AP-1 were significantly downregulated. Furthermore, hemin therapy attenuated TGF- β_1 and extracellular matrix (ECM) proteins such as fibronectin and collagen, with corresponding reduction of cardiac histopathological lesions, including longitudinal/cross-sectional muscle fiber thickness, scarring, muscular hypertrophy, coronary arteriolar thickening and collagen deposition. Similarly, hemin attenuated structural lesions in the kidney such as glomerular hypertrophy, glomerular sclerosis, mononuclear cell infiltration, tubular cast formation, tubular dilation and renal arteriolar thickening with concomitant improvement of kidney function as evidenced by reduction of plasma creatinine, proteinuria, but enhanced creatinine clearance.

Collectively, these results suggest that the HO system suppressed hypertension, cardiac and renal fibrosis, and hypertrophy in the DOCA-salt hypertensive rat by downregulating transcription factors such as NF- κ B and AP-1, reducing ECM proteins

such as fibronectin and collagen, decreasing local tissue production of angiotensin-II and aldosterone, and improved renal functional capacity.

ACKNOWLEDGEMENTS

Primarily, all thanks to my family who allowed me to go to higher studies away from the home. I would like to thank my supervisor Dr. Joseph Fomusi Ndisang for his continuous support and guidance at all stages of my graduate studies, which had a great impact on my graduate career. I also sincerely thank him for supporting my attendance at several scientific conferences. I am indebted to all members of advisory committee, Dr. Kailash Prasad, Dr. Linda Heibert, Dr. Paul Lee, Dr. Nigel West and Dr. Prakash Sulakhe for their guidance and support throughout my graduate studies. I am grateful to Dr. Jim Thornhill, Associate Dean (Research and Graduate studies), College of Medicine for providing me financial support during my graduate studies and providing funding for the remaining experiments needed for my studies. My thanks to Dr. Wolfgang Walz, Head, Department of Physiology for providing support throughout my graduate studies. I am very thankful to Mrs. Maureen Webster, Mrs. Cynthia green, Mrs. Barbara Raney, Mrs. Lois, Mrs. Lorelie, Mrs. Carol Ross, Ms. Gladys Wiebe, and Mr. Dilip Singh in the Department of Physiology for their help throughout my graduate studies. Special thanks to Mr. James Talbot, Mrs. Nina Lane, Mr. Zoran and the animal house personnel for helping me through out my research. Finally, I would like also to thank Dr. Emina Torlakovic and Heather for their fruitful collaboration and providing help for the histopathological studies. Most importantly, I am very grateful to vivek, atul, amol, sunil, pramod, abhay, sandip, my friends from BOVET groups, Glenmark group and all family members those living overseas, for their everlasting support, motivation and love.

DEDICATION

To My Beloved Family, Friends and Country

TABLE OF CONTENTS

PERMISSION TO USE STATEMENT.....	i
ABSTRACT.....	ii
ACKNOWLEDGMENTS	v
DEDICATION.....	vi
TABLE OF CONTENTS.....	vii
LIST OF FIGURES	xii
LIST OF TABLES	xiv
LIST OF ABBREVIATIONS	xv
LIST OF CHEMICALS AND ANTIBODIES.....	xvii
1. INTRODUCTION.....	1
1.1.	
Hypertension.....	1
1.1.1. Angiotensin-II and aldosterone.....	2
1.2.	
Oxidative stress.....	4
1.2.1. 8-isoprostane.....	6
1.2.2. Superoxide dismutase.....	7
1.3.	
Inflammation.....	8
1.4.	
Hypertrophy.....	10
1.4.1. Cardiac and renal hypertrophy.....	10
1.5.	
Mediators involved in hypertrophy and remodelling.....	13
1.5.1. Nuclear factor kappa B.....	13
1.5.2. Activating Protein-1.....	15
1.5.3. Transforming growth factor beta.....	15
1.5.4. Extracellular matrix proteins.....	17
1.5.4.1. Collagen.....	17
1.5.4.2. Fibronectin.....	18
1.6.	
Cardiac and renal structural and functional alterations.....	19
1.6.1. Cell death by necrosis and apoptosis.....	23
1.7.	
Heme oxygenase system and heme catabolised products.....	25
1.7.1. Bilirubin.....	26
1.7.2. Iron and ferritin.....	26
1.7.3. Carbon monoxide.....	27
1.8.	
Cyclic guanosine monophosphate.....	28

1.9.	
Hemin.....	29
1.10.	
Deoxycorticosterone acetate (DOCA)-salt-induced hypertension.....	30
2. RATIONALE, HYPOTHESIS AND OBJECTIVES	
.....	34
2.1.	
Rationale.....	34
2.2.	
Hypothesis.....	35
2.3.	
Objectives.....	35
3. MATERIALS AND METHODS	
.....	36
3.1.	
Animal experiments.....	36
3.1.1. Measurement of systolic blood pressure.....	38
3.1.2. Estimation of hematocrit.....	39
3.1.3. Plasma ferritin assay.....	40
3.2.	
Determination of hypertrophy of heart and kidney.....	40
3.2.1. Determination of left ventricular hypertrophy.....	40
3.2.2. Assessment of kidney hypertrophy.....	40
3.3.	
Assay for the quantification of heme oxygenase-1.....	41
3.4.	
Assay for heme oxygenase activity.....	42
3.5.	
Measurement of cyclic guanosine monophosphate levels.....	43
3.6.	
Superoxide dismutase assay.....	44
3.7.	
Total antioxidant capacity assay.....	45
3.8.	
Measurement of aldosterone in the heart and kidney.....	47
3.9.	
Assessment of angiotensin-II levels in the heart and kidney.....	47
3.10.	
Urine analysis.....	48
3.10.1. Measurement of urine excretion.....	48
3.10.2. Total urinary protein assay.....	48
3.10.3. Creatinine clearance rate.....	49

3.11.	
Assay for urinary 8-isoprostane.....	50
3.12.	
Western immunoblotting expression of HO-1, TGF-β and fibronectin.....	51
3.13.	
Total RNA isolation and quantitative RT-PCR for NF-κB and AP-1.....	52
3.14.	
Histological analysis of left ventricle and kidney.....	53
3.14.1. Left ventricular morphological lesions: semi-quantitative analysis.....	53
3.14.2. Quantification of cardiac muscular hypertrophy.....	54
3.14.3. Assessment of perivascular fibrosis.....	54
3.14.4. Morphometric analysis of small coronary and renal arteries.....	55
3.14.5. Semi-quantitative analysis of morphological lesions in kidney....	55
3.14.6. Quantitative analysis of glomerular hypertrophy.....	55
3.15.	
Immunohistochemical detection of TGF-β and fibronectin.....	56
3.16.	
Statistical analysis.....	57
4. RESULTS	
.....	58
4.1.	
Effect of hemin on systolic blood pressure.....	58
4.2.	
Effect of hemin treatment on body weight and hematocrit values.....	61
4.3.	
Effect of hemin regimen on cardiac and renal hypertrophy.....	62
4.4.	
Effect of hemin on cardiac and renal HO-1 expression, HO activity and cGMP content.....	66
4.5.	
Measurement of aldosterone and angiotensin-II levels in cardiac and renal tissue after hemin therapy.....	70
4.6.	
Effect of hemin therapy on markers/mediators of oxidative stress such as urinary 8-isoprostane, NF-κB and AP-1.....	73
4.6.1. Urinary 8-isoprostane.....	73
4.6.2. NF-κB and AP-1.....	74
4.7.	
Assessment of hemin regimen on antioxidant defense systems (ferritin and SOD) and total antioxidant capacity.....	78
4.8.	
Effect of hemin therapy on TGF-β in the left ventricle and kidney.....	81

4.9.	
Effect of hemin treatment on ECM proteins	84
4.9.1. Fibronectin expression and levels in the kidney.....	84
4.9.2. Perivascular collagen depositions in the left ventricle.....	86
4.10.	
Assessment of hemin therapy on morphological changes in the left ventricle.....	89
4.10.1. Left ventricular myocyte scarring.....	89
4.10.2. Left ventricular myocyte hypertrophy.....	89
4.10.3. Morphometry of small coronary arteries in the left ventricle.....	92
4.11.	
Effect of hemin therapy on DOCA-salt-induced renal injury.....	94
4.11.1. Renal morphological lesions.....	94
4.11.2. Glomerular hypertrophy, and sclerotic/damaged glomeruli in the kidney.....	97
4.11.3. Tubular cast formation in the kidney.....	100
4.11.4. Small renal arteries morphometry in the kidney.....	100
4.12.	
Effect of hemin regimen on functional parameters of the kidney.....	102
4.12.1. Polyurea and proteinuria.....	102
4.12.2. Creatinine clearance rate.....	102
5. DISCUSSION	106
5.1.	
Physiological parameters such as systolic blood pressure, body weight and hematocrit.....	107
5.2.	
Heme oxygenase and cyclic guanosine monophosphate.....	111
5.3.	
Aldosterone and angiotensin-II.....	113
5.4.	
Oxidative stress, inflammation and heme oxygenase system.....	118
5.5.	
Cardiac and renal hypertrophy, transcription factors, and heme oxygenase system.....	122
5.6.	
Improvement in cardiac and renal morphological lesions, and function.....	124
5.7.	
Limitation of the study.....	136
6. SUMMARY AND CONCLUSIONS	138
7. FUTURE DIRECTIONS	140

8. REFERENCES141

9. APPENDIX162

LIST OF FIGURES

Figure 1.1. Renin-angiotensin-aldosterone system.....	3
Figure 1.2. Hemin structure.....	30
Figure 1.3. The catalysis of heme and its end products by heme oxygenase.....	33
Figure 4.1. Effect of 4 weeks hemin treatment on systolic blood pressure of DOCA-salt-induced hypertensive rats.....	59
Figure 4.2. Hemin therapy inhibits DOCA-salt-induced cardiac and left ventricular hypertrophy.....	63
Figure 4.3. Hemin reduces left-to-right ventricular ratio and left ventricular wall thickness in DOCA-salt hypertensive rats.....	64
Figure 4.4. Hemin therapy abates DOCA-salt-induced kidney hypertrophy.....	65
Figure 4.5. Effect of hemin and CrMP on HO-1, HO activity and cGMP levels in cardiac tissue of DOCA-salt hypertensive rats.	67
Figure 4.6. Hemin therapy enhances HO-1 expression, HO activity and cGMP in the kidney.....	68
Figure 4.7. Hemin therapy prevents upregulation of cardiac and renal aldosterone levels.....	71
Figure 4.8. Effect of hemin treatment on cardiac and renal angiotensin-II levels.....	72
Figure 4.9. Hemin therapy attenuates urinary 8-isoprostane.....	74
Figure 4.10. Hemin prevents activation of NF- κ B in cardiac and renal tissue.....	75
Figure 4.11. Hemin therapy abates cardiac and renal AP-1 expression.....	76
Figure 4.12. Hemin treatment restores plasma ferritin and kidney SOD levels.....	79
Figure 4.13. Hemin enhances total antioxidant capacity in heart and kidney.....	80
Figure 4.14. Effect of hemin therapy on TGF- β expression in cardiac tissue.....	82
Figure 4.15. Hemin therapy attenuates TGF- β in the kidney.....	83

Figure 4.16. Hemin therapy prevents mobilization of fibronectin in the kidney.....	85
Figure 4.17. Effect of hemin on perivascular fibrosis in the cardiac tissue section.....	87
Figure 4.18. Hemin attenuates left ventricular myocytes scarring.....	88
Figure 4.19. Representative photomicrographs of left ventricle myocytes from different groups with H. & E. stain, magnification 400X.....	90
Figure 4.20. Hemin therapy attenuates cardiac myocytes hypertrophy.....	91
Figure 4.21. Effect of hemin on small coronary arterial remodeling in cardiac tissue....	93
Figure 4.22. Hemin abrogates renal morphological lesions such as mononuclear cell infiltration, glomerulosclerosis and tubular dilation.....	95
Figure 4.23. Hemin reduces morphological lesions and damaged and sclerotic Glomeruli numbers in the kidney.....	96
Figure 4.24. Hemin attenuates glomerular hypertrophy.....	98
Figure 4.25. Hemin reduces tubular cast formation in the kidney of the DOCA-salt rat...99	
Figure 4.26. Hemin prevents small renal arterial remodeling.....	101
Figure 4.27. Hemin treatment decreases urine excretion and proteinuria.....	103
Figure 4.28. Hemin therapy reduces plasma and urine creatinine levels and creatinine clearance.....	104
Figure 5.1. Multifaceted interaction of the HO system.....	135

LIST OF TABLES

Table 4.1. Effect of hemin on body weight and hematocrit values.....	61
--	----

LIST OF ABBREVIATIONS

Acetylcholine	(ACh)
Activating protein-1	(AP-1)
Angiotensin converting enzyme	(ACE)
Angiotensin-II receptor subtype-1	(AT ₁)
Chromium (III) mesoporphyrin IX chloride	(CrMP)
Cyclic adenosine monophosphate	(cAMP)
Cyclic guanosine monophosphate	(cGMP)
Cytochrome P450 monooxygenases	(CYP450)
Deoxycorticosterone acetate-salt	(DOCA-salt)
Dimethyl sulfoxide	(DMSO)
Endothelin-1	(ET-1)
Endothelial NOS	(eNOS)
Enzyme Immuno Assay	(EIA)
Ethylenediaminetetraacetic acid	(EDTA)
Extracellular matrix	(ECM)
Glyceraldehyde 3-phosphate dehydrogenase	(GAPDH)
Heme oxygenase-1	(HO-1)
Haematoxylin and eosin	(H&E)
High performance liquid chromatography	(HPLC)
Hours	(Hrs)
Inducible NOS	(iNOS)
2-kidney-1 clip	(2K1C)
Messenger ribonucleic acid	(mRNA)
Microlitre	(μ l)
Micrometer	(μ m)
Micrimole	(μ M)
Milimeter of mercury	(mmHg)
Milimole	(mM)
Minutes	(min)
Nitric Oxide	(NO)
Nitric oxide synthase	(NOS)
Nuclear factor kappa B	(NF- κ B)
Pixel	(Px)
Potassium chloride	(KCl)
Reactive oxygen species	(ROS)
Real time-Polymerase chain reaction	(RT-PCR)
Reduced nicotinamide adenine dinucleotide	(NADH)
Reduced nicotinamide adenine dinucleotide phosphate	(NADPH)
Renin-angiotensin-aldosterone system	(RAAS)
Sodium nitroprusside	(SNP)
Soluble guanylate cyclase	(sGC)
Sparague-Dawley	(SD)

Spontaneously hypertensive rat	(SHR)
Stannous chloride	(SnCl ₂)
Superoxide dismutase	(SOD)
Tin protoporphyrin IX	(SnPPIX)
Transforming growth factor beta	(TGF-β)
Trolox equivalent antioxidant capacity	(TEA C)
Uninephrectomized	(UnX)
Vascular smooth muscle cells	(VSMC)
Zinc protoporphyrin	(ZnPP)

LIST OF CHEMICALS, ANTIBODIES, AND KITS

The following chemicals and antibodies were obtained as shown in the list below:

Ammonium Sulphate	Sigma-Aldrich, Inc
Aldosterone EIA kit-Monoclonal	Cayman chemical
Anti HO-1 antibody	Calbiochem
Angiotensin-II EIA kit	Cayman chemical
Chemiluminescence reagent	Perkin Elmer Life science
Chromium Mesoporphyrins	Frontier Scientific, Inc
Creatinine analysis	DXC, Beckman Coulter
Cyclic GMP EIA kit	Cayman chemical company
Dako Envision immunoperoxidase staining kit	Santa Cruz Biotechnology
Deoxycorticosterone acetate	Sigma-Aldrich, Inc
EDTA	Sigma-Aldrich, Inc
Ferritin analysis	Abbott Architect i2000SR
First Strad cDNA synthesis kit	Novagen
Fibronectin (P1H11): sc-18825	Santa Cruz Biotechnology, Inc
Hemin	Sigma-Aldrich, Inc
Horseadish peroxide	Sigma-Aldrich, Inc
8-isoprostane assay	Cayman chemical
Monoclonal anti β -actin antibody	Sigma-Aldrich, Inc
Monoclonal Anti-GAPDH antibody	Sigma-Aldrich, Inc
Pyridine spectrophotometric reagent (99%)	Sigma-Aldrich, Inc
Potassium phosphate	Sigma chemicals
Rat HO-1 ELISA kit	Stressgen chemicals
Sodium chloride	Sigma chemicals
Sodium dithionite	Sigma chemicals
Sodium phosphate	Sigma chemicals
Sodium dodecyl sulphate	Sigma chemicals
Superoxide dismutase assay	Cayman Chemical

Tris-HCL

Total antioxidant capacity assay

Total Bilirubin Kit

Total protein assay

TGF β 1/2/3 (H-112): sc-7892

Trizol reagent

Sigma chemicals

Cayman chemical

Diagnostics Chemicals Limited

Bio-Rad kit

Santa Cruz Biotechnology, Inc

Invitrogen Life technologies

1. INTRODUCTION

1.1. Hypertension

The control of blood pressure depends on sodium and fluid balance, and vasomotor tone. It is also regulated by numerous factors including environmental, genetical, paracrine and hormonal as well as the nervous systems and intracellular feedback mechanisms. The interactions between these factors lead to alteration in the heterogeneous patterns of hemodynamics, which finally results in high blood pressure [1]. High blood pressure/hypertension is clinically defined as a systolic blood pressure ≥ 140 mmHg, and/or diastolic blood pressure ≥ 90 mmHg and is endemic in westernized societies. An epidemiological study showed that people having blood pressure between 120/80 and 140/90 mmHg are considered to be prehypertensive and have greater the risk of heart disease than those with lower blood pressure [2]. The majority of hypertensive patients (~90 %) have elevated blood pressure of unknown origin; it is termed primary or essential hypertension [3]. Essential hypertension is a frequent, chronic, age-related disorder, which finally leads to cardiovascular and renal complications. Similarly, systemic hypertension is also a common cause of cardiac, vascular, and renal hypertrophy. More than 50 % of essential hypertensive patients have salt-sensitive hypertension [4] with abnormal renal sodium handling [5], and this is accompanied by progressive renal damage [6]. Hypertension affects 25-35 % of the adult population, and about 60-70 % of those above 70 year of age in developed and developing countries [1]. The prevalence of hypertension in the United States and Canada is around 20-22 % of population. By the year 2025, hypertension is expected to increase to about 60 % of the population worldwide, affecting around 1.5 billion people. Developing

countries will experience an 80 % increase, which translates that approximately 1.15 billion people will be affected with hypertension [7].

1.1.1. Angiotensin-II and aldosterone

Among the factors that control blood pressure, the renin-angiotensin-aldosterone system (RAAS) is an essential regulatory component of the cardiovascular and renal system (Fig.1.1). It is a hormone system that regulates blood pressure and water (fluid) balance. When blood pressure is low, the kidneys secrete renin, which stimulates the production of angiotensin. Angiotensin causes an increase in blood pressure directly by vascular constriction or indirectly through stimulation of aldosterone production, which causes sodium and water retention. If the RAAS is too active, blood pressure will be too high. Interestingly, with decrease in cardiac function, the system will start to activate adaptive and positive mechanisms to counteract the underlying condition. However, as time progresses, prolonged alteration of the RAAS becomes maladaptive, leading to the development of severe hypertension and oxidative stress, followed by cardiac and renal hypertrophy, fibrosis, and vascular remodeling [8]. Although, the systemic RAAS is depressed in the DOCA-salt hypertensive rat, local production of angiotensin-II [9] and aldosterone [10] in the heart and kidney tissue contribute to the cardiac and renal end-stage-organ damage.

Angiotensin-II is a potent vasoconstrictor and plays an important role in blood pressure regulation. In addition, angiotensin-II stimulates the production of aldosterone from the adrenal gland, which in turn causes the tubules of the kidneys to retain sodium and water, and thus, increases blood pressure. Angiotensin-II is an oligopeptide and has hormonal properties. It is derived after a series of conversions from the precursor

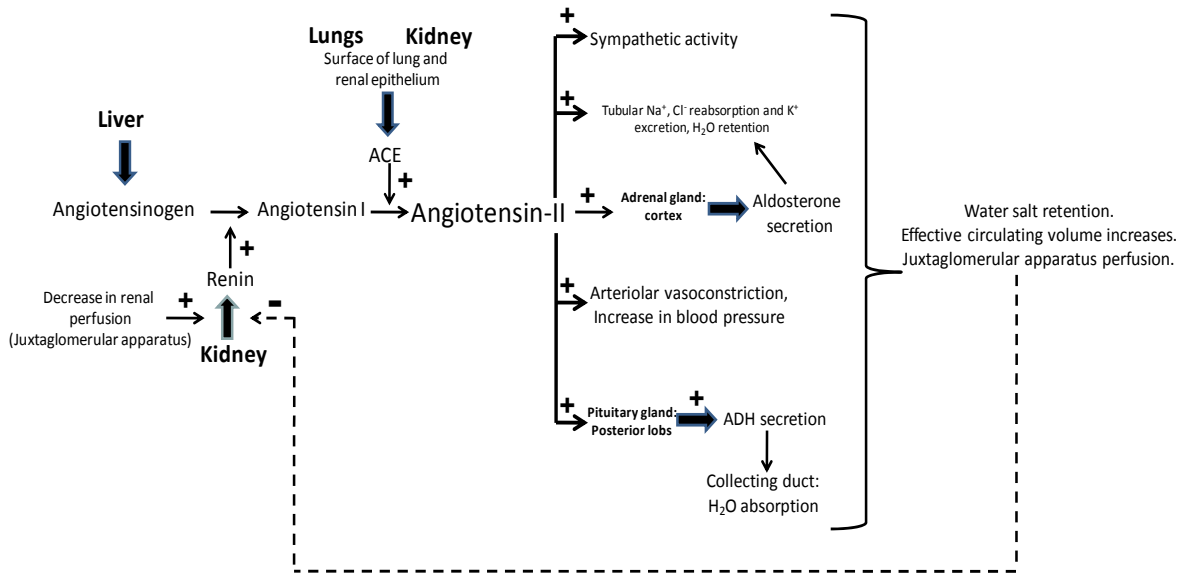


Figure 1.1. Renin-angiotensin-aldosterone system (+, stimulatory and -, inhibitory)
 [modified from <http://images.google.ca/RAAS>, A. Rad, 2006]

molecule angiotensinogen, a serum globulin released from the liver. Renin is produced in kidneys in response to both a decrease in intra-renal blood pressure at the juxtaglomerular cells and/or decrease in the delivery of sodium and chloride ion to the macula densa [11]. It converts angiotensinogen into angiotensin-I, which is a precursor to angiotensin-II. Subsequently, angiotensin-converting enzyme, which is found predominantly in the capillaries of the lung, converts angiotensin-I into angiotensin-II. Angiotensin-II thus formed acts as an endocrine, paracrine/autocrine, and intracrine hormone [11]. Recent studies show that angiotensin-II production occurs in tissues such as heart and kidney [9]. Angiotensin-II also stimulates local tissue production of aldosterone in heart and kidney and causes organ-damage.

Aldosterone is a steroid hormone secreted from the adrenal gland, which controls sodium and potassium balance [12, 13]. Aldosterone acts by promoting unidirectional reabsorption of salt across a variety of epithelial tissues, sweat glands, salivary glands,

intestine, and the kidney. It is synthesized from cholesterol in the zona glomerulosa section of the adrenal gland. Although hormones and electrolytes affect the secretion of aldosterone, the renin-angiotensin system (RAS) is the major and primary regulator of its secretion. Angiotensin-II and potassium are known to stimulate the secretion of aldosterone by enhancing the rate of synthesis of the hormone [14]. However, recently many researchers have reported cardiac and kidney tissue production of aldosterone [10].

Interestingly, both angiotensin-II and aldosterone interacts synergistically and stimulates synthesis of oxygen free radicals, which further contributes to end-organ damage. Moreover, there is an interrelationship between the development of hypertension, local production of angiotensin-II and aldosterone, and oxidative stress. Many studies in animal and human hypertension have shown that increased oxidative injury might play an important role in the etio-pathogenesis of hypertension. Increased oxidative stress has been reported in several hypertensive models including the spontaneously hypertensive rat (SHR), stroke-prone SHR, Dahl salt-sensitive rat and the DOCA-salt hypertensive rat [15-18].

1.2. Oxidative stress

Oxidative stress is an imbalance between prooxidants and antioxidants in favour of former [19]. Reactive oxygen species (ROS) are the natural byproducts of normal oxygen metabolism and are involved in normal intracellular signaling. However, ROS are highly reactive small molecules that result from the presence of unpaired valence shell electrons [20]. During oxidative stress, various ROS, including the superoxide anion ($O_2^{\cdot-}$), a hydroxyl radical (HO^{\cdot}) or hydrogen peroxide (H_2O_2) are produced

intracellularly or generated exogenously from different sources [21]. The majority of the intracellular ROS are produced in the mitochondria, while cytosolic enzymes such as nicotinamide adenine dinucleotide phosphate [NAD(P)H] oxidases, xanthine oxidases, and lipoxygenases are also responsible for generating ROS [22]. Intracellular ROS production is normally counteracted by an endogenous antioxidant defense system [21-23]. However, during hypertension, increases in oxidative stress are commonly seen due to the production of ROS from xanthine oxidase, uncoupled endothelial (nitric oxide) NO synthase and NAD(P)H oxidase, or by a decrease in antioxidant capacity. In hypertension, elevated RAAS triggers the generation of ROS in part through the activation of membrane-bound nicotinamide adenine dinucleotide (NADH) and NAD(P)H oxidase. These oxidase enzymes are present in phagocytic mononuclear cells, fibroblasts, endothelial cells and vascular smooth muscle cells [24, 25]. Superoxides formed from the activation of NAD(P)H bind to nitric oxide to form peroxynitrite, a potent oxidant, which further causes endothelial dysfunction and vasoconstriction, the characteristics of many vascular diseases including hypertension [26]. Interestingly, deoxycorticosterone, along with salt, activates NAD(P)H oxidase through both the mineralocorticoid receptor (MR)-dependant mechanism and angiotensin-II receptor subtype 1 (AT₁), resulting in the generation of ROS and endothelial dysfunction through the formation of peroxynitrite as well as oxidation of the nitric oxide synthase co-factor 5,6,7,8-tetrahydrobiopterin (BH₄) [27]. In addition, aldosterone decreases the expression of glucose-6-phosphate dehydrogenase (G6PD) leading to the reduction of NADP⁺ to NAD(P)H, and thus promotes oxidative stress and endothelial dysfunction [28]. Furthermore, aldosterone also stimulates the uncoupling of nitric oxide synthase (NOS) by induction of Ser1177 dephosphorylation through protein phosphatase 2A (PP2A)

[29]. Thus, the oxygen radicals formed oxidize tissue phospholipids and release isoprostane, direct markers for oxidative stress [30] and antioxidant deficiency.

1.2.1. 8-isoprostane

The isoprostanes belong to the family of eicosanoids and are produced non-enzymatically by the random oxidation of tissue phospholipids caused by increased superoxide radicals. Isoprostanes normally appear in the plasma and urine under normal conditions and are increased by oxidative stress. Isoprostanes appear as an artifact in the tissue and plasma samples due to prolonged oxidative degradation or improper storage. One of the isoprostanes, 8-isoprostane has biological activity; it is a potent pulmonary and renal vasoconstrictor. It is one of the causative mediators of hepatorenal syndrome and pulmonary oxygen toxicity [31]. Elevated levels are found in heavy smokers [32]. 8-isoprostane is a marker of oxidative stress and indicator of a deficiency of antioxidants. The 8-isoprostane levels in plasma of normal healthy volunteers is 40-100 pg/ml, while, urinary levels range between 10-50 ng/mmol creatinine, which is higher than any other enzymatically derived eicosanoids. Moreover, quantification of urinary 8-isoprostane has been proposed to be a precise index of chronic and systemic non-enzymatic lipid peroxidation [33]. Therefore, a lowered level of 8-isoprostane indicates strong antioxidant capacity and/or decreased oxidative stress [34].

One of the strategies of reduction or prevention of hypertension, and cardiovascular and renal tissue damage is to minimize the ROS production or to enhance the antioxidant defense mechanism. The mechanisms of scavenging of ROS can be categorized into two groups, the first one is enzymatic, which includes superoxide dismutase (SOD) [35], catalase [36], and glutathione peroxidase [37]; while the second group comprises nonenzymatic molecules, including vitamins A, C and E. Other potent

antioxidant scavenging systems are glutathione-ascorbic acid [38] and thioredoxin [39]. These antioxidants are able to ameliorate hypertension caused specifically by oxidative stress; however, there are many other factors responsible for the development of hypertension. Importantly, previous study showed that decreased total antioxidant capacity and SOD were noted in the SHR and DOCA-salt hypertensive rat [40].

1.2.2. Superoxide dismutase

Among all the endogenous scavenging system of ROS, SODs are metalloenzymes, which have a role in the cellular antioxidant defense mechanism by catalyzing the dismutation of the superoxide anion to molecular oxygen and hydrogen peroxide.



According to their metal components, SODs have been classified as copper/zinc (Cu/Zn), manganese (Mn), and iron (Fe), and are widely distributed in plants and animals. They occur in high concentrations in brain, erythrocytes, liver, heart, and kidney. In humans, SODs are found in three forms, cytosolic Cu/Zn-SOD, mitochondrial Mn-SOD, and extracellular SOD [41]. Extracellular SOD is found in extracellular fluids and in the interstitial spaces of tissues, which constitutes the majority of SOD activity in plasma, lymph, and synovial fluid. The amount of SOD present, both cellular and extracellular, is crucial for the prevention of diseases linked with increased oxidative stress. The presence of sufficient amounts of SOD in cells and tissues keeps the concentration of superoxide ($\text{O}_2^{\cdot-}$) very low through an extremely fast catabolic mechanism with turnover of $2 \times 10^9 \text{ M}^{-1} \text{ sec}^{-1}$. In hypertension, its concentration decreases and nitric oxide competes with SOD for the superoxide leading to formation of

peroxynitrite, which further converts to hydroxyl radicals, causing oxidative stress and tissue injury. Therefore, a reduction in the superoxide dismutase level indicates oxidative stress in diseased states. Interestingly, increase in the heme oxygenase-1 (HO-1) protein and activity has been associated with enhanced SOD activity and decreased oxidative stress [42].

Accumulation of ROS in tissue has been implicated in the activation of the oxidative/inflammatory transcription factor, nuclear factor kappa B (NF- κ B), which involves the induction of a wide variety of biological responses [43]. NF- κ B regulate many of the cellular genes implicated in early immune, acute phase, and inflammatory reactions, including interleukin-(IL)1 β , tumor necrosis factor- α , IL-2, IL-6, IL-8, inducible nitric oxide synthase, cyclooxygenase-2, intracellular adhesion molecules, growth regulatory factors and many antioxidant systems [44].

1.3. Inflammation

Inflammation is a complex biological response of tissue and vasculature to harmful stimuli such as irritants, damaged cells and pathogens. It is a protective attempt of organisms to remove the injurious stimuli as well as the initiation of the healing process for the tissue. Inflammation is classified into two major groups depending on the time-frame and type of inflammatory cells present at the site of injury. Acute inflammation is characterized by rapid influx of plasma and neutrophils from blood into the injured tissue; it is an early response of the body to harmful stimuli. During acute inflammation a series of reactions take place including, vascular changes, leucocytes extravasation and phagocytosis, chemotaxis and leucocyte activation, phagocytosis, and release of leucocyte products. Leucocyte metabolites and proteases are toxic and may

damage tissues. In general, however, acute inflammation may have different outcome, as it resolves completely, healing may take place by connective tissue replacement, abscess formation in pyogenic organisms and progresses to chronic inflammation. Chronic inflammation is characterized by progressive shifting of cells from neutrophils to mononuclear cells (lymphocytes and monocytes) at the site of injury, which subsequently causes destruction and healing of the tissue from the inflammatory process [45]. When the monocyte reaches the extravascular tissue, it undergoes transformation to form a large phagocytic cell, the macrophage. To perform phagocytic action macrophages are activated by signals such as cytokines (interferon- γ) secreted by T lymphocytes, other chemical mediators, bacterial endotoxins, and extracellular matrix (ECM) proteins like fibronectin. After activation, macrophages release a wide variety of biologically active ingredients that are important mediators of the tissue destruction, vascular proliferation, and fibrosis. If etiological factors are not eliminated then further recruitment of monocytes from the circulation takes place by certain chemotactic factors such as cytokines of the IL-8 family, growth factors like transforming growth factor beta₁ (TGF- β_1) and platelet derived growth factor (PDGF), fragments from the breakdown of collagen and fibronectin, and fibropeptides. Although, macrophages act as a powerful defense against unwanted invaders, it can damage tissue significantly when activated inappropriately. Interestingly, NF- κ B is also known to regulate pro-inflammatory cytokines, which in turn causes infiltration and activation of neutrophils and mononuclear cells during acute and chronic inflammatory events.

There is strong link between hypertension, oxidative stress, inflammation, and fibrosis due to the involvement of NF- κ B, which modulates cellular genes, participated

in all of these signaling cascades. Mineralocorticoid-salt-induced cardiac and renal injury, and fibrosis are associated with infiltration of leucocytes and expression of pro-inflammatory cytokines suggesting that inflammation is an important part of cardiac and renal fibrosis. Moreover, Beswick et al., demonstrated that leucocyte infiltration in DOCA-salt hypertensive model is accompanied by ROS accumulation and increased expression of NF- κ B [46]. Furthermore, NF- κ B has been involved in hypertrophy, and together with inflammation, stimulates growth factors like TGF- β .

1.4. Hypertrophy

Hypertrophy is an increase in the size of an organ due to an increase in the cell size rather than cell number. The increase in size of the cells is due to an enhanced synthesis of structural components. Hypertrophy should not be confused with increase in size of cells due to an increased intake of fluid, referred as cellular swelling or edema whereby the hypertrophic organ has no extra cells, just larger sized cells. On the other hand, hypertrophy should be distinguished from hyperplasia where there is an abnormal increase in number of normal cells in normal tissue arrangement. Hypertrophy may be physiologic or pathologic and is caused by increased functional demand or specific hormonal stimulation. The striated muscle cells in both skeletal muscles and the heart are most capable of hypertrophy, because they cannot adapt to increased metabolic demands by mitotic division and formation of more cells to share the work [47].

1.4.1. Cardiac and renal hypertrophy

Cardiac hypertrophy is a morphological adaptation characterized by an increase in myocardial mass due to chronic work overload. Myocardial hyperfunction induces an increase in myocyte size, which leads to an increase in the overall mass and size of the

heart. The diameter of the cardiac myocyte increases about 65 % or more in cardiac hypertrophy in humans. The adult cardiac myocyte cannot divide; therefore an increase in the number of myocytes cannot occur in the adult heart [47]. For a long time, the heart has been considered as a post-mitotic organ without having regenerative potential. Based on this paradigm, it was known that cardiomyocytes undergo cellular hypertrophy but do not enter into cell cycle of a subpopulation of nonterminally differentiated myocyte or activates a pool of primitive cells. Cardiac biology has relied on this dogma for a long time, however, with the advent of regenerative medicine and the advancement of stem cell research the regenerating capacity of myocardial tissue by resident progenitor stem cells has gained considerable attention with potential of novel stem cell based therapy, to treat cardiac diseases. Efforts have been made to identify and characterize the resident pool of stem cells that can generate myocytes, and endothelial cells and smooth muscle cells organized in coronary vessels [48]. Given all this, the adult myocardium has a robust intrinsic reparative capacity and it resides in the cardiac stem cells. Moreover, acute ischemic injury or chronic cell apoptosis/necrosis causes a decrease in the viable cardiomyocyte, which is not balanced by adaptive hypertrophy of the remaining cardiomyocytes [49]. Therefore, the imbalance between myocardial hypertrophy and apoptosis has also been one of the proposed mechanism for cardiac failure [50, 51].

Cardiac hypertrophy is traditionally classified as either physiological or pathological depending on the underlying factors. **A)** Physiological cardiac hypertrophy is an adaptive response to growth signals and is characterized by a proportional increase in length and width of the cardiac myocyte. This type of hypertrophy is commonly seen in athletes. Traditionally, cardiac hypertrophy is considered as an adaptive response required from sustained stress due to elevated cardiac output. Generally, prolonged

hypertrophy is associated with a significant increase in the risk of sudden death or progression to heart failure [52], indicating that the hypertrophic process is not entirely beneficial [53].

B) Pathological cardiac hypertrophy is a response to stress signals and is associated with an increase in cardiac myocyte size, upregulation of protein synthesis, and organization of the sarcomere. Phenotypically, pathological cardiac hypertrophy is divided into two different subtypes: a) concentric hypertrophy, in which there is parallel addition of sarcomeres and lateral growth of the individual cardiac myocyte due to pressure overload; and b) eccentric hypertrophy characterized by addition of sarcomeres in a series, and longitudinal cell growth of myocytes takes place as a result of volume overload or prior infarction [54].

In hypertension, increase in the afterload causes left ventricular wall stress, which further stimulates the development of myocardial hypertrophy. Systolic and diastolic blood pressure depends on left ventricular mass and wall thickness, respectively. Therefore, both volume and pressure overload accelerates the development of left ventricular hypertrophy in the hypertensive condition [55]. Recently, epidemiological studies showed that hypertension along with left ventricular hypertrophy leads to an increased risk of congestive heart failure, ventricular arrhythmias, and stroke [52, 56], all of which are considered risk factors for cardiac morbidity and mortality [57]. However, various studies showed that the prevalence of left ventricular hypertrophy not only depended on hypertension but that various hemodynamic and neurohumoral factors also contribute to the development and maintenance of left ventricular hypertrophy [58-60]. In these the most important are the sympathetic nervous system [61], and the activated RAAS [62], which are known to

induce myocardial hypertrophy and fibrosis [55]. In addition, local tissue production of angiotensin-II and aldosterone stimulates myocardial hypertrophy and fibrosis, which leads to structural and functional alterations in cardiac tissue.

In the DOCA-salt model, cardiac hypertrophy results from chronic pressure overload, whereas the kidney develops hypertrophy due to increased workload resulting from uninephrectomy (removal of one kidney), also referred to as compensatory hypertrophy. The hypertrophic process involves both individual cell hypertrophy and fibrosis, which may occur either in combination or separately depending on underlying causative factors. These hypertrophic processes are associated with activation of growth stimulatory transcription factors such as NF- κ B, activating protein-1 (AP-1), which triggers activation of TGF- β_1 and ECM proteins such as collagen and fibronectin.

1.5. Mediators involved in hypertrophy and remodeling

1.5.1. Nuclear factor kappa B

NF- κ B is a transcription factor, which after activation is found in the nucleus. The NF- κ B transcription family is composed of several structurally related proteins, such as c-Rel, Rel A, Rel B, p50/p105, and p52/p100. These proteins normally give diverse combinations of dimeric complexes by forming either homodimers or heterodimers. Dimeric complexes regulate the gene expression by binding to DNA target sites known as kappa-B (κ B) sites. A commonly known NF- κ B consists of a p50/RelA or p50/p65 heterodimer. NF- κ B dimers bind to Inhibitory κ B (I κ B) which blocks the nuclear localization sequence and prevents translocation into the nucleus [63]. Thus, the inactive form of NF- κ B is normally present in the cytoplasm and bound with

I κ B. Therefore, agents activate NF- κ B by inducing the phosphorylation of I κ B, which in turn causes degradation of I κ B. Once the signal is received, I κ B α phosphorylates at two conserved serine residues (S32 and S36) in its N terminal regulatory domain. The complex of I κ B kinase consists of three major components, of which IKK α and β serve as kinases while IKK γ functions as the regulatory subunit. After phosphorylation, I κ Bs undergoes post-translational modification via a series of mechanisms by (E-highly specified enzymatic processes) E1 ubiquitin-activating enzyme, E2 ubiquitin-conjugating enzyme, and E3 ubiquitin protein ligases, referred as polyubiquitination. Once ubiquitinated, I κ B degrades into 26S proteasomes and leads to the release of NF- κ B dimmers, which translocate into the nucleus [64]. Activation of NF- κ B is a tightly regulated process and only takes place after appropriate stimulation to cause the modulation of targeted genes. NF- κ B is activated by a variety of stimuli, including proinflammatory cytokines such as IL-1 β , tumor necrosis factor- α (TNF- α), epidermal growth factor (EGF), viruses, viral proteins, bacteria, lipopolysaccharides (LPS), double-stranded RNA, ROS, physical and chemical stresses, and T- and B-cell mitogens [65]. In addition, cellular stresses such as chemotherapeutic agents and ionizing radiation activates NF- κ B [65]. Nuclear translocation of NF- κ B activates I κ B α gene prior to other genes. It is an autoregulatory mechanism which brings activated NF- κ B back to the cytoplasm [66].

Hypertension-induced cardiac and renal hypertrophy, and end-stage-organ damage is associated with activation of NF- κ B. Furthermore, DOCA-salt-induced hypertension, cardiac and renal fibrosis is accompanied with increased expression of NF- κ B [46]. NF- κ B has a binding site on the consensus promoter region of the HO-1

gene, thus modulation and transcription of genes, which are involved in inflammation, hypertrophy, and growth regulatory processes, occur through upregulation of the HO system [67].

1.5.2. Activating protein-1

The mammalian AP-1 proteins are homodimers and heterodimers consisting of basic regions-leucine zipper (bZIP) proteins, which include Jun, Fos, Jun dimerization partners, and the closely related activating transcription factors subfamilies. AP-1 is activated by several growth factors, proinflammatory cytokines, and a variety of environmental stressors. These stimulations cause induction of fos genes that further heterodimerize with jun protein to form a stable AP-1 dimer. Thus, different AP-1 dimers formed are known to execute specific cellular programs. Activated AP-1 plays an important role in the control of cell proliferation, neoplastic transformation and apoptosis [68]. Mechanical stress, angiotensin-II, and hypoxia have been shown to activate AP-1 in the cardiac tissue [69, 70]. In addition, both angiotensin-II and aldosterone cause development of inflammatory lesions and fibrosis through activation of transcription factors such as NF- κ B and AP-1 in the liver [71]. Potential AP-1 binding sites have been identified on the promoter region of both HO-1 [67] and TGF- β genes [72] indicating that AP-1 may act as a mediator for the modulation of growth factors by the activated HO system during pathological alterations.

1.5.3. Transforming growth factor beta

TGF- β is a regulatory cytokine that belongs to the TGF- β superfamily. It is a protein, which has three isoforms, TGF- β_1 , TGF- β_2 , and TGF- β_3 . The TGF- β superfamily is composed of different protein precursors made up of TGF- β_1 with 390

amino acids, and TGF- β_2 and TGF- β_3 each containing 412 amino acids [73, 74]. Out of these, TGF- β_1 is an important cytokine, performing different cellular functions, including cellular proliferation, cell growth, and differentiation. TGF- β_1 is released in response to injury, via autocrine and/or paracrine mechanisms to maintain cellular homeostasis. The regulation of TGF- β_1 in cardiac, vascular, and renal tissue is under the influence of metabolic, hormonal (for example, angiotensin-II and aldosterone) and cyclomechanical stretch [75-77]. TGF- β_1 contributes to target organ damage in hypertension [75], and its overexpression has been commonly seen in chronic hypertension, left ventricular hypertrophy and remodeling [78, 79] as well as vascular remodeling [80] and progressive renal diseases [81]. Every rat model of hypertension shows left ventricular hypertrophy, which is a normal adaptation to increased pressure and volume overload [82]. However, the prolonged hypertrophic process is maladaptive. It is characterized by activation of TGF- β_1 that further stimulates ECM protein production and deposition, [83] and eventually leads to excess scarring and fibrosis [75]. Interestingly, angiotensin-II and aldosterone play important roles in the development of glomerular sclerosis, tubular fibrosis, which is mediated by activated renal TGF- β_1 and down-regulated endothelial nitric oxide synthase (eNOS) levels [75, 84]. Similarly, the activation of the oxidative transcription factor, AP-1, has been implicated in renal fibrosis, tubular injury and renal damage [85]. Mineralocorticoid-mediated as well as ROS-stimulated activation of AP-1 upregulates TGF- β_1 that subsequently enhances the production of fibronectin, and the development of renal fibrosis [86]. Alternatively, inappropriate activated TGF- β_1 stimulates cellular transformation of fibroblasts, synthesis of ECM proteins and integrins by decreasing the production of matrix

metalloproteinases (MMPs), and subsequently, promotes the development of fibrosis and tissue remodeling [87].

1.5.4. Extracellular matrix proteins

ECM does not remain as a structural form, but it performs a wide range of biological functions. The components of ECM interact with specific adhesion receptors on cell surfaces and control various cellular functions, which include differentiation, migration, proliferation, and apoptosis. Within the matrix, fibroblasts produce ECM proteins. Two major components of ECM are: i) fibrous proteins that provide structural support and resistance to deformation (e.g. collagen and elastin), or adhesion (e.g. fibronectin and laminin); and ii) glycosaminoglycans (GAGs) which link to protein to form proteoglycans [47].

1.5.4.1. Collagen

The collagen molecule consists of a central core with long, stiff, triple helical conformation. Three chains (glycine-proline-hydroxyproline) are wound around each other into a superhelix forming the core. Both ends of the helix are flanked by globular domains. Each of the collagen chains are encoded by separate genes, which are expressed in different combinations in different tissues. Connective tissue contains mainly fibrillar collagen that includes type I, II, III, IV and XI, and after secretion, these molecules polymerize to form long bound collagen fibrils in the ECM. Collagen type-I is abundantly present in most mammals. Total collagen in the myocardium is distributed as 85 % collagen type-I, 11 % collagen type-III, with the remaining being collagen type-IV and type-V which are associated with the basement membrane [47].

Chronic left ventricular pressure overload causes an increase in the number and size of collagen fibers. The proportional changes in both collagen type-I and type-III cause

improper alignments of cardiomyofibroblast. The adaptive mechanism changes to pathological, which results in increased reactive and reparative fibrosis. Moreover, pathological myocardial fibrosis is characterized by excessive collagen deposition, which results from an imbalance between collagen synthesis and degradation. In addition, TGF- β_1 can modulate both synthesis and degradation of collagen by regulating matrix metalloproteinase [88]. Therefore, substances like HO inducers, which are known to suppress TGF- β_1 could be used to reduce excessive collagen deposition and fibrosis [88]. Excessive collagen deposition is associated with hypertension-induced myocardial hypertrophy and increased thickness and density of the perimysial weave (interconnection of the bundles) of cardiac muscle fibers. Both interstitial and perivascular fibrosis are the characteristics of chronic hypertension-induced myocardial hypertrophy [89].

1.5.4.2. Fibronectin

Fibronectin is involved in many cellular processes, including blood clotting, cell migration/adhesion, tissue repairs, and embryogenesis. Fibronectin exists in two main forms: 1) as a soluble disulphide linked dimer found in the plasma, and 2) an insoluble glycoprotein dimer that acts as linkers in the ECM [47]. The extracellular form is synthesized by fibroblasts, chondrocytes, endothelial cells, macrophages, and by certain epithelial cells whereas, the plasma form is produced by hepatocytes. Fibronectin looks like a rod having three different types of homologous and repeating modules (I, II and III). Small linkers join these modules with each other as beads on a string. Module-I has twelve different subtypes, which can bind to fibrin and collagen. Module-II with two subtypes is structured to bind collagen. The most abundant form is module-III that binds

to integrins, and heparin. Fibronectin molecules also forms two disulphide bridges at their carboxy terminal producing a covalently linked dimer [47]. Fibronectin serves as a cell adhesion molecule by anchoring cells to the proteoglycan substrate or collagen. Fibronectin receptors, which are present on the cell membrane binds with different parts of ECM to organize cellular interactions [90]. In addition, fibronectin acts as a chemotactic factor to attract monocytes into the injured site during the progression of chronic inflammatory conditions.

1.6. Cardiac and renal structural and functional alterations

The multifactorial pathology of hypertension is closely linked to enhanced oxidative stress, inflammation, and the development of cardiovascular and renal remodeling. Histopathologically, cardiac remodeling is characterized by a structural rearrangement of the wall of a normal heart that involves hypertrophy of cardiomyocytes, proliferation of cardiac fibroblasts, fibrosis and cell death [91]. In fibrosis, disproportionate accumulation of fibrillar collagen type-I leads to stiffness of the ventricles and subsequently, impair both the relaxation and contraction of the ventricles. Furthermore, fibrosis separates myocytes from ECM proteins and impairs the electrical coupling of cardiomyocytes. In addition, fibrosis causes a reduction in the capillary density and increased oxygen diffusion distance and subsequently hypoxia of myocytes, thus it affects myocyte metabolism, performance and ventricular function resulting in cardiac end-stage damage [69]. Left ventricular fibrosis is common in many models of hypertension leading to alteration of cardiovascular function, and its reversal is indicative of improved cardiac function [92]. In the DOCA-salt hypertensive rat, cardiac fibrosis is characterized by a disproportionate increase in the synthesis and/or

inhibition of degradation of ECM protein. Specifically, the reactive fibrosis appears as interstitial and perivascular fibrosis and is not directly associated with myocyte death. In interstitial fibrosis, fibrillar collagen deposits in intermuscular spaces, while in perivascular fibrosis collagen accumulates within the adventitia of intramyocardial coronary arteries and arterioles [69]. Interestingly, adult cardiac myocardial cells/cardiomyocytes have the capacity to undergo hypertrophic changes. Systemic hypertension causes an increased hemodynamic load on the cardiomyocytes over time, which leads to increases in the synthesis of proteins and filaments in the cardiomyocytes. The overall effect is the advancement of cardiomyocyte hypertrophy and finally, increase in the size and weight of the heart. Moreover, chronic hypertension involves myocyte hypertrophy as well as fibrosis, with increased, irregular deposition of ECM proteins, especially collagen [62]. Therefore, it is necessary to characterize two different phenomenon of cardiac hypertrophy i.e. cardiomyocyte hypertrophy and cardiac fibrosis at the cellular level. Recent evidence suggests that a functional aldosterone system present in the heart, which is regulated by angiotensin-II, may cause cardiac fibrosis during the process of remodeling in hypertension [93]. Moreover, aldosterone also stimulates the expression of several profibrotic molecules that may contribute to the pathogenesis of cardiac and renal remodeling, and fibrosis [94].

Similarly, end-stage renal damage is characterized by glomerular hypertrophy, glomerular sclerosis, tubular dilation, infiltration of mononuclear cells, interstitial fibrosis, arterial remodeling, and tubular cast formations. In malignant hypertension, glomeruli of the kidney undergo hypercellular changes by cellular proliferation of mesangial, endothelial cells and leucocyte infiltration. Furthermore, it is accompanied by thickening of the basement membrane, hyalinization, and sclerosis of the glomerular tuft

with fibrin deposition. Tubular necrosis is often associated with rupture of the basement membrane and occlusion of the tubular lumen by casts. The straight portion of the proximal tubule and the ascending thick limb in the renal medulla are especially vulnerable, however focal tubular necrotic lesions occur in the distal tubules in conjunction with casts. Eosinophilic hyaline and granular casts are present in distal tubules and collecting ducts. These casts consist of Tamm-Horsfall proteins (urinary glycoprotein secreted by ascending and distal thick limb of tubules) along with hemoglobin, myoglobin and plasma proteins [47]. In addition, essential hypertension is associated with changes in the peripheral as well as tissue arterial vessels. High blood pressure causes progressive thickening of the walls of muscular arteries, with characteristic symmetric hypertrophy of the muscular media, reduplication of elastic lamina and further fibrotic thickening of the intima. Overall, these changes lead to reductions in the lumen diameters of the arteries and contribute to further hypertension [95]. Hypertension is known to cause progressive damage of the kidney, and microscopically the tubules undergo a series of changes. Tubules are shrunken or atrophied and undergo fibrosis. Some of the atrophied tubules may dilate cystically with cast formation. These casts are made up of inspissated proteinaceous material with highly eosinophilic (pink colored) characteristic, which is also termed thyroidisation [95]. Tubular interstitial nephritis can be either acute or chronic. Acute tubular interstitial nephritis is characterized by interstitial edema, accompanied with leucocyte infiltration and focal tubular necrosis, while in the chronic interstitial nephritis there is infiltration of mononuclear cells, intense interstitial fibrosis, and diffuse tubular atrophy. Clinically, the condition is associated with impaired ability to concentrate urine, polyurea, salt wasting, reduced ability to excrete acids (metabolic acidosis), and defects

in tubular reabsorption and secretion. With the aggravation of these pathological conditions, it is difficult to accurately diagnose and separate damage of the glomeruli and tubules from other causes of renal insufficiency [47].

The functional capacity of the kidney declines in end-stage renal damage, which can be clinically confirmed by increased proteinuria, increased plasma and urine creatinine, and glomerular filtration rate. Proteinuria has been considered as a marker of glomerular disease and increased excretion of protein in the urine reflects glomerular injury. Further, proteinuria has an important role in the progression of renal disease by causing tubular injury as it passes down through tubular lumen. As soon as tubular epithelial cells are exposed to plasma proteins, a variety of chemoattractants, proinflammatory cytokines, and extracellular matrix proteins are released, which ultimately lead to the development of interstitial inflammation and fibrosis [96, 97]. Furthermore, the glomerular filtration rate is also associated with glomerular and tubular diseases such as glomerular sclerosis, glomerulonephritis, and tubular injury. Generally, the levels of plasma, and urinary creatinine as well as the rate of creatinine clearance assess glomerular filtration rate. Therefore, it is important to know definition of clearance, which is defined as the volume of plasma from which a measured amount of substance such as creatinine can be completely eliminated (cleared) into the urine per unit time. Creatinine clearance depends on plasma and urinary concentration of creatinine; which in turn involves the glomerular filtration rate and renal plasma flow. Creatinine clearance is a better estimate of the glomerular filtration rate than any other test of urine analysis [98]. Creatinine is a marker of end-organ damage, because its level determines the overall renal function in patients with renal damage.

1.6.1. Cell death by necrosis and apoptosis

Cell necrosis is a morphological expression of cell death, resulting from the progressive degradative action of enzymes on lethally injured cell in living tissue. Cell necrosis is either enzymatic digestion of the cell and/or denaturation of proteins. When catalytic enzymes are derived from the lysosomes of the dead cell the process is referred to as autolysis, whereas heterolysis is when degradature components are released from the immigrant leucocytes [47]. There are two different types of cell necrosis: 1) coagulative necrosis when denaturation of protein takes place, 2) liquifactive necrosis occurs due to catalysis of cell structure. Morphologically, necrotic cells show increased eosinophilic staining, attributed in part due to loss of the normal basophilic intensity imparted by the RNA in the cytoplasm. It is also caused by increased binding of eosin color to denatured intracytoplasmic proteins. Moreover, the cell appears more glassy and homogenous than normal cells because of loss of glycogen particles. On the other hand, in liquifactive necrosis, an enzyme digests the cytoplasmic organelles leading to formation of cytoplasmic vacuoles, which appears moth-eaten. Nuclear changes may appear in different forms, 1) karyolysis is characterized by fading of basophilia of the chromatin reflective of DNase activity, 2) Pyknosis is a pattern in which DNA condense into a solid, shrunken basophilic mass, and appear as nuclear shrinkage and increased basophilia, and 3) karyorrhexis is associated with the pyknotic or partial pyknotic changes in the nucleus due to fragmentation [47].

Apoptosis is another type of morphologic cell death, which can be either physiological or pathological. It is different from the common coagulative necrosis. Histologically, the apoptotic cell appears as a round oval mass of intensely eosinophilic cytoplasm with dense nuclear chromatin fragments. The cell shrinkage and

fragmentation of apoptotic bodies are rapid, which are quickly phagocytosed, degraded, or extruded into the lumen. Additionally, apoptosis does not elicit inflammation as compared to necrosis, making it more difficult to detect histologically [47]. Apoptotic and necrotic cell death have different consequences on cardiac remodeling. Myocyte necrosis leads to an accelerated inflammatory reaction, macrophage infiltration, proliferation of the vasculature, activation of fibroblasts, and finally the formation of scars. Conversely, apoptosis does not activate any reparative fibrotic process and apoptotic bodies are removed by neighboring cells without any changes in the morphology of the tissue. However, apoptosis can induce restructuring of the ventricular wall and reduces the tension development capacity of ventricular myocytes [99]. In addition, there is evidence that apoptosis precedes necrosis and constitutes the prevailing form of myocyte death. Immediately, after an ischemic event, apoptosis affects more than 80 % and necrosis less than 20 % of myocytes in the affected region of ischemia [100]. However, as time progresses, the percentage of these two types of cell death overlap, and stimulates reparative processes and myocardial scarring [50].

To combat multiple disease conditions in patients, the present clinical strategy is to give poly-drug therapy. Although multiple drug therapy showed beneficial effects to counteract different pathological conditions, the interaction between these drugs also showed significant detrimental side effects. Therefore, we need to search alternative therapies, which can counteract multiple risk factors or diseased conditions, without having side effects. Recently, major interest has been directed towards cytoprotection by the HO system, an anti-stress/antioxidant defense enzyme system [101-105]. The HO system is present in the body and the activation of the HO-1 protein plays an important role in the modulation of pathophysiological conditions. However, in severe

pathological alterations, the HO system is not able to play a significant role due to insufficient activation of the HO-1 protein. Therefore, pharmacological or genetical intervention would be approaches to achieve long term overexpression of HO-1 protein and total HO activity to combat severe, multiple diseased conditions such as hypertension and diabetes that are associated with cardiac and renal end-organ damage [106].

1.7. Heme oxygenase system and heme catabolized products

HO is a microsomal enzyme having three distinct isoforms: HO-1, HO-2, and HO-3, of which HO-3 is an inactive isoform, and not present in humans [107]. HO-2 is a 36-kDa protein constitutively present in the mitochondria, which regulates normal physiological functions. It is mainly present in the heme protein containing enzymes of the liver and testis [108] and also expressed in the brain, endothelium, distal nephron segment, myenteric plexus and gastrointestinal tract. HO-1 is a 32-kDa inducible isoform protein localized in microsomes, which is ubiquitously expressed in a variety of mammalian cells after exposure of different stimuli [109], tissue injury and pharmaceutical agents. The rate-limiting enzymatic reaction of heme catabolism by the HO protein was first described by Tenhunen and his colleagues [110, 111]. Subsequent studies have highlighted the important role of the HO system in cellular defence. For example, reports have shown the HO-1 is critical for survival in HO-deficient mice (HO-1 $-/-$), especially against oxidative stress induced injuries [105]. Heme degradation is considered to be critical in the cellular defense mechanism, due to the removal of pro-oxidant heme, and increased production of bilirubin and carbon monoxide which are antioxidant and vasodilatory, respectively [106] [**Fig. 1.3**]. Iron, is another compound

released by heme degradation which can induce free radical formation, but rapidly binds to ferritin by ferritin reductase enzyme [106]. Importantly, the products of heme degradation upregulated by HO activity, mediate antioxidant, anti-inflammatory, antinecrotic, anti-apoptotic and antihypertrophic actions. Although the cytoprotective effect of the HO system has been confirmed in a number of experimental models, the complete mechanism of action needs to be clearly elucidated.

1.7.1. Bilirubin

Bilirubin is a four-pyrrole open chain ring (tetrapyrrole). In the adult human about 250-350 mg of bilirubin is produced daily [112]. About 80-85 % of bilirubin is derived from the breakdown of hemoglobin, which is released from aging and damaged erythrocytes. The reducing properties of bilirubin and biliverdin make them potential antioxidants. Bilirubin in the presence of hydrogen peroxide or organic hydroperoxide serves as a reducing agent for certain peroxidases such as horseradish peroxidase and prostaglandin H (PGH) synthase [107]. The cardioprotective properties of bilirubin, which are derived from the HO system, have been shown in the cardiovascular system [101, 113]. Similarly, the anti-inflammatory action of biliverdin has been confirmed in renal tissue, pretreated with biliverdin, when challenged with lipopolysaccharide (LPS), and showed attenuation of P- and E-selectin expression, and reduction of pro-inflammatory cytokines [114].

1.7.2. Iron and ferritin

Plasma iron is bound to transferrin which transfers iron to the intracellular compartment via cell surface receptors [106]. Iron is a pro-oxidant and leads to the generation of ROS, potentially resulting in damage to various cellular components. In addition, it can integrate into the phospholipid bilayer of the cell membrane and may

oxidize the inner components. Iron formed in the process of heme degradation is rapidly converted into ferritin by ferritin synthase, which stays in an oxidized (ferric) state, by H-chain ferroxidase activity [115].

Ferritin is a 24-unit oligomeric protein, with a macromolecular complex of 450 kDa (heavy- H: ~21 kDa and light- L:~ 19 kDa) chain. Ferritin has a cytoprotective effect which has been investigated in various in vitro models [116, 117]. When endothelial cells and primary human skin fibroblast preconditioned and challenged with oxidants, and sub-lethal doses of UV irradiation. Both HO-1 and ferritin synthase acts as a cytoprotectant [104, 118]. Furthermore, upregulation of HO and increased ferritin synthesis was shown to abate glycerol-induced renal injury [119]. Similarly, the overexpression of ferritin H-chain reduced apoptosis in liver ischemic injury [120]. All of these in vitro and in vivo studies suggest that either overexpression and/or chemical induction of ferritin leads to cytoprotection [115].

1.7.3. Carbon monoxide

Carbon monoxide is a diatomic molecule of low molecular weight (F.W. 28.01), which occurs naturally in the gaseous state under atmospheric temperature and pressure. It is soluble in aqueous media and organic solvents [121]. Physiologically carbon monoxide is produced in the body [122]. In biological systems, carbon monoxide is relatively stable compared to nitric oxide, which is a small gaseous molecule of similar structure and molecular size. Both nitric oxide and carbon monoxide form complexes with hemoproteins and metalloenzymes by forming heme-iron ligands. Nitric oxide binds with ferrous and ferric heme, while carbon monoxide binds to ferrous iron (reduced form) only [115]. Most of the carbon monoxide that is produced in the body

results from heme degradation by the HO system [107]. The antihypertensive effect of the HO system in SHR was known even before the discovery of the blood pressure lowering effect of carbon monoxide [123]. In addition, cytoprotective effects of carbon monoxide such as anti-apoptosis [124] and anti-inflammatory effects [125] in lung injury is mediated through physiological stress signals such as p38 mitogen activated protein kinases (MAPK) pathway [112, 126]. Interestingly, carbon monoxide binds the heme moiety of soluble guanylyl cyclase (sGC), and activates cyclic guanosine monophosphate (cGMP), which results in vascular relaxation [127-129], inhibition of vascular smooth muscle cell proliferation [130, 131], and platelet aggregation [132], an antiapoptotic effect on pancreatic beta cells [133], neurotransmission [134, 135], and bronchodilatation [136]. Overall, the HO-mediated production of carbon monoxide has been shown to suppress a variety of pathopathophysiological conditions, which made it important for the prevention of disease conditions.

1.8. Cyclic guanosine monophosphate

Cyclic GMP is a key intracellular second messenger molecule, which in response to a variety of hormones, autocooids and drugs, transduces cellular signaling events. cGMP is synthesized from GTP by both membrane-bound and sGC enzymes [137, 138]. The protein of particulate guanylate cyclase contains both the cGMP catalytic domain and a cell surface receptor function characterized previously by molecular studies. In mammals, out of six membrane forms of cGMP (GC-A-F) only three are known to have ligands. Soluble GC is a heterodimer consisting of α (α_1 or α_2) and β (β_1 or β_2) subunits [139, 140]. The α_1/β_1 heterodimer is activated by carbon monoxide, which results in accumulation of intracellular cGMP. The downstream mediators of cGMP dependent

kinases, cGMP-controlled events include cGMP-gated channels and cGMP-regulated phosphodiesterases. The relative abundance of cGMP within a given cell can serve as a marker for activation by agonists acting through particulate guanylate cyclase at the cell surface or intracellular activation of soluble guanylate.

1.9. Hemin (Molecular formula: $C_{34}H_{32}ClFeN_4O_4$; Molecular weight: 651.94)

Heme (iron protoporphyrin IX) exists as the prosthetic group of hemo-proteins, which include cytochrome P450, catalase, nitrophorins, peroxidases, nitric oxide synthases (NOS), guanylyl cyclases, cyclic nucleotide phosphodiesterases, hemoglobins, myoglobins, nitrite reductase, respiratory cytochromes and transcription factors. Heme and hemo-proteins are involved in a variety of biological and cellular functions needed for the survival of organisms [141]. Hemin (ferric chloride heme) is an oxidized form of iron protoporphyrin IX. Hemin is also a potent globin gene activator and growth promoter of early hematopoietic progenitors [141]. Synthetic heme analogues are commonly used to induce HO activity in animals and humans, especially in the newborns to prevent the development of severe hyperbilirubinemia [142]. Hemin stimulates the HO system, which plays a major role in the catabolism of heme, thus it protects the organism from free heme-induced cytotoxicity due to formation of oxygen free radicals and lipid peroxidation. The U. S. Food and Drug Administration have approved hemin, as an active ingredient of a biological therapeutic agent for the treatment of acute porphyrias [106].

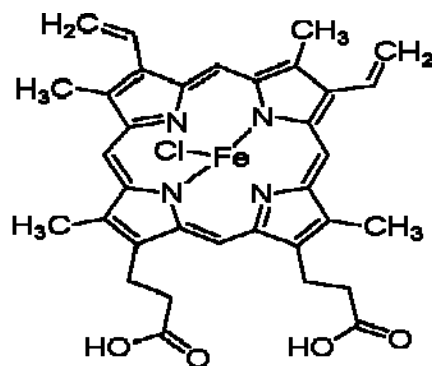


Figure 1.2. Hemin structure.

[Adapted from <http://www.sigmaaldrich.com/catalog/search/ProductDetail/SIGMA/H9039>].

1.10. Deoxycorticosterone acetate (DOCA)-salt-induced hypertension

The etiology and pathogenesis of human hypertension have been studied widely using different animal models of hypertension. These models have been used in research to study the prevention of hypertension or to develop a therapy, and to identify different risk factors involved in human hypertension. The studies in animal models of hypertension are important for the success of clinical trials, even though they do not encompass all traits of human essential hypertension. According to hypertension etiology; animal models of hypertension are divided into two different types, primary and secondary hypertension [143]. Depending on the manner of induction, primary hypertension includes environmentally-induced and genetically-induced models, whereas, secondary hypertension includes renal-induced and pharmacologically-induced hypertension. The DOCA-salt-induced model of hypertension is a type of pharmacologically-induced hypertension, which involves administration of a high dose of deoxycorticosterone, unilateral nephrectomy and isotonic salt (0.9 % NaCl) water as the sole drinking fluid. This animal model is a low renin, volume overload, and human primary aldosteronism type of hypertension [143] with a different natural history, and

different response to antihypertensives, compared to high renin models such as SHR, 2 kidney-1 clip (2K1C), and transgenic rats overexpressing the mouse Ren-2 gene (TGR[mRen2]²⁷) [144]. The DOCA-salt-induced hypertensive model is also characterized by enhanced oxidative stress [6, 19], upregulation of both endothelial system [145, 146] and local tissue RAAS, which results in severe hypertension, cardiac and renal hypertrophy, and end-stage-organ damage, accompanied by proteinuria and a decrease in the creatinine clearance rate [144]. In the DOCA-salt model, angiotensin I converting enzyme inhibitors and angiotensin-II receptor blockers are ineffective [147, 148], while aldosterone receptor blockers and diuretics are effective in reducing blood pressure [149]. There are some limitations in the DOCA-salt-induced hypertensive rat model as compared to genetically-induced models. These are as follows, 1) a large dose of deoxycorticosterone acetate is necessary, 2) surgical removal of one kidney, and 3) continuous ingestion of salt water is required [143]. Even with all these limitations, however, this model is easy to develop and cost effective. The role of sodium in the development of hypertension has consequently been widely studied.

Hypertension in the DOCA-salt model has been divided into different phases; it proceeds with increase in plasma volume and later shifts to pressure natriuresis leading to a transient decrease in blood volume and increase in blood viscosity. Subsequently, reduction in arteriolar blood flow and activation of the intravascular coagulation pathway causes deposition of fibrin and impairment of vascular wall diffusion. Further, vascular alterations causes fibrinoid necrosis and plasmatic vasculitis, leading to cardiovascular complications and nephrosclerosis [150]. Patients with chronic essential hypertension also present the symptoms observed in the DOCA-salt model, having volume overload, vascular remodeling and elevated blood pressure with associated renal

damage [151]. Salt retention is one of the characteristics of chronic human essential hypertension, which can be achieved rapidly in the mineralocorticoid hypertensive rat model. We chose the DOCA-salt hypertensive rat model because it depicts end stage cardiac and renal damage. Moreover, in this low renin model, local production of angiotensin-II and aldosterone, which triggers cardiovascular and renal inflammatory responses results from accumulation of ROS and subsequent activation of NF- κ B and AP-1 [46].

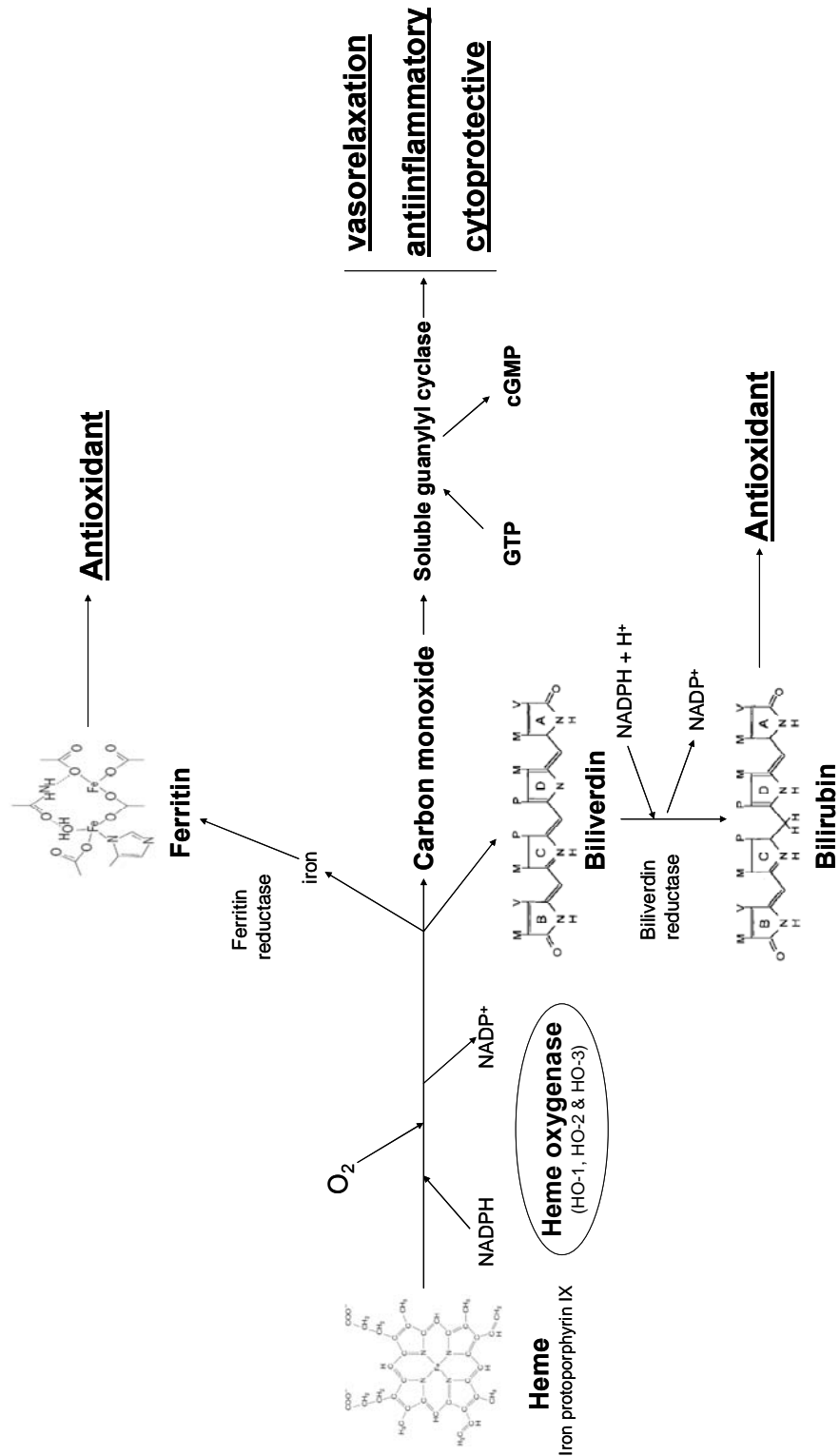


Figure 1.3. The catalysis of heme and its end products by heme oxygenase
 [Modified from Ndisang et.al., J Hypertens. 2004 Jun;22(6):1057-74, and Abraham and Kappas; Free Radical Biology & Medicine; (2005)39: 1-25)].

2. RATIONALE, HYPOTHESIS, AND OBJECTIVES

2.1. Rationale

The HO system has been implicated in the modulation of several diseases, including hypertension, cardiac and renal injury [152]. Upregulation of the HO system has beneficial effects either by degradation of the pro-oxidant heme or by increase in the production of bilirubin and carbon monoxide [Fig.1.3], which are now regarded as beneficial and critical to the cellular defense mechanism [106]. Acute 4 day hemin therapy (i.p.) reduced blood pressure in the young SHR, however, it failed to lower blood pressure in the adult SHR as a result of a non-surmountable increase in HO-1, sGC, cGMP [153, 154]. Whether, this was due to inadequate translation and/or transcription of proteins involved in the HO signal transduction pathway remains to be fully elucidated. However, subsequent studies have now shown that chronic treatment with hemin leads to the prolonged expression of the HO-1 protein, reduced blood pressure and modestly decreased cellular heme in the adult SHR [155]. Similarly, initial data from our laboratory showed that chronic hemin therapy for 23 days lowered systolic blood pressure to physiological normal levels in the adult SHR [40]. Therefore, to counteract disease conditions, it is imperative to boost the HO-1 protein before the onset of chronic disease [156]. Moreover, chronic hemin therapy significantly enhances total HO activity, HO-1 expression, and agents involved in the carbon monoxide signaling cascade to normalize blood pressure in arteries of adult SHR and DOCA-salt hypertensive rats [40, 155]. However, the effect of the chronic hemin regimen on local production of angiotensin-II and aldosterone in the heart and kidney of DOCA-salt hypertensive rat is still unknown. Given the pivotal role of angiotensin-II and aldosterone in the pathophysiology of end-stage renal damage, novel agents capable of

suppressing angiotensin-II, aldosterone, oxidative stress and its mediators such as NF- κ B and AP-1 would be very beneficial and would limit the risk associated with multiple drug therapy in the treatment of cardiac and renal disease.

To date no systemic study has been carried out to correlate the hemin-induced changes in histopathological lesions of the heart such as myocyte scarring, fibrosis or kidney lesions such as glomerular hypertrophy, glomerular sclerosis, tubular cast formation, and small renal arterial thickening in the DOCA-salt hypertensive rat model. Moreover, the effect of an upregulated HO system in DOCA-salt-induced hypertension, oxidative stress, inflammatory and hypertrophic insults needs further clarification.

2.2. Hypothesis

Chronic hemin therapy would counteract cardiac and renal histopathological lesions in DOCA-salt-induced hypertension and prevent end-stage organ damages.

2.3. Objectives

To characterize the effects of hemin on the pathophysiological changes and underlying mechanisms of the HO system, that is responsible for the protection of the heart and kidney in DOCA-salt hypertensive rats.

3. MATERIAL AND METHODS

3.1. Animal experiments

The experimental protocol was approved by the University of Saskatchewan Standing Committee on Animal Care and Supply, which is accordance with the principles and guidelines of the Canadian Council on Animal Care. Hemin (Sigma-aldrich, St. Louis, Mi, USA) was triturated, dissolved in 0.1 M NaOH, and diluted with 1 X phosphate buffer solution (PBS), pH 7.2. The pH of solution was titrated to 7.4 by using 0.1 M HCl. Care was taken that the volume of NaOH was not exceed above 10 % of the final volume of hemin solutions [154]. Chromium (III) mesoporphyrin IX chloride (CrMP) [Frontier Scientific, Logan, Utah, USA] was dissolved in 1 X PBS and pH was titrated to 7.4 with 0.1 M HCl and final volume was adjusted using PBS. To prepare DOCA strips, Elastomer Part A (MDX4-4210, Factor II, Inc. AZ, USA) was weighed about 18 grams, then 1.23 gram DOCA (044K3492, Sigma-Aldrich, USA) was added and mixed thoroughly. This gave a creamy white semi-solid product without any lumps. Further, 1.8 grams of the catalyst (crosslinker, Part B) was added to the elastomer/DOCA mixture and mixed thoroughly. This final product was scooped quickly and gently onto the casting tray and the elastomer mixture was forced into the slot with a metal spatula. Care was taken that the mixture should be evenly distributed along the wells and bubbles were avoided. This ratio provided 4 complete lanes of DOCA inserts (30 c.m. each). The elastomer was allowed to polymerize for 48 hours (hrs) at room temperature. After polymerization DOCA strips were gently removed from the mold and cut into 5 cm. pieces, which were stored in a sealed plastic bag till further use [157, 158]. The above procedure was followed again depending on total requirements of DOCA-strips for the study.

Male Sprague Dawley (SD) rats were purchased from Charles River (Willington, MA, USA) at 8 weeks of age and were housed under standardized conditions. At 9 weeks of age, all animals except the normal control rats (normal SD) were anaesthetized by inhalant anaesthesia (Isoflurane), and the right kidney removed through a dorsal flank incision [159]. Animals that received surgical intervention were injected with the pain-killer Buprenorphine (3 µg/ml/kg body weight) before and 12 hrs after surgery. All uninephrectomized animals recovered very well after the surgery, and began eating and drinking water normally.

A total of 74 rats were used in the study, and were divided into seven different groups: A) DOCA-salt + hemin, n=22; B) DOCA-salt, n=22; C) DOCA-salt + hemin + chromium mesoporphyrin (CrMP), n=6; D) uninephrectomized-DOCA (UnX-DOCA) + water, n=6; E) uninephrectomized-salt (UnX-salt), n=6; F) UnX-sham + water, n=6 and G) surgery-free control (normal SD), n=6. In the DOCA-salt group, a silastic strip impregnated with DOCA was implanted subcutaneously in the midscapular region of uninephrectomized rats and animals were given a 0.9 % NaCl and 0.2 % KCl solution (salt water) for drinking *ad libitum* for 4 weeks, until they became hypertensive [160-162]. DOCA-salt + hemin group rats were treated the same as the DOCA-salt group with the addition of an intraperitoneal injection of the HO inducer, hemin (30 mg/kg body weight) daily, for 4 weeks. Then DOCA-salt + hemin + CrMP group rats were treated the same as DOCA-salt + hemin group with the addition of CrMP injection, 4 µmol/kg (2.61mg/kg) body weight, i.p., daily (for 4 weeks), a HO blocker [163]. Many HO inhibitors available are nonspecific and affect other hemo enzymes as well as increases level of HO-1 proteins. We used CrMP, which is a selective competitive

inhibitor of HO activity [153, 164]. Further, the UnX-DOCA group rats were treated like the DOCA-salt group, however *ad libitum* access to tap water was given. In the UnX-salt and UnX-sham groups, a DOCA free silastic strip was implanted and the animals had access to salt water and tap water *ad libitum*, respectively. The last group was the normal control where rats had no surgery or treatment.

At the end of the study, the animals were kept in metabolic cages and urine samples were collected for 24 hrs. Thereafter the rats were weighed, anaesthetized and sacrificed. Blood and plasma samples were collected, and the kidney and heart tissues were isolated in ice-cold phosphate-buffered saline (PBS), cleaned, and weighed. Subsequently, the mid left ventricular portions of the heart and half of the left kidney of each rat were collected in formalin phosphate buffer for histopathological studies and remaining tissues were snap-frozen in liquid nitrogen and stored at -80°C for further analysis by molecular assays. Some of the gross parameters from the DOCA-salt and DOCA-salt + hemin groups were measured in half of the animals used in the total study. However, most of the molecular studies were done using n=6 and/ or n=4 samples for all groups.

3.1.1. Measurement of systolic blood pressure

Systolic blood pressure was measured in conscious animals using a standard tail-cuff noninvasive blood pressure measurement system (Model 29 SSP, Harvard Apparatus, Montreal, Canada) weekly for the 4 week period of treatment. According to the standard protocol of Harvard Apparatus, in the initial setting of the machine the Biopac system was connected to the analog system. Further pressure and pulse plugs were connected to analog channels 2 and 4, respectively. To set the blood pressure machine, all knobs such as pressure adjust, Lo pass/ band pass, pulse gain, offset, filter

gain were adjusted as per the company's manual. Then the tail cuff was plugged into the input channel and the air tubing was attached to the tail cuff, sphygmomanometer, and air in channel of the Biopac system. After all these settings, NIBP software was opened in the computer, which was connected with the Biopac. Further using MP100 tool pressure was calibrated by applying a clamp onto the tube, which was attached to the tail cuff. Calibration was done using channel 1, when reading on the manometer was zero, 0 mmHg was calibrated. Channel 2 was used to calibrate the highest reading, i.e. 220 mmHg, when air was pumped through the bulb. The calibration of the tail cuff was done before starting every experiment.

Before starting the blood pressure measurement, the rat was restrained and the rat's tail was inserted into the tail cuff. The restrainer was kept on a heating pad to maintain the temperature (27-30°C). In addition, a heating coil with airflow was directed towards the restrainer to ensure an increase in the core body temperature of rat and increase blood flow towards the tail. Rats were allowed to settle for 5 minutes and baseline pressure was recorded. Raw systolic pressure was measured by pumping air through the tail cuff to about 220 mmHg reading on manometer, waiting for 2-3 seconds and then releasing the pressure slowly to get peak raw systolic pressure. On the screen, a bell shaped curve was recorded indicative of a good reading. The final systolic pressure reading was calculated by subtracting the basal pressure reading from the raw systolic reading. The final value of systolic blood pressure was a mean of six recorded readings per rat [154].

3.1.2. Estimation of hematocrit

The blood samples were collected in BD vacutainers spray-coated K₂-EDTA tubes (Ref. 367861) and thoroughly mixed with K₂-EDTA anticoagulant by 8-10

inversions. Heparinized capillary tubes were filled with blood by capillary action, and the other end sealed with nonabsorbent sealing clay. These capillaries were placed in a slot on a microcapillary centrifuge (Biofuge A, Baxter, Canlab) with the plugged end facing outward. Samples were centrifuged at the auto set point for 5 minutes (mins). After centrifugation the hematocrit value was determined using a ruler as a percentage of the packed cells to the total volume [165].

3.1.3. Plasma ferritin assay

Plasma ferritin was assayed in the Biochemical Laboratory, Royal University Hospital (RUH), College of Medicine, using a standard ferritin kit supplied with Architech- i2000 system using a biochemical autoanalyzer (Abbott Architect i2000SR, USA).

3.2. Determination of hypertrophy of heart and kidney

3.2.1. Determination of left ventricular hypertrophy

The heart was isolated, cleaned in PBS, blotted, and weighed using an analytical balance (Precisa XR 205SM-DR, Precisa Instruments, Ltd. Switzerland). The heart weight-to-body weight ratio was calculated. Subsequently, the atria were cut off, and left ventricle with intraventricular septum and right ventricle were separated and weighed [166]. The left ventricle-to-body weight ratio and left ventricle-to-right ventricle ratio were calculated [167]. In addition, the left ventricular wall thickness was measured using a Vernier caliper [168].

3.2.2. Assessment of kidney hypertrophy

The kidney weight-to-body weight ratio is a widely accepted index of kidney hypertrophy [169]. Body weights were recorded prior to sacrificing the animals. After

sacrifice, the left kidneys were rapidly removed from the animal and placed into ice cold PBS. Fat and connective tissues were trimmed off, kidneys were blotted dry, and weighed using an analytical balance. After weighing, the left kidney-to-body weight ratio was established.

3.3 Assay for the quantification of heme oxygenase-1

Detection and quantification of HO-1 protein was done in the cardiac tissue by using rat HO-1 ELISA kit (Stressgen bioreagents, Ann Arbor, USA). It is a quantitative sandwich immunoassay. The anti-rat HO-1 immunoassay plate is precoated with a mouse monoclonal antibody specific for HO-1 on the wells. HO-1 is captured by the immobilized antibody and is detected with rabbit polyclonal antibody specific for the HO-1. The polyclonal antibody is subsequently bound by an anti-rabbit IgG antibody, which is conjugated with horseradish peroxidase. The assay is developed with tetramethylbenzidine substrate (TMB) and a blue color forms in proportion to the amount of HO-1 bound.

To prepare the tissue samples. Cardiac tissue samples were homogenized in 1X extraction reagent (supplied with kit) consisting of protease inhibitors such as 0.1mM PMSF, 1µg/ml leupeptin, 1µg/ml aprotinin, 1µg/ml pepstatin. The homogenate were centrifuged at 21,000 x g for 10 mins at 4°C and supernatants were aliquotted and stored at -80°C untill assayed. All the reagents were brought to room temperature. Rat HO-1 standard and samples were diluted in sample diluents. Subsequently, 100 µl of prepared standards and samples were added in duplicates to the wells of the anti-rat HO-1 immunoassay plate and the plate was covered. The plate was allowed to incubate for 1

hr at room temperature and then wells were washed 4 times with 1X wash buffer. Then 100 μ l of diluted rat HO-1 conjugate was added to each well and the plate was incubated at room temperature for 30 min. Again, wells were washed with 1X wash buffer 4 times and 100 μ l of TMB substrate was added. Further incubation of the plate was done in the dark for 15 mins and the reaction was stopped by adding 100 μ l of stop solution in the wells. Finally, the plate was read at 450 nm using a microplate reader (SpectraMax 340PC, Molecular Device, CA, USA). The blue color intensity is directly proportional to the amount of HO-1 enzyme present in the wells. The standard curve was plotted using a linear scale concentration (ng/ml) on the X-axis and absorbance, corresponding rat HO-1 standard, on the Y-axis. The sample concentrations were determined by multiplying by the dilution factor and presented as ng/ml of sample.

3.4. Assay for heme oxygenase activity

The HO activity was evaluated as bilirubin production using an established method [154, 170]. To perform this assay, bilirubin reductase was initially extracted from the liver cytosol as described below. The liver homogenates were prepared using ice-cold 0.25 M sucrose solution containing phenylmethylsulfonyl fluoride (1 mM), EDTA (0.2 mM) and 50 mM potassium phosphate buffer (pH 7.4). The homogenates were centrifuged at 20,000 g for 20 mins and supernatant fractions were centrifuged at 150,000 g for 90 min. The microsomal pellets thus obtained were washed, and further resuspended in 20 mM potassium phosphate buffer (pH 7.4), containing 135 mM KCl, 1 mM phenylmethylsulfonyl fluoride, and 0.2 mM EDTA to a protein concentration of 10 mg/ml. The 150,000 g supernatant obtained from the microsomal preparation was

fractionated by addition of ammonium sulphate (AS), and the 40-60 % AS fraction was dissolved in 10 mM potassium phosphate buffer.

To measure HO activity, both cardiac and kidney tissues (1 gram) were homogenized on ice in 4 ml of 5:1 K/Na 100 mmol/L phosphate buffer with 2 mmol/L $MgCl_2$ (HO-activity buffer), then centrifuged at 13,000 rpm for 15 min. Aliquots of 100 μ l were collected from the supernatant, and placed in tubes containing 500 μ l of a mixture of 0.8 mmol/L nicotinamide dinucleotide phosphate, 20 μ mol/L hemin, 2 mmol/L glucose-6-phosphate, 0.002 U/ μ l glucose-6-phosphate dehydrogenase, and 100 μ l liver cytosol as a source of biliverdin reductase. The reaction was started in the dark at 37°C for 1 hr, and then stopped by adding 500 μ l of chloroform. To extract bilirubin, tubes were vigorously agitated and centrifuged at 13,000 rpm for 5 mins. The chloroform layer was collected and read on a spectrophotometer, at 464 nm minus the background at 530 nm. The amount of bilirubin in each sample was determined by the spectrophotometric assay using (extinction coefficient for bilirubin 40 $mM^{-1}cm^{-1}$), and was expressed as nmole/mg protein/hr. The protein content was measured using Bradford assay [171]. Spleen tissue was used as a positive control [154].

3.5. Measurement of cyclic guanosine monophosphate levels

The quantification of cGMP was performed using Cayman's competitive enzyme immunoassay (EIA) method directly from cardiac and kidney tissue homogenates [172]. In short, this assay is based on the competition between free cGMP and a cGMP-acetylcholinesterase (AChE) conjugate (cGMP tracer) for a limited number of cGMP specific rabbit antibody binding sites. Briefly, the kidney and cardiac tissue

samples were homogenized in 6 % trichloroacetic acid at 4°C in the presence of 3'-isobutyl-1-methylxanthine to inhibit phosphodiesterase activity and centrifuged at 2000 g for 15 mins. The supernatant was recovered, washed with water-saturated diethyl ether and the upper ether layer was aspirated and discarded while the aqueous layer containing cGMP was recovered and lyophilized. The dry extract from the samples were dissolved in assay buffer. EIA buffer, samples or cGMP standards, cGMP AchE tracer and cGMP antiserum were added in wells sequentially as described in the manufacturer's protocol. After incubation for 18 hrs at 4°C, the plate was washed to remove any unbound reagents and then Ellman's Reagent (which contains the substrate to AchE) was added to the well. The product of this enzymatic reaction develops a distinct yellow color after 90-120 mins. Finally, the plate reading was done at 412 nm using a microplate reader (SpectraMax 340PC, Molecular Device CA, USA). The intensity of this colour, determined spectrophotometrically, was proportional to the amount of cGMP tracer bound to the well, which was inversely proportional to the amount of free cGMP present in the well during the incubation and expressed as picomol of cGMP per mg of protein.

3.6. Superoxide dismutase assay

Superoxide dismutase assay was performed using an EIA kit (Cayman Chemical, Ann Arbor, MI, USA) according to the manufacturer's instruction [40, 173] in kidney tissue. The assay was performed to detect total SOD activity (cytosolic and mitochondrial).

Kidney tissue samples were homogenized in 5-10 ml of cold 20 mM HEPES buffer pH 7.2, containing 1 mM EGTA, 210 mM mannitol and 70 mM sucrose per gram of tissue and centrifuged at 1500 x g for 5 mins at 4°C. Supernatants were collected and stored at -80°C until assayed. In the present assay, tetrazolium salt was used for the detection of superoxide radicals generated by xanthine oxidase and hypoxanthine, and 1 unit of SOD was defined as the amount of enzyme needed to produce 50 % dismutation of the superoxide radical. All reagents were equilibrated at room temperature and samples were thawed and kept on ice. The stock SOD standard solution was prepared by diluting 20 µl of SOD standard with 1.98 ml of sample buffer and a range between 0 to 0.25 U/ml standards were used for the assay. Then 200 µl of diluted radical detector and 10 µl of samples or standards were added to the wells and the reaction was initiated by adding 20 µl of diluted xanthine oxidase to all wells. Then all the contents from the plate were mixed carefully, subsequently, plate was covered and incubated on a shaker for 20 mins. at room temperature. The absorbance was read at 450 nm using a plate reader (SpectraMax 340PC, Molecular Device, CA, USA). The results were calculated as units/ml of samples.

3.7. Total antioxidant capacity assay

In tissues, the antioxidant system comprises different enzymes including catalase, glutathione peroxidase and superoxide dismutase as well as substances such as α -tocopherol, β -carotene, ascorbic acid, ferritin, biliverdin, uric acid, reduced glutathione and bilirubin [104, 174-179]. The total antioxidant capacity is the sum of

endogenous and food-derived antioxidants. As compared to a single antioxidant, the additive effects of all the different antioxidants provide a greater protection.

The total antioxidant capacity assay in both heart and kidney tissue [173, 174] was determined using an EIA kit (Cayman Chemical Company, Ann Arbor, MI, USA) according to the manufacturer's instruction [40, 173]. This assay was based on the ability of the antioxidants in the samples to inhibit the oxidation of 2,2-azino-di-3-ethylbenzthiazoline sulphonate (ABTS) to ABTS plus metmyoglobin. In brief, kidney and left ventricular tissue samples were homogenized in the presence of protease inhibitors in 1 ml of cold buffer pH 7.4, containing 5 mM potassium phosphate, 0.9 % sodium chloride and 0.1 % glucose. Samples were centrifuged at 10,000 x g for 15 mins at 4°C. Supernatants were separated, and total protein of the samples were determined by the Bio-Rad method [171]. Samples were stored at -80°C until assaying. Before beginning the assay, all reagents, except samples were equilibrated to room temperature. Trolox standards were prepared between the ranges of 0 to 0.330 mM Trolox. Then 10 µl of either standard or samples, 10 µl of metmyoglobin, and 150 µl of chromogen were added in the designated wells on the plate. Subsequently, the reaction was started by adding 40 µl of the hydrogen peroxide working solution to all the wells, as quickly as possible. The plate was covered and incubated on a shaker for 5 mins at room temperature. Finally, the absorbance was recorded after removing the plate cover at 750 nm using the Synergy Microplate Reader (BioTek Instruments, Inc., VT, USA) with Gen5 Data Analysis Software. The results were presented as trolox equivalent antioxidant capacity (TEA C) per mg protein [173].

3.8. Measurement of aldosterone in the heart and kidney

Cardiac and kidney tissue aldosterone concentrations were quantified using an aldosterone EIA kit-Monoclonal (Cayman Chemical Company, Ann Arbor, MI, USA) [12, 180]. The tissues were homogenized in 10 mM Tris-buffered saline (20 mM Tris-HCl of pH 7.4, 0.25 M sucrose, and 1 mM EDTA) in the presence of a freshly prepared cocktail of protease inhibitors, and centrifuged at 8500 rpm for 10 mins at 4°C using a method described previously [154] and total protein estimation was determined using the Bio-Rad method [171]. The assay was based on the competition between aldosterone and a tracer (aldosterone-acetylcholinesterase) using a fixed amount of aldosterone monoclonal antibody. This antibody-aldosterone (either free or tracer) complex was bound to the goat polyclonal anti-mouse IgG that had previously been attached in the well. The plate was washed to remove excess unbound tracers and subsequently, Ellman's reagent was added in the well according to the protocol. The products of this enzymatic reaction give a yellow color, which was quantified spectrophotometrically using a standard curve generated by reading the absorbance at 412 nm with a microplate reader (SpectraMax 340PC, Molecular Device, CA, USA). The intensity of the distinct yellow color was proportional to the amount of aldosterone tracer bound to the well, which was inversely proportional to the amount of free aldosterone present in the well during the incubation. Finally, the aldosterone concentration was equalized by calculation of aldosterone pg/mg protein in the tissue.

3.9. Assessment of angiotensin-II in the heart and kidney

Cardiac and kidney tissue angiotensin-II concentrations were quantified using an angiotensin-II EIA kit (SPI-BIO bertin group F-91741 - Massy Cedex, France). A

specific monoclonal anti-angiotensin-II was immobilised on a 96 well microtiter plate. Angiotensin-II of samples and standards was allowed to react immunologically for 24 hrs at 4°C. Wells were then washed to remove the excess unbound molecules of angiotensin-II while the trapped molecules were covalently linked to the plate by glutaraldehyde via amino groups. In addition, denaturing treatment followed so that angiotensin-II could react again with the acetylcholinesterase-labelled mAb used as tracer. Finally, the plate was washed and Ellman's reagent (enzymatic substrate for AChE and chromogen) was added to the wells. The AChE tracer acts on the Ellman's reagent to form a yellow compound. Levels of angiotensin-II were quantified using a standard curve generated by reading the absorbance at 412 nm with a microplate reader (SpectraMax 340PC, Molecular Device, CA, USA) and represented as pg/mg protein [180, 181].

3.10. Urine analysis

3.10.1. Measurement of urine excretion

Patients having kidney problems are associated with frequent urination and increased excretion of urine (polyurea). Similarly, in the DOCA-salt hypertension either by pressure natriuresis or due to severe renal damage causes increase in urine excretions. Antihypertensive effect and improved renal lesions would reduce urine excretion. Therefore, at the end of the study, all the animals were kept in metabolic cages and urine was collected for 24 hrs. Total urine excreted per group was calculated as ml/24 hrs in all the groups.

3.10.2. Total urinary protein assay

Total protein concentrations in urine samples were measured using the Bradford protein assay (Bio-Rad kit) [171]. The Bio-Rad protein assay used was a dye-binding assay, in which various concentrations of protein displayed different colors. The working dye solution was prepared by diluting 1 part dye reagent concentrate with 4 parts distilled deionized water, and filtering through Whatman filter paper #1 to remove particulate. Bovine serum albumin (Fract V, Fisher BiReagents, USA) was used for the assay standard to determine a linear range of 0.2 to 0.9 mg/ml. Then 25 µl each of the standard and sample solutions were pipetted out into a clean, dry test tube (duplicates); 1 ml of diluted dye reagent was added to each tube and finally the solutions were mixed by vortex. Tubes were incubated for 10 mins at room temperature and absorbance was measured at 595 nm. The protein concentration in the urine was calculated and presented in the form of total protein excretion in mg for 24 hrs urine collection [152].

3.10.3. Creatinine clearance rate

Creatinine is a metabolic product of creatine-phosphate dephosphorylation in muscle. It is produced daily and is present in the blood at stable levels. It has a constant rate of production and is excreted through a combination of glomerular filtration (70-80 %) and tubular secretion. With a decrease in the glomerular filtration rate, the creatinine clearance value becomes increasingly inaccurate due to the shift towards tubular secretion fractions as a greater proportion of total urinary creatinine (it may go to 60 % in renal insufficiency) [98].

$$\text{Creatinine clearance} = \frac{\text{Urinary creatinine concentration} \times \text{urine flow/ volume}}{\text{Plasma creatinine concentration}}$$

Plasma creatinine, urine creatinine and creatinine clearance were measured in the Biochemical Laboratory (RUH), College of Medicine, with the help of the laboratory supervisor as per their standard protocol using a biochemical autoanalyser machine and kit (DXC, Beckman Coulter, CA, USA) [182].

3.11. Assay for urinary 8-isoprostane

8-isoprostane, under normal condition appears in the plasma and urine, and when its levels are elevated, it signifies intense oxidative activities. Quantification of urinary 8-isoprostane has been proposed to be a precise index of chronic and systemic non-enzymatic lipid peroxidation and increased ROS [33].

Urinary 8-isoprostane assay was done using an EIA kit (Cayman Chemical Company, Ann Arbor, MI, USA) according to the manufacturer's instructions [46]. Urine samples were purified using an immunoaffinity method as described in the manufacture's instruction before assaying. The assay is based on the competition between 8-isoprostane and an 8-isoprostane-acetylcholinesterase (AChE) conjugate (8-isoprostane tracer) for a specific 8-isoprostane rabbit antiserum binding site. Concentrations of 8-isoprostane were varied while the 8-isoprostane trace was constant, therefore, the amount of 8-isoprostane tracer that bound to rabbit antiserum was inversely proportional to the concentration of 8-isoprostane in the well. The complex of rabbit antiserum-8-isoprostane (either free or tracer) was bound to the rabbit IgG mouse monoclonal antibody, which was previously attached to the well. The plate was washed to remove excess unbound 8-isoprostane and reagents, then Ellman's reagent containing the substrate AChE were added to obtain a yellow color, which absorbs at 412 nm. The intensity of yellow color determined spectrophotometrically is directly proportional to

the amount of 8-isoprostane tracer bound to the well. Where as it is indirectly proportional to the amount of free 8-isoprostane present in the well during the incubation; or

$$\text{Absorption } \alpha [\text{Bound 8-Isoprostane Tracer}] \propto 1/ [8\text{-Isoprostane}].$$

3.12. Western immunoblotting expression of HO-1, TGF- β and fibronectin

Kidney tissues were homogenized in 10 mM Tris-buffered saline (20 mM Tris-HCl of pH 7.4, 0.25 M sucrose, and 1 mM EDTA) in the presence of a freshly prepared cocktail of protease inhibitors, and centrifuged at 8500 rpm for 10 mins at 4°C as described previously [154]. The supernatant was decanted and total protein concentration was determined by the Bio-Rad method [171]. Aliquots of 50 μ g of proteins were loaded on a 10 % SDS-polyacrylamide gel. The fractionated proteins were electrophoretically transferred to nitrocellulose paper and non-specific binding was blocked with 3 % non-fat milk. Thereafter, the membranes were incubated overnight with primary rabbit anti-HO-1 antibody (Calbiochem, USA, 1:500), rabbit anti-pan TGF- β (Sigma-Aldrich, Inc., USA, 1:200), and mouse monoclonal anti-fibronectin antibody (Santa Cruz Biotechnology, Inc., CA, USA, 1:200) for HO-1, TGF- β and fibronectin, respectively. After several washes, the nitrocellulose blot was incubated with secondary goat anti-rabbit antibody conjugated to horseradish peroxidase (Sigma-Aldrich, Inc., USA) for HO-1, TGF- β , while goat anti-mouse antibody for fibronectin, and the immuno-reactivity were visualized with enhanced horseradish peroxidase/luminol chemiluminescence reagent (Perkin Elmer Life Sciences, Boston, MA, USA). A monoclonal antibody produced in mouse of glyceraldehyde-3-phosphate

dehydrogenase (GAPDH) and β -actin (Sigma-Aldrich, Inc., USA, 1:5000), and horseradish peroxidase conjugated secondary goat anti-mouse antibody (Sigma-Aldrich, Inc., USA) were used for cardiac tissue and kidney tissue, respectively as a house keeping protein control to ascertain equivalent loading [183]. Relative densitometry analyses of respective bands of blots were carried out using UN-SCAN-IT software (Silk Scientific, Utah, USA). TGF- β and fibronectin expression were utilized in the kidney samples, however HO-1 expression was incorporated in both heart and kidney samples.

3.13. Total RNA isolation and quantitative RT-PCR for NF- κ B and AP-1

Heart and kidney tissue, about 300 mg, was homogenized in 0.5 ml Trizol Reagent (Invitrogen Life Technologies, Carlsbad, CA, USA) according to the manufacturer's specifications. Reverse transcription was carried out using the First Strand cDNA Synthesis Kit (Novagen, Madison, WI, USA) with 0.5 μ g Oligo (dT)₆, 50 mM Tris-HCl (pH 8.3 at 25°C), 75 mM KCl, 75 mM KCl, 3 mM MgCl₂, 50 mM DTT, 10 mM each free dNTP and 100 U of MMLV reverse transcriptase according to manufacturer's instruction. Quantitative PCR was done with Applied Biosystems 7300 Real Time PCR system (Foster City, CA, USA), iQ SYBR Green Supermix (Bio-Rad, Hercules, CA, USA) containing 50 mM KCl, 20 mM Tris-HCl (pH 8.4), 0.2 mM each free dNTP, hot start enzyme iQ^{Taq} DNA polymerase (25 U/ml), 3 mM MgCl₂, SYBR Green 1, and 10 nM fluorescein as passive reference [184]. Triplicate samples containing 1 μ l of cDNA were run using a template of 3.2 pmol of primers for NF- κ B (forward, 5'CATGCGTTTCCGTTACAAGTGCGA-3' and reverse 5'TGGGTGCGT

CTTAGTGGTATCTGT-3'), AP-1 (forward, 5' AGCAGATGCTTGAGTTGAGAGCC A-3' and reverse, 5' TTCCATG GGTCCCTGCTTTGAGAT-3'), β -actin (forward, 5' TCATCACTATCGGCAATGAGCGGT-3' and reverse, 5' ACAGCACTGTGTTGGCA TAGAGGT-3') and for heart house keeping gene GAPDH was used (forward, 5'CCAGCCAAGGATACTGAGAGCAAGA-3' and reverse, 5' TCTGGGATGGAATT GTGAGGGAGA-3') in a final volume of 25 μ l. The National Research Institute of Canada, Saskatoon, confirmed the sequences of all primers used. The program for the thermal cycle was 10 mins at 95°C followed by 40 cycles of 15 secs at 95°C, 30 secs at 56°C and 15 secs at 72°C. The melting points of the PCR product were determined by incubating at 65°C for 1 min followed by a 1°C per min rise over 30 mins.

3.14. Histopathological analysis of left ventricle and kidney

The middle portion (midpapillary level) of the left ventricle and half of kidney were separated, fixed in 10 % formalin phosphate buffer for 48 hrs, processed and paraffin embedded. Then sections of 5 μ m thicknesses were cut and stained with hematoxylin and eosin for histological analysis.

3.14.1. Left ventricular morphological lesions: semi-quantitative analysis

The left ventricular sections were obtained from the middle portion of the left ventricle to avoid differences in regional cardiomyocyte size in different regions of the left ventricle [185]. Observation of the degree of scarring was conducted in a blind fashion using light microscopy (Eclipse 80i, Nikon Canada Inc., Ontario, Canada) semi-quantitatively on a 0-2 scale (0= normal or almost normal; 1= focal mild; and 2= severe patchy lesions) in each cardiac tissue section, and the mean score was calculated per group [186].

3.14.2. Quantification of cardiac muscular hypertrophy

Cardiac hypertrophy is a combination of myocyte hypertrophy and reactive fibrosis, therefore it was decided to measure cardiomyocyte size along with myocardial weight (cardiac or left ventricular weight) to exclude the confounding influence of non-myocyte on cardiac hypertrophy [187]. Cardiac muscular hypertrophy was initially scored blindly using a semi-quantitative method (0= no hypertrophy and 1= positive hypertrophy). It was further confirmed quantitatively by measuring muscle fiber thickness and myocyte diameter using image analyses software. To get consistent results, myocytes were positioned perpendicularly to the plane of the section with a visible nucleus and cell membrane clearly outlined. Unbroken areas were selected for measurement [188]. Left ventricular myocyte width (both longitudinal and cross/transverse sections separately) were measured randomly in 20 cardiac muscle fibers from each left ventricular tissue section. All sections were imaged at 400X using NIS-elements BR-Q imaging software (Nikon) [0.95 $\mu\text{m}/\text{Pixel}$ (Px)]. Muscle fiber thickness was quantified and analyzed between different groups [189, 190].

3.14.3. Assessment of perivascular fibrosis

Left ventricular paraffin sections of 5 μm thick were obtained and stained with Masson's trichrome/collagen blue stain [191]. The tissue collagen was stained distinctly blue in the focal lesions of patchy fibrosis. The perivascular areas were also stained with blue color, indicative of fibrosis. All vessels from the left ventricular sections were selected and imaged at 200X, then photomicrographed by using NIS-element BR-Q imaging software (Nikon) [0.95 $\mu\text{m}/\text{Px}$]. Total areas of vessel and perivascular fibrosis were measured using the area measurement tool. Finally, assessment of the perivascular

fibrosis was done by calculating the ratio of the fibrosis area surrounding the vessel to the total vessel area, and averaged per group. [192].

3.14.4. Morphometric analysis of small coronary and renal arteries

All small coronary and renal arteries from left ventricle and kidney sections were selected and imaged at 200X, respectively. Using NIS-elements BR-Q imaging software (Nikon) [0.95 $\mu\text{m}/\text{Px}$] the inner and outer diameters of arteries were measured and wall thickness calculated. In addition, the media-to-lumen ratio and medial cross-sectional areas of arteries were calculated and compared between the experimental groups [193-195].

3.14.5. Semi-quantitative analysis of morphological lesions in kidney

Morphologic evaluation of glomerular hypertrophy, glomerular sclerosis, tubular dilation, cast formation and mononuclear cell infiltration was conducted in a blind fashion using light microscopy semi-quantitatively on a 0-3 scale (0= normal or almost normal; 1= mild; 2= moderate; 3= severe) in each kidney section and the mean score was calculated [196]. Quantitative assessments of renal glomerular and tubular lesions were done by counting the damaged and sclerotic glomeruli and tubular protein casts in each section [197].

3.14.6. Quantitative analysis of glomerular hypertrophy

The cortex regions of the kidney sections were imaged at 200X and 30 glomeruli were selected randomly. Then the diameters of the glomeruli were measured using NIS-elements BR-Q imaging software (Nikon) [0.95 $\mu\text{m}/\text{Px}$] and compared between groups [182, 198].

3.15. Immunohistochemical detection of TGF- β and fibronectin

Paraffin embedded sections of left ventricle and kidney tissue were taken for the detection of TGF- β whereas, only kidney tissue sections were utilized for the fibronectin detection in the three groups (UnX-sham, DOCA-salt and DOCA-salt + hemin) of the study. Five-micrometer thick sections were placed on the slides, deparaffinized, and rehydrated. The endogenous peroxidases were blocked by pre-treating sections with 3 % H₂O₂ in methanol for 10 mins, and then digested with pepsin at 37°C for 20 min. Dako autostainer universal staining system was used to perform all further procedures. Later, sections were incubated in protein-blocking serum for 60 mins. at room temperature followed by incubation with anti-rabbit TGF- $\beta_{1/2/3}$ (1:50 dilutions) antiserum for TGF- $\beta_{1/2/3}$, while fibronectin (P1H11) mouse monoclonal antibody (1:50 dilution) raised against a cell binding domain of fibronectin of human origin (Santa Cruz Biotechnology, Inc., CA, USA) for fibronectin about 30 mins. at room temperature. Sections were then washed in phosphate-buffered saline and incubated with an Envision plus chromagen linked secondary antibody (goat anti-rabbit or anti-mouse antibody, Santa Cruz Biotechnology, Inc., CA, USA) for 30 mins. Diaminobenzidine was used to localize peroxidase conjugates as a chromogen for 10 min. Finally, sections were counter-stained with hematoxylin and examined under the light microscope. Specific products utilized were included in the Dako Envision immunoperoxidase staining kit (Santa Cruz Biotechnology, Inc., CA, USA).

The immunostaining intensity of TGF- β and fibronectin was scored on 50 different fields per tissue section by semi-quantitative method, blindly. The staining intensity score per high power field was given on a 0-3 scale, where 0= no staining, 1=

mild, 2= moderate and 3 = maximum staining [199]. Further, the expressions of TGF- β and fibronectin were further confirmed by quantitative Western immunoblot method in the renal tissue only.

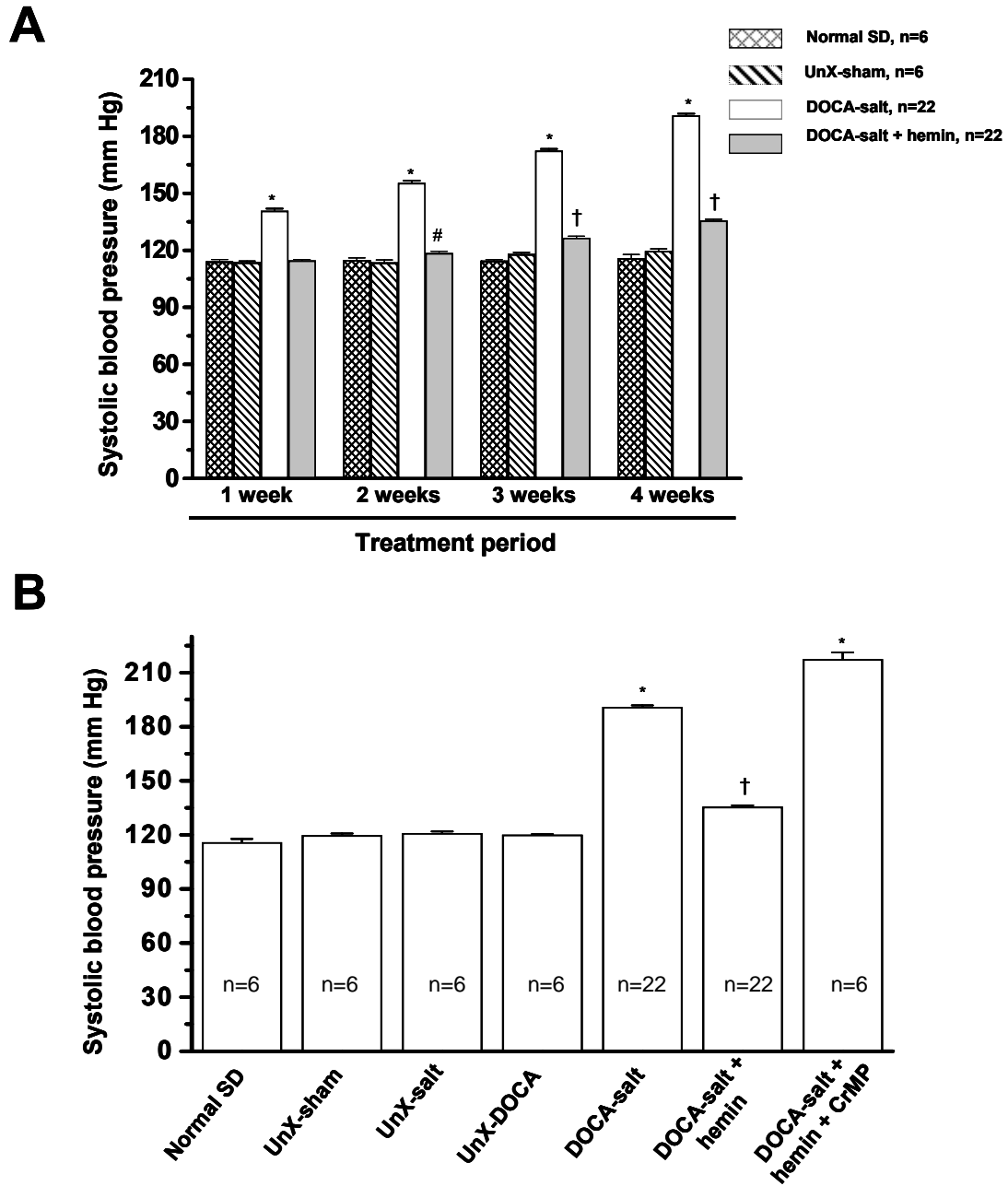
3.16. Statistical analysis

All data was expressed as mean \pm SEM. Statistical analyses were done with a one way ANOVA for repeated measures wherever appropriate. Groups were compared using Bonferroni test for multiple comparisons. P values of $p < 0.05$ were considered statistically significant.

4. RESULTS

4.1. Effect of hemin on systolic blood pressure

Systolic blood pressure was measured using a standard tail-cuff noninvasive blood pressure measurement system in the animals every week for 4 weeks during the protocol. Two normotensive groups and hemin-treated DOCA-salt group rats were compared with the DOCA-salt treated rats to observe the progression of development of the hypertension [Fig. 4.1.A]. However, at the end of study all rats from all groups were subjected to the standard tail-cuff noninvasive blood pressure measurement system to measure systolic blood pressure [Fig. 4.1.B]. The systolic blood pressure reading was determined from the mean of six readings per rat, and was averaged per group [154]. Hemin therapy given to DOCA-salt rats progressively lowered blood pressure over a four weeks period. Figure, 4.1.A demonstrated that the average systolic blood pressure in DOCA-salt hypertensive rats was significantly higher after the first week than in hemin-treated DOCA-salt, UnX-sham and normal SD [(140.8 ± 1.10 mmHg, n=22 vs. hemin-treated DOCA-salt, 114.7 ± 0.54 mmHg, n=22 and controls (113.7 ± 0.66 mmHg and 114.2 ± 1.05 mmHg, n=6), p< 0.01]. A gradual increase in blood pressure in the DOCA-salt rat was observed throughout the study. In the second week, the trend remained similar to that noted in the first week, as the blood pressure in DOCA-salt hypertensive rats was notably higher compared to hemin-treated and normotensive controls (155.4 ± 1.19 mmHg, n=22 vs. all groups, p< 0.01) [Fig. 4.1.A]. However, hemin-treated DOCA-salt rats showed significant increased blood pressure as compared to UnX-sham (118.5 ± 0.96 mmHg, n=22 vs. 113.6 ± 1.32 mmHg n=6, p< 0.05), but remained comparable to normal SD rats (114.8 ± 1.12 mmHg, n=6).



([#]p< 0.05 vs. UNX-sham and DOCA-salt, *p< 0.01; †p< 0.01 vs. all other groups). Bars represent means ± SEs.

[**Normal SD**- normal rat, **UnX-sham**- uninephrectomized rat + elastic strip + normal water, **UnX-salt**- uninephrectomized rat + elastic strip + salt water, **UnX-DOCA**- uninephrectomized rat + DOCA elastic strip + normal water, **DOCA-salt**- uninephrectomized rat + DOCA elastic strip + salt water and **DOCA-salt + hemin**- uninephrectomized rat + DOCA elastic strip + salt water + hemin, **DOCA-salt + hemin + CrMP**- uninephrectomized rat + DOCA elastic strip + salt water + hemin + CrMP].

Blood pressure in the third week was consistently higher in DOCA-salt hypertensive rats than controls [172.4 ± 0.91 mm Hg, n=22 vs. (UnX-sham, 118.0 ± 0.80 and normal SD, 114.9 ± 0.83 mm Hg, n=6), p< 0.01]. However, hemin treated DOCA-salt rats showed significantly increased blood pressure compared to controls, but it was still within the normotensive range (126.6 ± 0.88 mm Hg, n=22 vs. controls, p< 0.01) [**Fig. 4.1.A**].

In the fourth week DOCA-salt hypertensive rat showed severe hypertension with blood pressure reaching 190.9 ± 0.90 mm Hg, n=22, (p< 0.01) compared to all other experimental groups [**Fig. 4.1.B**]. Although, blood pressure of hemin-treated DOCA-salt hypertensive rats was within the normotensive range, it remained higher than that of control animals [135.6 ± 0.74 mm Hg, n=22 vs. (UnX-DOCA, 119.0 ± 0.79 mm Hg, UnX-salt, 121.0 ± 0.91 mm Hg, UnX-sham, 120.0 ± 0.4 mm Hg and normal SD, 115.9 ± 1.95 mm Hg, n=6), p< 0.01]. In contrast, CrMP a HO blocker, nullified the effect of hemin and showed significantly higher systolic blood pressure in the DOCA-salt + hemin + CrMP group (217.5 ± 3.7 mm Hg, n=6, p< 0.01) compared to all other groups [**Fig. 4.1.B**]. Importantly, in the present study blood pressure of the normotensive controls did not differ significantly, suggesting that uninephrectomy, DOCA and salt alone in the SD rat did not affect blood pressure up to 4 weeks of the study.

4.2. Effect of hemin treatment on body weight and hematocrit values

At the end of the study, all animals were weighed and compared within groups to determine the effect of hemin on the body weight. The average body weight of the UnX-sham (471 ± 23.2 g, n=6), UnX-salt (454 ± 10.5 g, n=6) and UnX-DOCA (450 ± 14.2 g, n=6) were significantly higher than the DOCA-salt hypertensive (405 ± 11.6 g, n=22), hemin-treated DOCA-salt (415 ± 5.8 g, n=22) and both CrMP + hemin-treated DOCA-salt (408 ± 10.1 g, n=6) rats, $p < 0.05$. Whereas, it did not differ from the normal SD (444 ± 19.1 g, n=6) [Table 4.1]. Hemin therapy did not affect the body weight of the experimental rats.

Parameter	Normal SD (n=6)	UnX-sham (n=6)	UnX-salt (n=6)	UnX-DOCA (n=6)	DOCA-salt (n=22)	DOCA-salt + hemin (n=22)	DOCA-salt + hemin + CrMP (n=6)
Body weight (grams)	444 ± 19.1	471 ± 23.2 [†]	454 ± 10.5 [†]	450 ± 14.2 [†]	405 ± 11.6	415 ± 5.8	408 ± 10.1
Hematocrit (%)	53 ± 0.9	54 ± 0.5	53 ± 0.5	52 ± 0.4	59 ± 2.2*	50 ± 2.2	54 ± 0.4

Table 4.1. Effect of hemin on body weight and hematocrit values.

([†] $p < 0.05$ vs. DOCA-salt, DOCA-salt + hemin and DOCA-salt + hemin + CrMP; * $p < 0.01$ vs. all other group; **Mean ± SE**)

Normal hematocrit values in the rat ranges from 36–54 % (juvenile to adult rat) [200]. In the present study, hematocrit values in the normotensive controls, hemin-treated, and both CrMP and hemin-treated DOCA-salt were within the normal range [normal SD, 53 ± 0.9 %, n=6; UnX-sham, 54 ± 0.5 %, n=6; UnX-salt, 53 ± 0.5 %, n=6, UnX-DOCA, 52 ± 0.4 %, n=6; DOCA-salt + hemin, 50 ± 2.1 %, n=22 and DOCA-salt + hemin + CrMP, 54 ± 0.4 %, n=6]. However, in the untreated DOCA-salt hypertensive rats, hematocrit values were significantly higher than all other groups (59 ± 2.2 %, n=22, $p < 0.01$) [Table 4.1].

4.3. Effect of hemin regimen on cardiac and renal hypertrophy

The effect of hemin on gross cardiac hypertrophy was determined by assessing heart-to-body weight ratio, left ventricle-to-body weight ratio, left-to-right ventricular weight ratio, and left ventricular wall thickness. A significant increase in the heart-to-body weight ratio was observed in the DOCA-salt hypertensive rats (3.8 ± 0.12 gram/kg, $n=22$, $p < 0.01$) as compared to normal SD (2.9 ± 0.9 gram/kg, $n=6$), UnX-sham (2.8 ± 0.08 gram/kg, $n=6$), UnX-salt (2.7 ± 0.09 gram/kg, $n=6$) and UnX-DOCA (2.8 ± 0.4 gram/kg, $n=6$). Hemin treatment significantly reduced the heart-to-body weight ratio in the DOCA-salt hypertensive rats (3.4 ± 0.07 gram/kg, $n=22$, $p < 0.05$), although not to control values. However, CrMP enhanced the heart-to-body weight ratio in the DOCA-salt hypertensive rats [**Fig. 4.2.A**]. Furthermore, left ventricle-to-body weight ratio in the DOCA-salt hypertensive rats (2.4 ± 0.14 gram/kg, $n=22$, $p < 0.01$) was higher than normotensive controls (normal SD, 2.0 ± 0.08 ; UnX-sham, 1.82 ± 0.12 ; UnX-salt, 1.9 ± 0.06 and UnX-DOCA, 2.0 ± 0.09 gram/kg, $n=6$) and was in a comparable range with DOCA-salt + hemin + CrMP, treated hypertensive rats (2.7 ± 0.09 gram/kg, $n=6$). Hemin therapy reduced left ventricular-to-body weight ratios to the level of controls (2.1 ± 0.08 gram/kg, $n=22$, $p < 0.05$) [**Fig. 4.2.B**].

Another important index for the assessment of hypertrophy is the left-to-right ventricular weight ratio. The left-to-right ventricular weight ratio did not differ between the normotensive controls (normal SD, 4.1 ± 0.20 ; UnX-sham, 4.4 ± 0.66 ; UnX-salt, 4.4 ± 0.09 and UnX-DOCA, 4.3 ± 1.02 , $n=6$), but was significantly elevated in DOCA-salt hypertensive rat (6.7 ± 0.62 , $n=22$, $p < 0.05$) and DOCA-salt + hemin + CrMP treated rats (6.8 ± 0.87 , $n=6$, $p < 0.05$) compared to controls. However, left-to-right ventricular

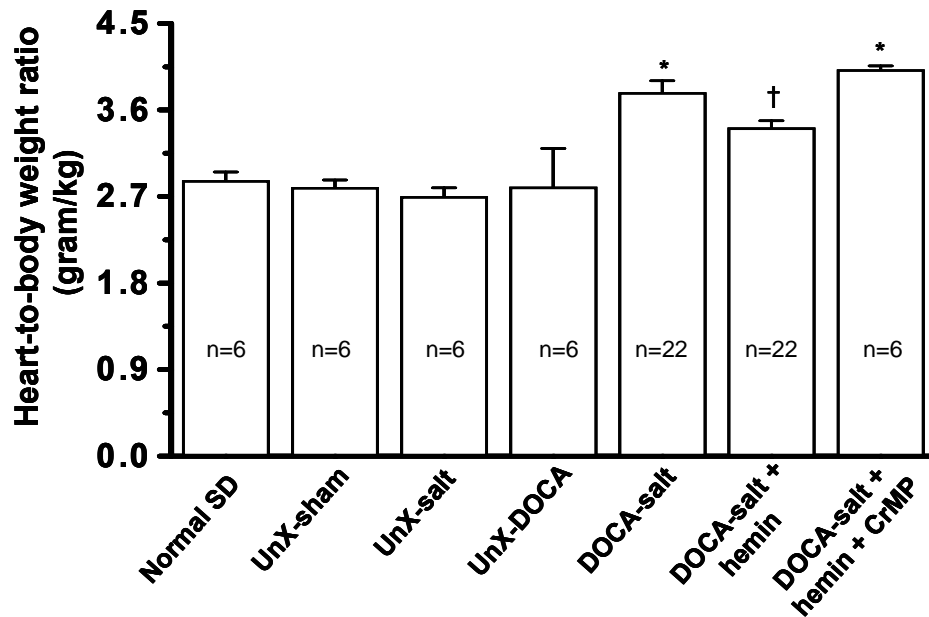
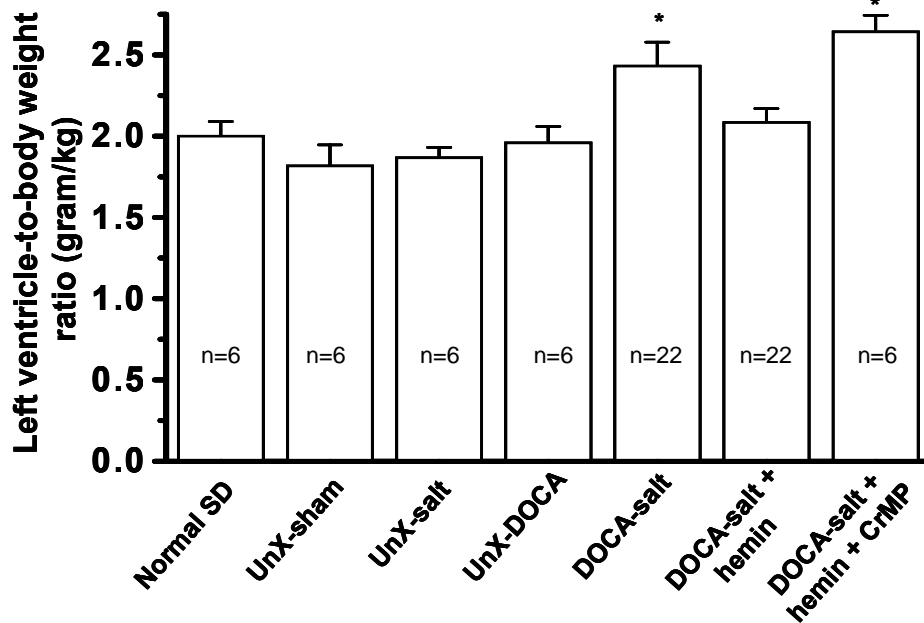
A**B**

Figure 4.2. Hemin therapy inhibits DOCA-salt-induced cardiac and left ventricular hypertrophy. Uninephrectomized rats receiving DOCA-salt showed significant increased (A) Heart-to-body weight ratio, (B) Left ventricle-to-body weight ratio. Hemin therapy significantly prevented development of cardiac and left ventricle hypertrophy in the DOCA-salt rats, whereas CrMP blocked the effect hemin. ([†]p < 0.05 vs. all other groups; *p < 0.05 vs. Normal SD, UnX-sham, UnX-salt, UnX-DOCA and DOCA-salt hemin groups). Bars represent means ± SEs.

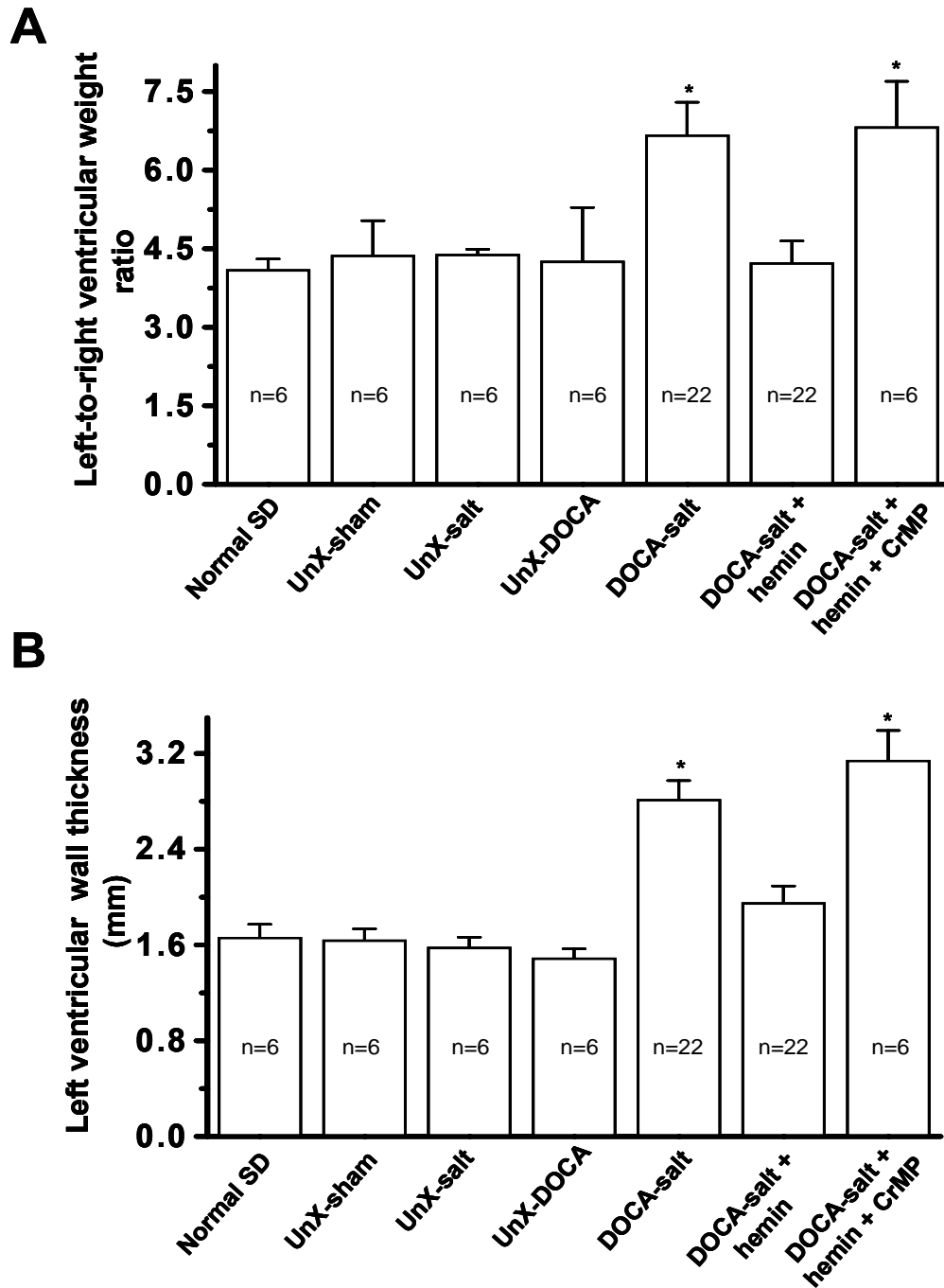


Figure 4.3. Hemin reduces left-to-right ventricular ratio and left ventricular wall thickness in DOCA-salt hypertensive rats. DOCA-salt and DOCA-salt + hemin + CrMP treated uninephrectomized rat showed significantly higher (A) left-right ventricular ratio and (B) left ventricular wall thickness. However, hemin treatment in DOCA-salt hypertensive rats restored left-to-right ventricular ratio and left ventricular wall thickness to control levels. (* $p < 0.05$ vs. Normal SD, UnX-sham, UnX-salt, UnX-DOCA and DOCA-salt hemin groups). Bars represent means \pm SEs.

weight ratio between DOCA-salt and DOCA-salt + hemin + CrMP groups were non-significant. Interestingly, hemin therapy reduced the left-to-right ventricular weight ratio in the DOCA-salt hypertensive rats (4.2 ± 0.41 , $n=22$, $p < 0.05$) to control levels [Fig. 4.3.A]. We also assessed the left ventricular wall thickness in the DOCA-salt hypertensive rat and relative controls. In a similar way this index was restored to control levels by hemin (2.82 ± 0.155 mm to 1.96 ± 0.138 mm, $n=11$, $p < 0.01$) [Fig. 4.3.B].

Similarly, at the end of study (4 weeks), DOCA-salt-induced hypertensive rats showed severe renal hypertrophy, which was assessed by the kidney-to-body weight ratio.

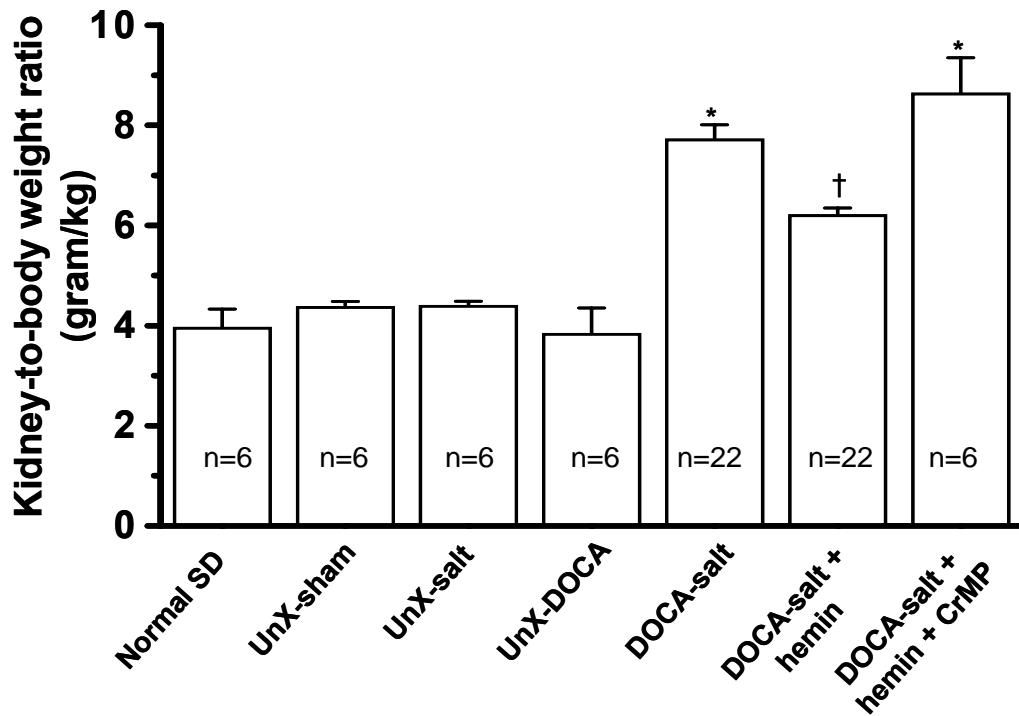


Figure 4.4. Hemin therapy abates DOCA-salt-induced by kidney hypertrophy. Uninephrectomized rats receiving DOCA-salt showed significant increased kidney-to-body weight ratio. Hemin therapy significantly prevented kidney hypertrophy. There is no difference of kidney-to-body weight ratio between the normotensive control groups. CrMP treatment nullified the effect of hemin and enhanced renal hypertrophy. († $p < 0.01$ vs. all other groups; * $p < 0.01$ vs. Normal SD, UnX-sham, UnX-salt, UnX-DOCA and DOCA-salt + hemin groups).

Kidney-to-body weight ratio was significantly increased in DOCA-salt hypertensive rats (7.73 ± 0.281 gram/kg, $n=22$, $p < 0.01$) as compared to control rats (normal SD, 3.97 ± 0.358 ; UnX-sham, 4.39 ± 0.094 ; UnX-salt, 4.41 ± 0.780 and UnX-DOCA, 3.85 ± 0.500 gram/kg, $n=6$). Hemin therapy significantly reduced renal hypertrophy (6.24 ± 0.129 gram/kg, $n=22$, $p < 0.01$), but not to control levels [Fig. 4.4]. Whereas, the HO blocker, CrMP exacerbated renal hypertrophy with ratios significantly higher than controls and DOCA-salt + hemin groups ($p < 0.01$).

4.4. Effect of hemin on cardiac and renal HO-1 expression, HO activity, and cGMP content

The HO-1 concentration in cardiac tissue of normotensive controls were not significant (normal SD, 11.05 ± 0.904 vs. UnX-sham, 11.68 ± 0.868 ng/ml, $n=6$). In the DOCA-salt hypertensive rats the HO-1 concentration increased by 1.5-fold compared to the controls (17.32 ± 1.617 ng/ml, $n=6$, $p < 0.05$). Interestingly, hemin therapy in DOCA-salt hypertensive rats showed a 6.3 fold increase in the HO-1 concentration compared to normotensive controls (71.75 ± 4.579 ng/ml, $n=6$, $p < 0.01$). Whereas, the HO blocker CrMP abolished the effect of hemin in the DOCA-salt hypertensive rats (16.26 ± 2.431 ng/ml, $n=6$, vs. controls and DOCA-salt + hemin, $p < 0.01$) [Fig. 4.5.A]. Alternatively, HO-1 expression in the kidney tissue was quantified by Western immunoblot technique, compared to the relative percentage against β -actin. The HO-1 expression in kidney tissue from the normotensive rats (normal SD, 10.3 ± 2.0 , and UnX-sham, 10.7 ± 1.6 HO-1/ β -actin %, $n=6$) were significantly lower compared to

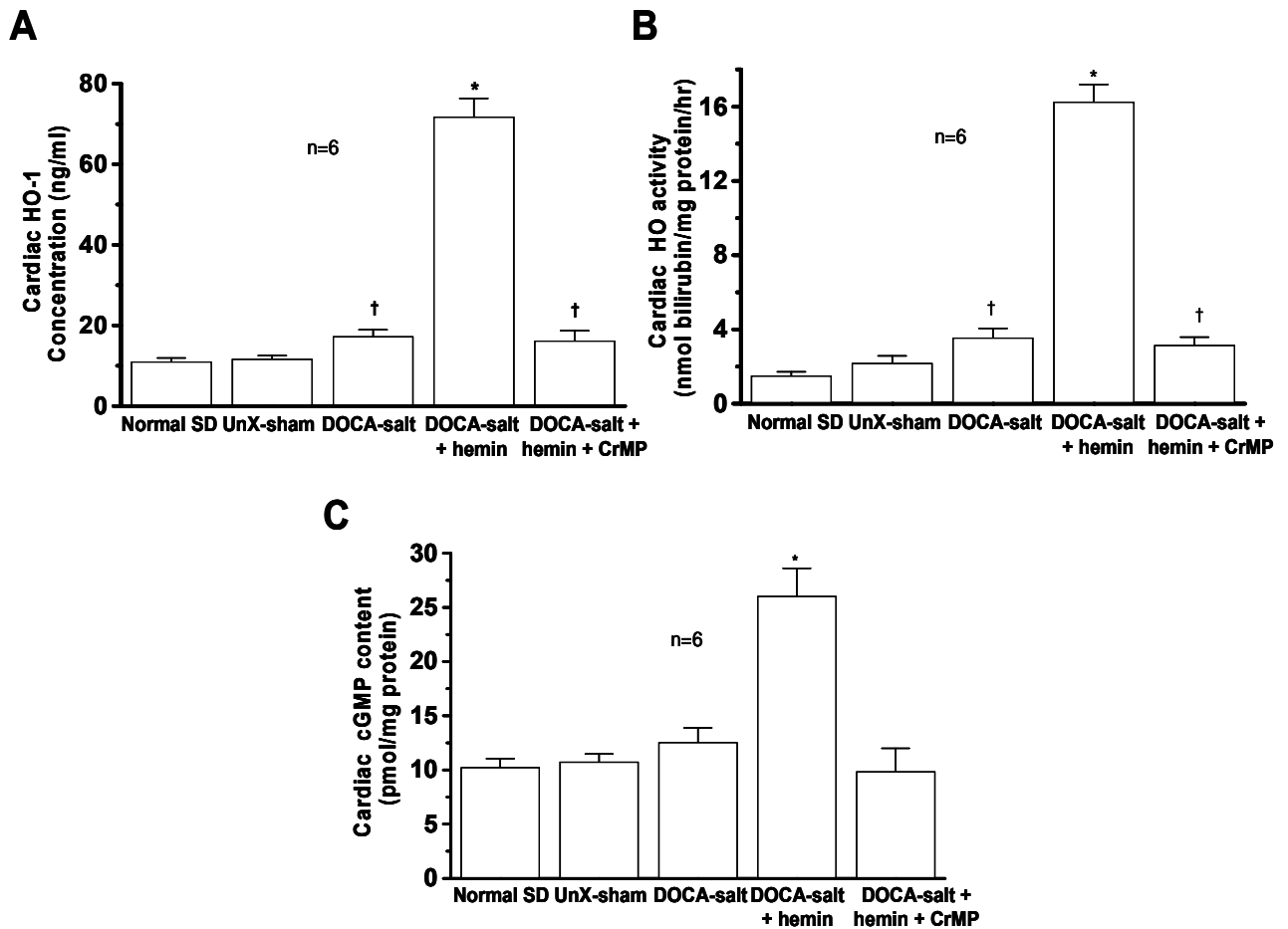


Figure 4.5. Effect of hemin and CrMP on HO-1, HO activity and cGMP levels in cardiac tissue of DOCA-salt hypertensive rats. (A) Cardiac HO-1 levels measured using anti-rat HO-1 ELISA kit. Cardiac HO-1 levels in the DOCA-salt significantly higher than the controls, however hemin therapy further boosted robustly. **(B)** Similar to the HO-1 levels, HO activity in the DOCA-salt was increased significantly compared to the control groups and hemin further enhanced HO activity. **(C)** Stimulation of the HO system enhanced production of cGMP in hemin-treated DOCA-salt rats whereas, CrMP abolished the effects of hemin.

([†] $p < 0.05$ vs. Normal SD, UnX-sham and DOCA-salt + hemin groups; ^{*} $p < 0.01$ vs. all other groups). HO-1= heme oxygenase-1, cGMP = cyclic guanosine monophosphate

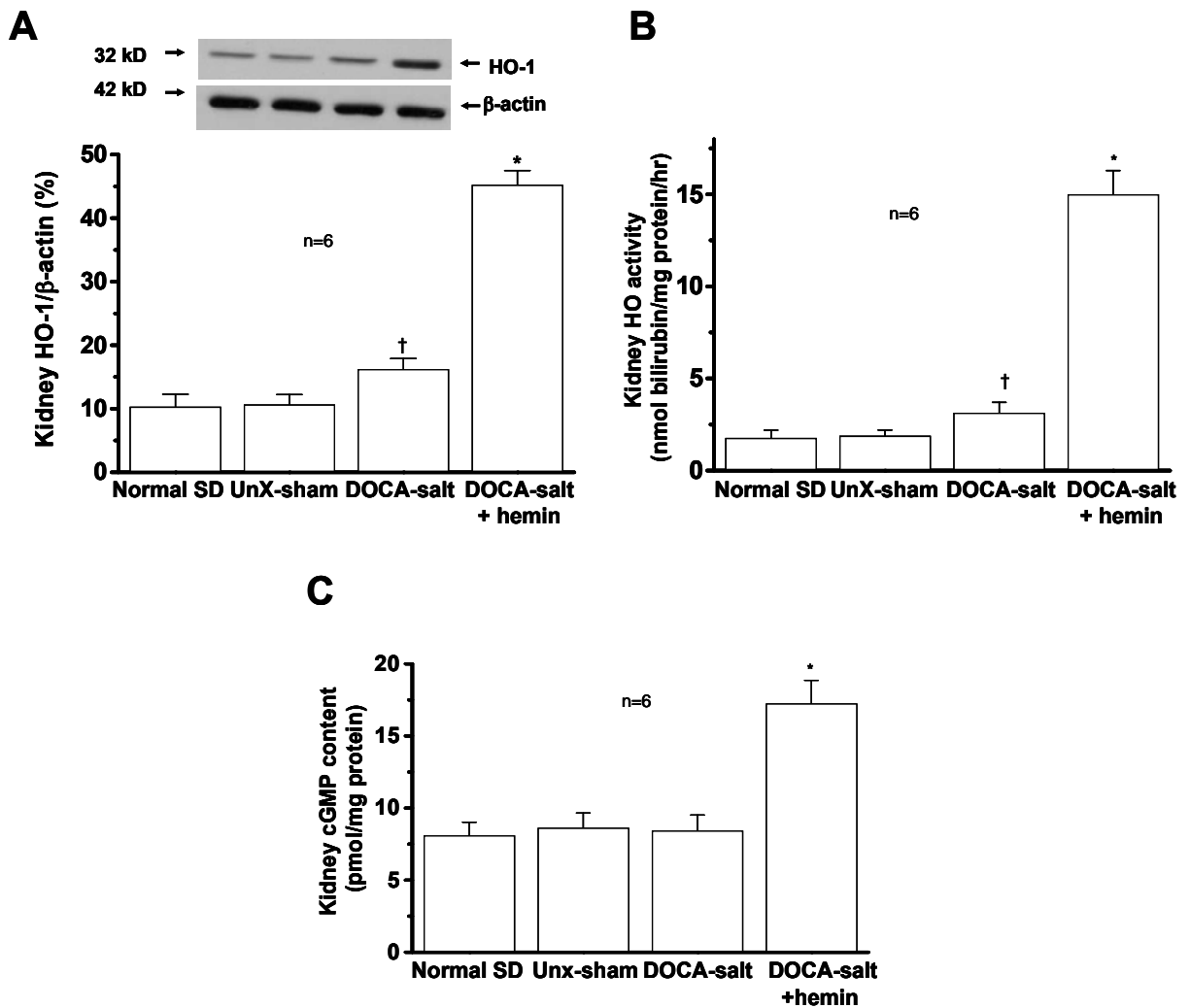


Figure 4.6. Hemin therapy enhances HO-1 expression, HO activity and cGMP in the kidney. (A) Representative western blot and densitometry analysis of HO-1 expression against β-actin in kidney tissue. HO-1 expression was higher in the DOCA-salt rat and was further boosted significantly higher level by hemin. (B) Significant increased activity was found in the kidney of DOCA-salt compared with control rats. Hemin treatment robustly increased HO activity in DOCA-salt hypertensive rats. (C) Hemin therapy greatly enhanced cGMP content in the kidney of DOCA-salt rats. (* $p < 0.01$; [†] $p < 0.05$ vs. all other groups). β-actin = beta actin

DOCA-salt hypertensive rats (16.2 ± 1.6 HO-1/ β -actin %, $n=6$, $p < 0.05$), suggesting basal HO-1 levels in the normal animal. Hemin therapy further boosted renal HO-1 expression compared to controls and only DOCA-salt alone treated hypertensive rats (45.2 ± 2.2 HO-1/ β -actin %, $n=6$, $p < 0.01$) [**Fig. 4.6.A**].

In cardiac tissue, HO activity in controls (normal SD and UnX-sham) were not significantly different from each other (1.5 ± 0.20 vs. 2.2 ± 0.40 nmol bilirubin/mg protein/hr, $n=6$). However, the HO activity of the controls were less than those of DOCA-salt alone treated hypertensive rats (3.6 ± 0.51 nmol bilirubin/mg protein/hr, $n=6$, $p < 0.05$) and combined hemin and CrMP treated DOCA-salt hypertensive rat (3.2 ± 0.43 nmol bilirubin/mg protein/hr, $n=6$, $p < 0.05$). Hemin therapy alone further enhanced cardiac HO activity in DOCA-salt hypertensive rats (16.3 ± 0.93 nmol bilirubin/mg protein/hour, $n=6$, $p < 0.01$) compared to DOCA-salt alone treated and control rats [**Fig. 4.5.B**]. Similar observations of HO activity were made in the kidney. In the kidney tissue of DOCA-salt hypertensive rat, the HO activity was significantly increased (3.1 ± 0.57 nmol bilirubin/mg protein/hr, $n=6$, $p < 0.05$) compared to controls (normal SD, 1.8 ± 0.42 and UnX-sham, 1.9 ± 0.32 nmol bilirubin/mg protein/hr, $n=6$). Similarly, as observed in the heart, hemin therapy further enhanced kidney HO activity by 7-fold than that of control rats [**Fig. 4.6.B**].

The basal cGMP in DOCA-salt hypertensive rats, which were comparable to the levels in normotensive controls were significantly elevated by hemin therapy. The basal cardiac tissue cGMP levels of UnX-sham, normal SD and DOCA-salt hypertensive rats were 10.77 ± 0.705 , 10.25 ± 0.804 , and 12.56 ± 1.327 , pmol/mg protein, $n=6$, respectively and were not significantly different from each other. However, hemin

therapy robustly boosted cardiac cGMP content (26.06 ± 2.561 pmol/mg protein, $n=6$, $p < 0.01$) in DOCA-salt hypertensive rats compared to controls and DOCA-salt hypertensive rats [**Fig. 4.5.C**]. In contrast to that combined hemin and CrMP therapy blocked the effect of hemin in the DOCA-salt hypertensive rats (9.87 ± 2.132 pmol/mg protein, $n=6$, vs. hemin treated DOCA-salt group, $p < 0.01$). Similarly, hemin therapy significantly enhanced kidney cGMP content [17.25 ± 1.607 pmol/mg proteins, $n=6$, $p < 0.01$ vs. untreated DOCA-salt hypertensive rats (8.43 ± 1.082 pmol/mg protein, $n=6$) and normotensive controls (normal SD, 8.10 ± 0.919 and UnX-sham, 8.63 ± 1.024 pmol/mg protein, $n=6$)] [**Fig. 4.6.C**].

4.5. Measurement of aldosterone and angiotensin-II levels in cardiac and renal tissue after hemin therapy

Hemin therapy significantly decreased cardiac aldosterone levels in DOCA-salt hypertensive rat (25.0 ± 5.65 to 7.1 ± 1.03 pg/mg protein, $n=6$, $p < 0.05$) compared to DOCA-salt alone to the level of controls (normal SD, 8.1 ± 2.74 and UnX-sham, 7.0 ± 2.73 , pg/mg protein, $n=6$) [**Fig. 4.7.A**]. Similarly, renal aldosterone levels in DOCA-salt hypertensive rats were substantially increased from the basal levels of normotensive controls (normal SD, 6.0 ± 2.24 and UnX-sham, 4.2 ± 2.03 , pg/mg protein, $n=6$). However, hemin-treatment in DOCA-salt rats showed significant attenuation of renal aldosterone levels (28.7 ± 7.01 to 6.4 ± 2.56 , pg/mg protein, $n=6$, $p < 0.05$) [**Fig. 4.7.B**].

In this study, there were no significant difference between cardiac angiotensin-II levels of normal SD, UnX-sham and hemin-treated DOCA-salt rats (4.5 ± 1.07 , 3.2 ± 1.17 and 5.8 ± 1.53 , pg/mg protein, $n=6$, respectively). However, in DOCA-salt hypertensive rats the levels of cardiac angiotensin-II were considerably increased ($16.8 \pm$

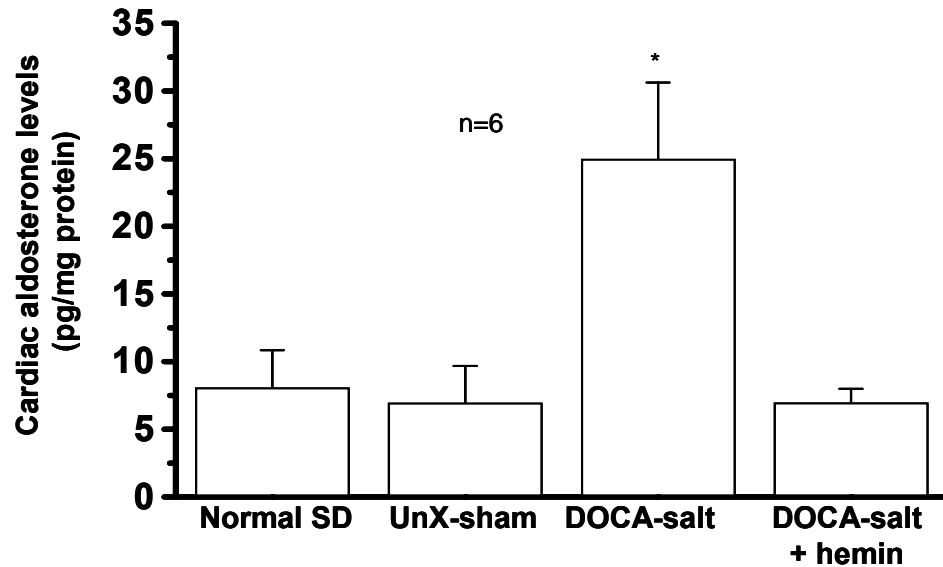
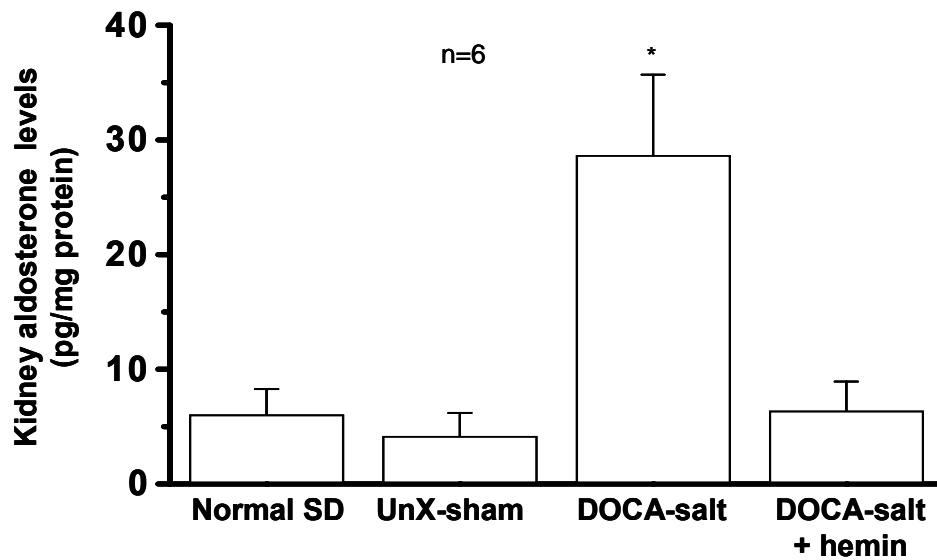
A**B**

Figure 4.7. Hemin therapy prevents the upregulation of cardiac and renal aldosterone levels. In DOCA salt hypertensive rat both cardiac (A) and renal (B) aldosterone were greatly increased compared with controls. Hemin therapy attenuated aldosterone levels in DOCA-salt hypertensive rats, which were comparable with controls. (* $p < 0.05$ vs. all other groups).

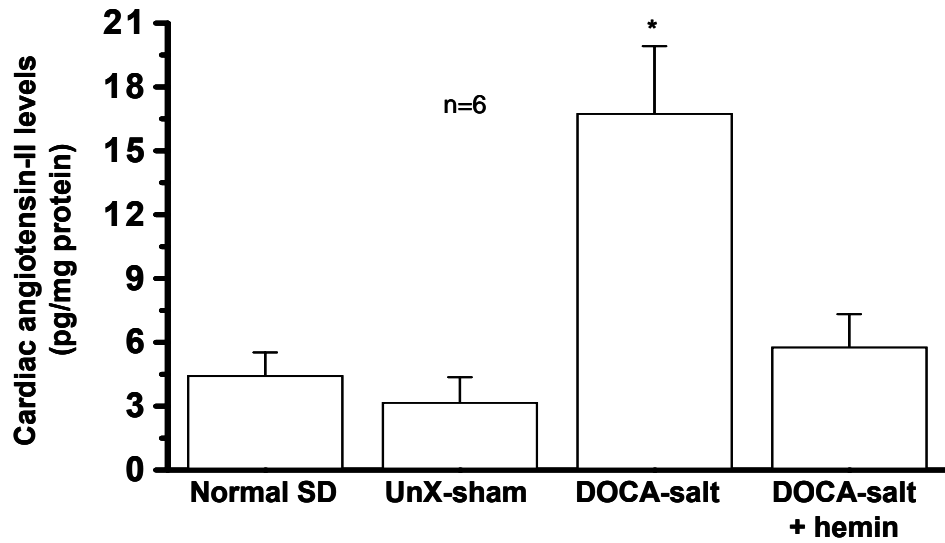
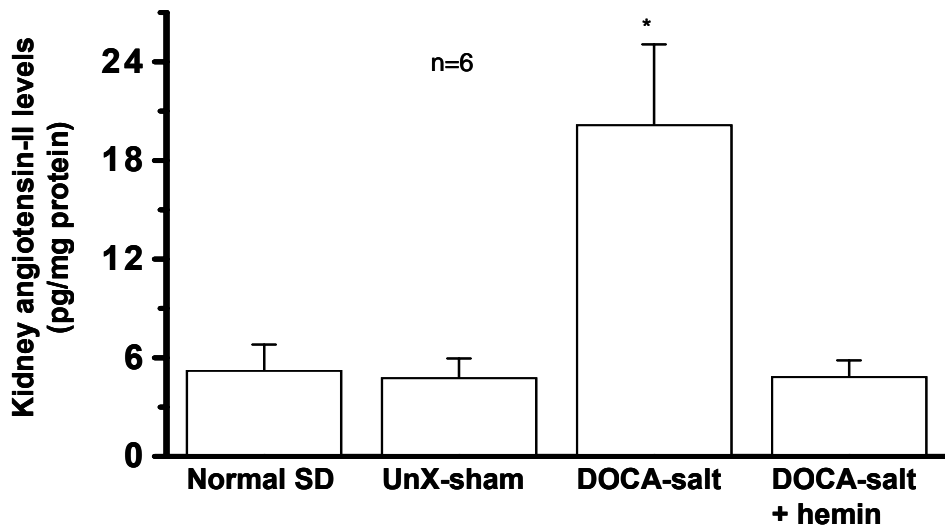
A**B**

Figure 4.8. Effect of hemin treatment on cardiac and renal angiotensin-II levels. DOCA-salt stimulated both cardiac (A) and renal (B) angiotensin-II levels with respect to controls, However, hemin therapy significantly downregulated angiotensin-II levels. (* $p < 0.05$ vs. all other groups).

3.15 pg/mg protein, n=6, p< 0.05) than those of the controls. Hemin therapy robustly reduced angiotensin-II to the basal levels noted in control rats [Fig. 4.8.A]. Similarly, hemin therapy abated renal angiotensin-II levels in the DOCA-salt hypertensive rats (20.2 ± 4.87 to 4.9 ± 0.97 , pg/ml, n=6, p< 0.05). Angiotensin-II levels were restored to the levels of controls (normal SD, 5.3 ± 1.56 , pg/mg protein and UnX-sham 4.8 ± 1.15 , pg/mg protein, n=6) [Fig. 4.8.B].

4.6. Effect of hemin therapy on markers/mediators of oxidative stress such as urinary 8-isoprostane, NF- κ B and AP-1

4.6.1. Urinary 8-isoprostane

Urinary 8-isoprostane was used as an oxidative maker in DOCA-salt hypertensive rats. The basal urinary 8-isoprostane levels in controls were found as, 8.78 ± 1.399 ng/24 hrs and 8.90 ± 1.654 ng/24 hrs, (n=6) in normal SD and UnX-sham, respectively. In the DOCA-salt hypertensive rat, enhanced excretion of urinary 8-isoprostane (57.94 ± 3.322 ng/24 hrs, n=6, p< 0.01) was observed with respect to controls. However, hemin-treated DOCA-salt hypertensive rat substantially decreased urinary 8-isoprostane levels (18.17 ± 2.300 ng/24 hrs, n=6, p< 0.01) as compared to DOCA-salt treatment alone. This decreased urinary 8-isoprostane was not restored to the normal control levels. In construct, CrMP nullified the effect of hemin and increased urinary 8-isoprostane levels (71.99 ± 7.522 ng/24 hrs, n=6, vs. all other groups, p< 0.01) [Fig. 4.9].

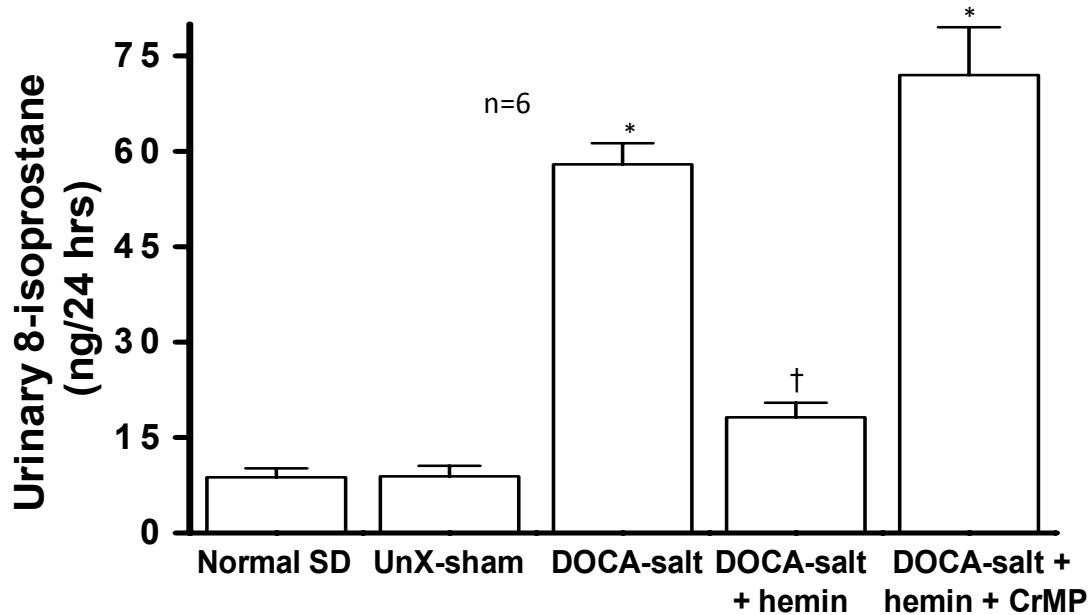


Figure 4.9. Hemin therapy attenuates urinary 8-isoprostane. Oxidation of tissue phospholipid membrane releases urinary 8-isoprostane, an index of systemic oxidative stress. DOCA-salt rats excreted significantly higher levels of urinary 8-isoprostane compared with controls. In hemin-treated rats, urinary 8-isoprostane was significantly abated, but levels remained significantly higher than controls. However, CrMP abolished the effect of hemin in DOCA-salt hypertensive rats. († $p < 0.05$; * $p < 0.01$ vs. all other groups).

4.6.2. NF- κ B and AP-1

For the evaluation of NF- κ B expression, mRNA levels of NF- κ B were measured by real-time RT-PCR and percentage arbitrary unit was expressed against mRNA of GAPDH and β -actin in both cardiac and renal tissue, respectively. As shown in **Figure 4.10.A**, significantly increased cardiac mRNA expression of NF- κ B levels was observed in DOCA-salt hypertensive rat [98.73 ± 6.631 NF- κ B/GAPDH % vs. controls (normal SD, 28.37 ± 3.157 and UnX-sham, 30.84 ± 3.215 NF- κ B/GAPDH %) $n=6$, $p < 0.01$]. Hemin, therapy significantly downregulated cardiac mRNA expression of NF- κ B in DOCA-salt rats with respect to DOCA-salt treatment alone (40.12 ± 2.429

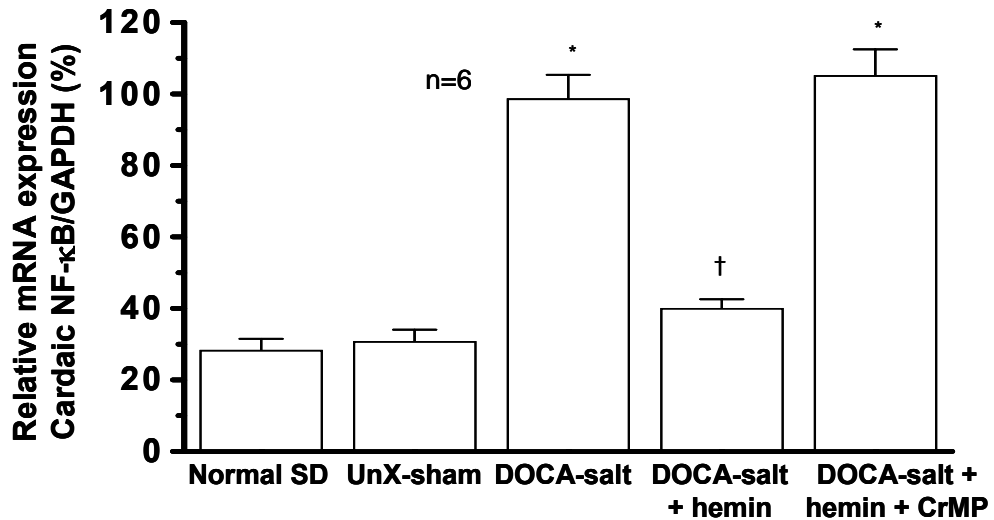
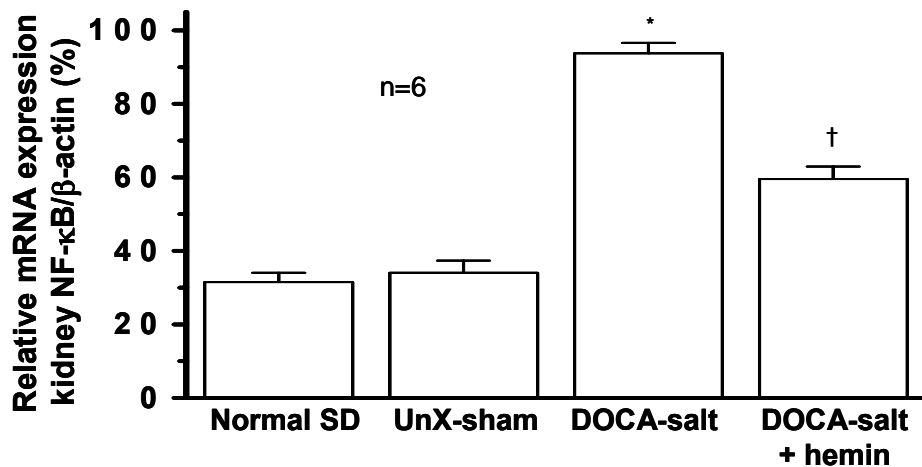
A**B**

Figure 4.10. Hemin prevents activation of NF-κB in cardiac and renal tissue.

Quantitative RT-PCR showing relative mRNA expression of NF-κB against GAPDH and β-actin, respectively. Hemin therapy significantly downregulated NF-κB expression in both cardiac (**A**) and renal (**B**) tissue as compared with DOCA-salt rats. However, NF-κB expression levels were significantly higher than the controls. CrMP treatment nullified the effect of hemin in DOCA-salt hypertensive rats. († $p < 0.01$ vs. all other groups; * $p < 0.01$ vs. Normal SD, UnX-sham and DOCA-salt + hemin groups).

NF-κB = Nuclear factor kappa B.

GAPDH = Glyceraldehyde 3-phosphate dehydrogenase.

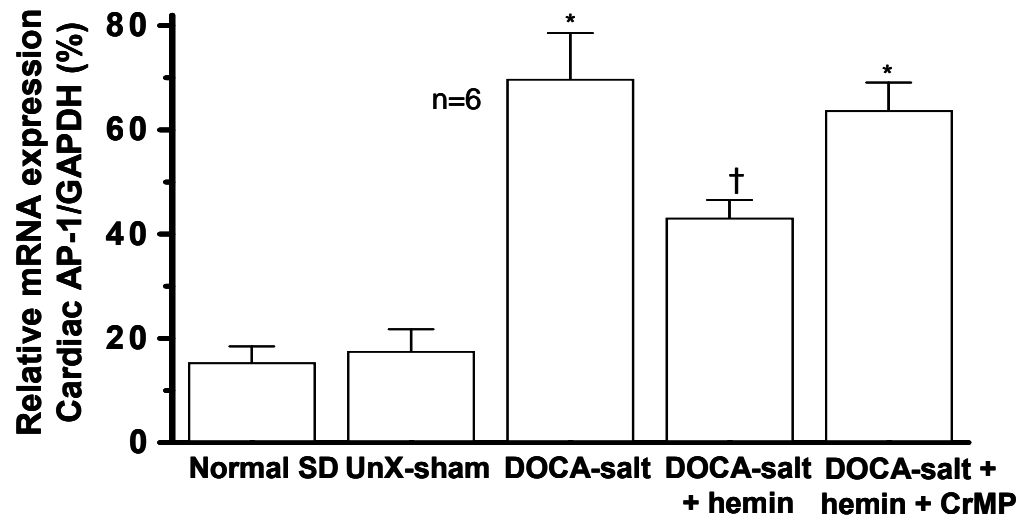
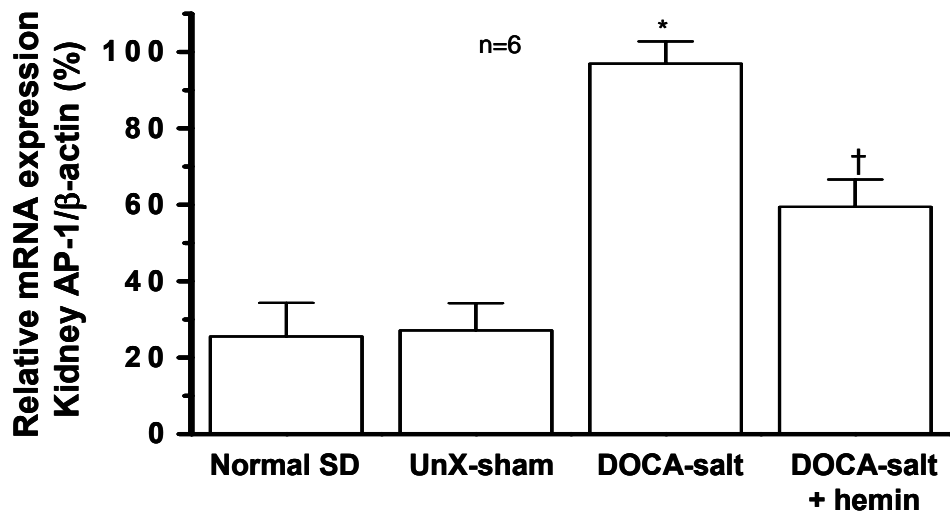
A**B**

Figure 4.11. Hemin therapy abates cardiac and renal AP-1 expression. Quantitative RT-PCR showing relative mRNA expression of AP-1 against GAPDH and β -actin, respectively. In DOCA-salt rat significant enhanced mRNA expression of AP-1 as compared to controls is shown. Both CrMP + hemin treatment also enhanced mRNA expression of AP-1 compared to all other groups. However, hemin regimen significantly attenuated mRNA expression of AP-1 in (A) cardiac and (B) renal tissue. This levels remained greatly higher than controls. ($\dagger p < 0.01$ vs. all other groups; $* p < 0.01$ vs. Normal SD, UnX-sham and DOCA-salt + hemin groups). AP-1 = activating protein-1

NF- κ B/GAPDH % n=6, p< 0.01). Although, hemin therapy abated mRNA expression of cardiac NF- κ B levels, it was not restored to the control levels. CrMP treatment abolished the effect of hemin and significantly enhanced level of mRNA expression of NF- κ B compared to all groups in DOCA-salt hypertensive rats (105.27 ± 7.215 NF- κ B/GAPDH % n=6, p< 0.01).

Analogically, in the normotensive controls, the basal kidney mRNA expression of NF- κ B levels were noted as follows, 31.5 ± 2.54 , NF- κ B/ β -actin % for normal SD and 34.1 ± 3.26 NF- κ B/ β -actin % for UnX-sham, n=6. In the DOCA-salt hypertensive rats enhanced activity of kidney NF- κ B was observed, however hemin therapy significantly alleviated but remained at levels significantly above controls (93.8 ± 2.82 vs. 59.6 ± 3.39 , NF- κ B/ β -actin %, n=6, p< 0.01) [**Fig. 4.10.B**].

The transcription factor AP-1 was quantified by real-time PCR in all the experimental groups. As illustrated in **Figure 4.11.A**, the cardiac tissue of DOCA-salt hypertensive rat (69.73 ± 8.231 AP-1/GAPDH %, n=6, p< 0.01) had a significantly higher AP-1 mRNA expression in relationship to those of controls. Hemin treatment significantly abrogated cardiac mRNA expression of AP-1 in the DOCA-salt hypertensive rats. However, cardiac mRNA expression of AP-1 in hemin-treated DOCA-salt rat was significantly higher levels than those of controls [43.12 ± 3.43 AP-1/GAPDH % vs. controls (normal SD, 15.37 ± 3.112 and UnX-sham, 17.35 ± 4.222 AP-1/GAPDH %) n=6, p< 0.01]. In contrast, cardiac mRNA expression of AP-1 in DOCA-salt + hemin + CrMP group was comparable with DOCA-salt group and significantly higher than controls and hemin treated DOCA-salt hypertensive rats (63.73 ± 5.324 AP-1/GAPDH %) n=6, p< 0.01). Similarly, kidney mRNA expression of AP-1

was reduced in hemin-treated DOCA-salt hypertensive rat (96.9 ± 5.83 , AP-1/ β -actin % to 59.4 ± 7.15 , AP-1/ β -actin %, $n=6$, $p < 0.01$). The reduction of mRNA expression of AP-1 was not restored to the level of normotensive controls (Normal SD, 25.6 ± 8.77 , and UnX-sham, 27.1 ± 7.11 , AP-1/ β -actin %, $n=6$, $p < 0.01$) [**Fig. 4.11.B**].

4.7. Assessment of hemin regimen on antioxidant defense systems (ferritin and SOD), and total antioxidant capacity

Plasma ferritin levels in control rats were 1.83 ± 0.401 $\mu\text{g/L}$ and 2.0 ± 0.365 $\mu\text{g/L}$ for normal SD and UnX-sham, respectively. However, in DOCA-salt hypertensive rats plasma ferritin levels decreased significantly as compared to the controls (0.92 ± 0.239 $\mu\text{g/L}$, $p < 0.01$). After hemin therapy, plasma ferritin levels were reestablished compared to control levels (2.5 ± 0.447 $\mu\text{g/L}$, $p < 0.01$) [**Fig. 4.12.A**].

DOCA-salt hypertensive rats were associated with significant decrease in the kidney SOD level (4.27 ± 0.827 U/ml, $n=6$, $p < 0.01$) with respect to controls (normal SD, 13.65 ± 0.966 U/ml and UnX-sham, 12.65 ± 1.026 U/ml, $n=6$). However, hemin therapy, restored the renal SOD levels in the DOCA-salt rat to control levels (12.37 ± 0.968 U/ml, $n=6$) [**Fig. 4.12.B**].

The total antioxidant capacity in cardiac tissue of controls (normal SD and UnX-sham) were comparable (0.97 ± 0.073 vs. 0.87 ± 0.088 mM of TEAC/mg protein, $n=6$). However, in the DOCA-salt alone (0.22 ± 0.009 mM of TEAC/mg protein, $n=6$, $p < 0.01$) and CrMP + hemin treated DOCA-salt (0.20 ± 0.051 mM of TEAC/mg protein, $n=6$, $p < 0.01$) hypertensive rats, significantly decreased total antioxidant capacity compared to controls. Hemin-treatment in DOCA-salt hypertensive rats revived the

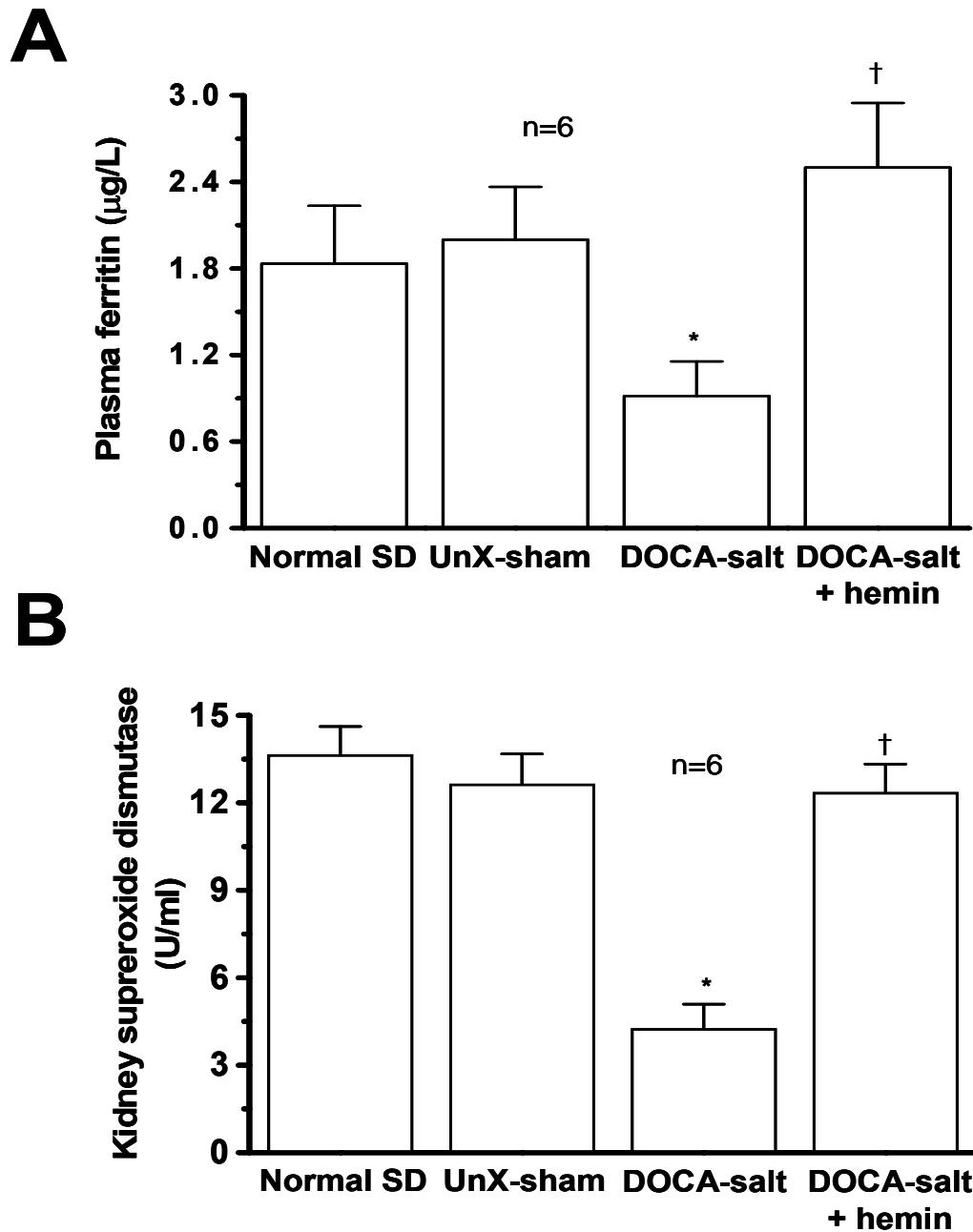


Figure 4.12. Hemin treatment restores plasma ferritin and kidney SOD levels. (A) Plasma ferritin in DOCA-salt rat was downregulated as compared to controls. Hemin regimen significantly augmented plasma ferritin levels in DOCA-salt rats, which remained comparable to controls. **(B)** Increased oxidative stress in the DOCA salt rat reduced relative SOD antioxidant defense system; however, hemin therapy enhanced its activity and was not significantly different from controls. (* $p < 0.01$ vs. all other groups; † $p < 0.01$ vs. DOCA-salt). SOD = Superoxide dismutase, a metalloenzyme scavenges superoxide radicals

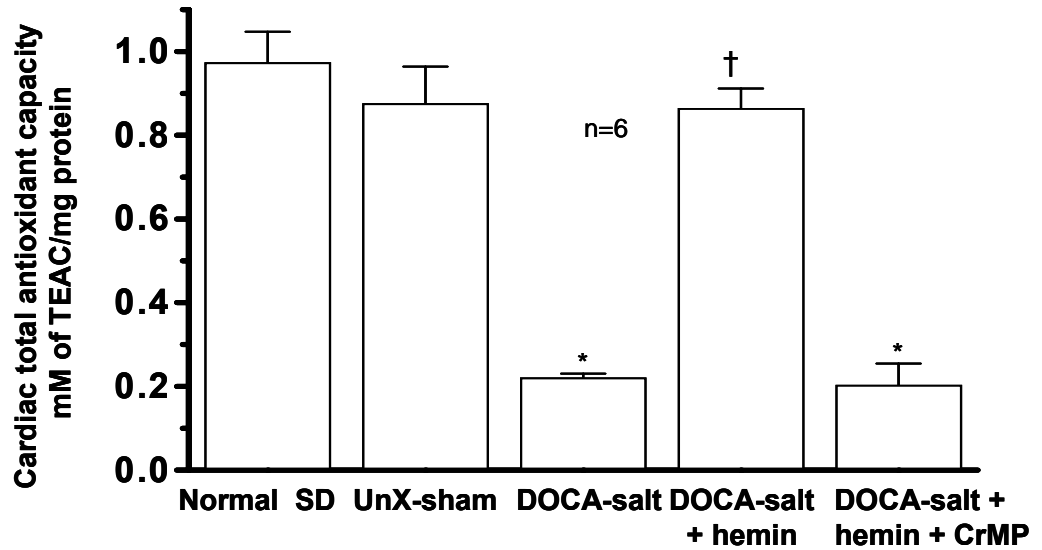
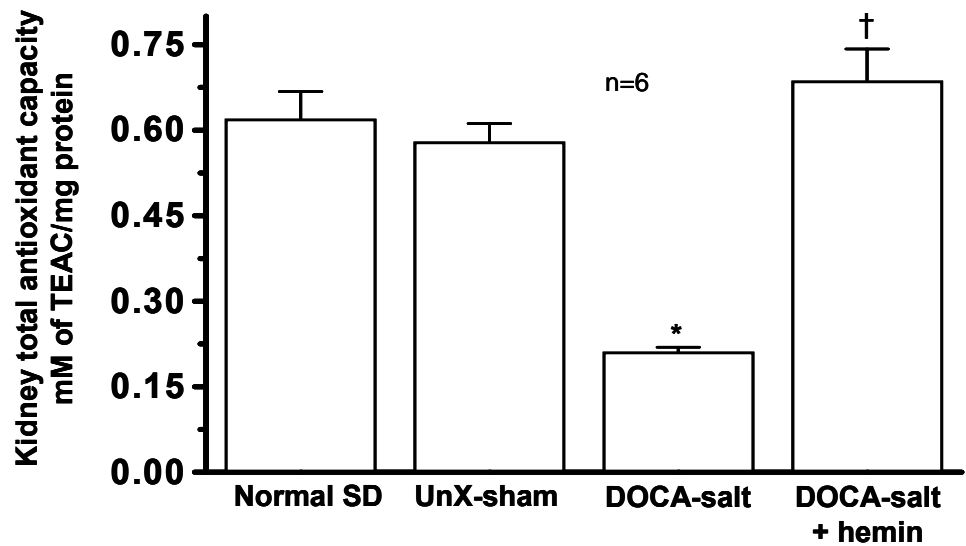
A**B**

Figure 4.13. Hemin enhances total antioxidant capacity in heart and kidney. Hypertension in DOCA-salt rat downregulated total antioxidant capacity of (A) heart and (B) kidney as compared with normotensive controls. Hemin, regimen significantly increased total antioxidant capacity compared with untreated DOA-salt and restored to the level of normotensive controls. (* $p < 0.01$ vs. normal SD, UnX-sham and DOCA-salt + hemin; † $p < 0.01$ vs. DOCA-salt and DOCA-salt + hemin + CrMP). TEAC = Trolox Equivalent Antioxidant Capacity

cardiac total antioxidant capacity (0.86 ± 0.047 mM of TEAC/mg protein, $n=6$, $p < 0.01$ vs. untreated) [Fig. 4.13.A]. Similarly, kidney total antioxidant capacity was restored by hemin therapy (from DOCA-salt, 0.21 ± 0.008 mM of TEAC/mg protein to 0.69 ± 0.055 mM of TEAC/mg protein, $n=6$, $p < 0.01$). Kidney total antioxidant capacity in hemin-treated DOCA-salt rats was comparable to controls (0.62 ± 0.048 vs. 0.57 ± 0.032 mM of TEAC/mg protein, $n=6$) [Fig. 4.13.B].

4.8. Effect of hemin therapy on TGF- β in the left ventricle and kidney

The remodeling of myocardium revealed the presence of TGF- β immunoreactivity, which was visualized as brown to reddish granules in myocardial tissue of the left ventricle [Fig. 4.14.A]. In the DOCA-salt hypertensive rats, a marked increase in the intensity of TGF- β immunostaining was observed in the lesions consisting of myocardial scarring, interstitial fibrosis and inflammatory lesions as compared to the UnX-sham ($p < 0.01$) [Fig. 4.14.A(ii)]. The intensity of the TGF- β immunoreaction was reduced in the left ventricle of hemin-treated DOCA-salt hypertensive rats compared with DOCA-salt treatment alone ($p < 0.01$) [Fig. 4.14.B]. However, the reduction of TGF- β staining intensity did not reach that in normotensive controls [Fig. 4.14.B].

Representative photomicrographs of different groups showing different intensities of kidney tissue TGF- β immunoperoxidase staining are shown in Figure 4.15.A (i-iii). Positive staining for TGF- β was most prominently observed within renal tubular epithelium (brown to reddish granules) giving a typical mosaic appearance [Fig. 4.15.A (ii)]. There was occasional mild staining of the interstitium; however, both

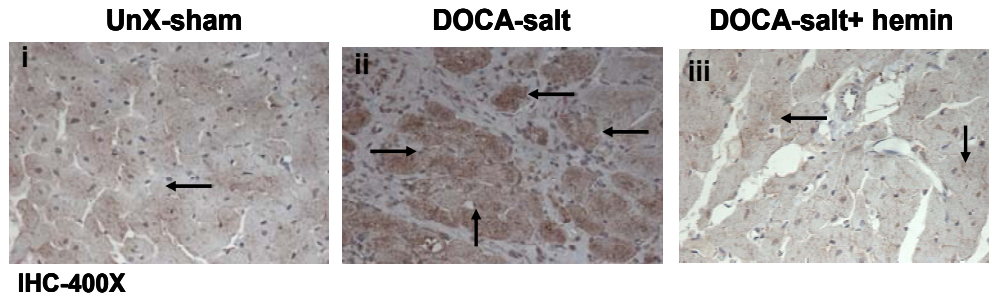
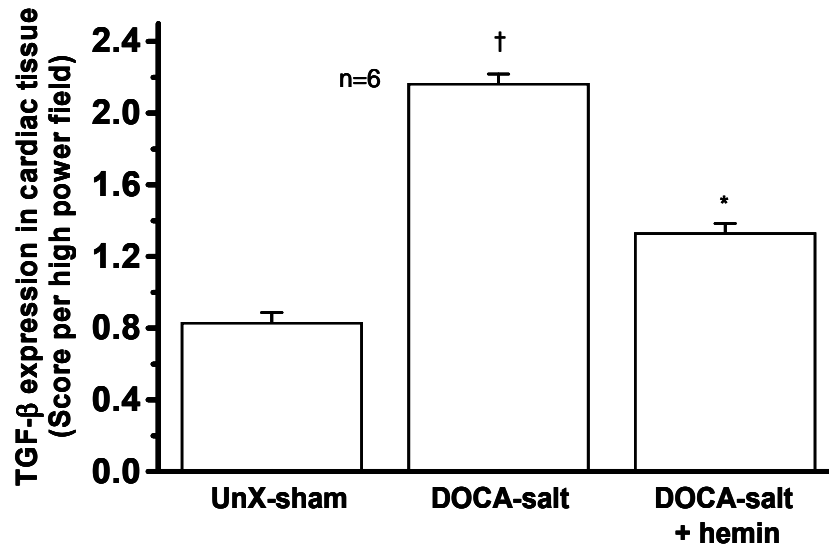
A**TGF- β expression in cardiac tissue****B**

Figure 4.14. Effect of hemin therapy on TGF- β expression in cardiac tissue. (A) Representative photomicrographs from different groups showing different intensity of TGF- β . Reddish brown granules of TGF- β (arrow) in the area consisting of myocardial scarring, interstitial fibrosis and inflammatory lesions. Immunohistochemistry magnification-400X. **(B)** TGF- β expression was assessed semi-quantitatively using a 0 to 3 scale (0- no staining, 1- very little stained area, 2- moderately stained area, 3- severely /all stained area). Fifty different fields in high power (per section) were scored and averaged per group. Cardiac tissue from a DOCA-salt treated rat shows increased immunostaining expression of TGF- β (**ii**) compared to UnX-sham (**i**), while hemin downregulated the TGF- β expression (**iii**). (* $p < 0.01$; † $p < 0.01$ vs. all other groups). TGF- β = transforming growth factor beta

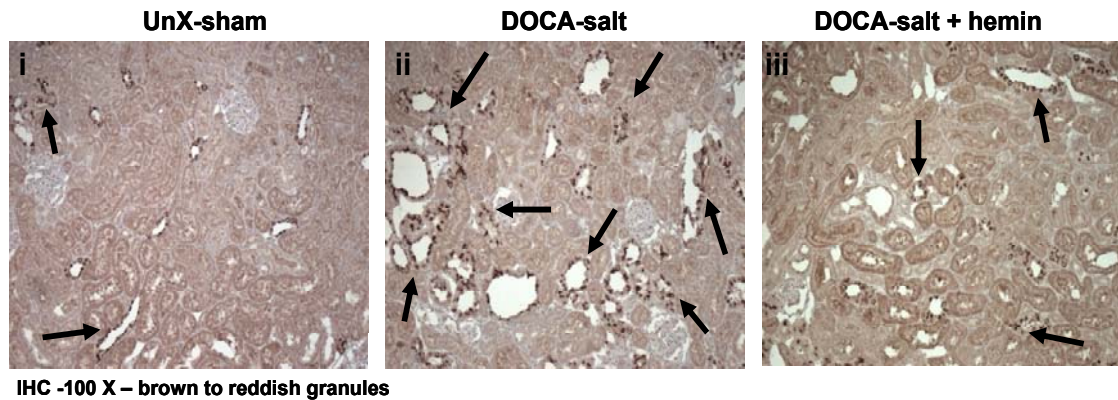
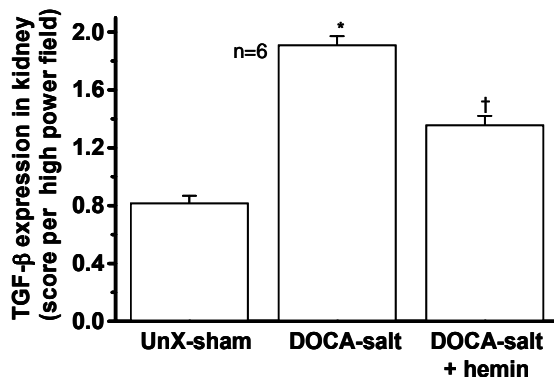
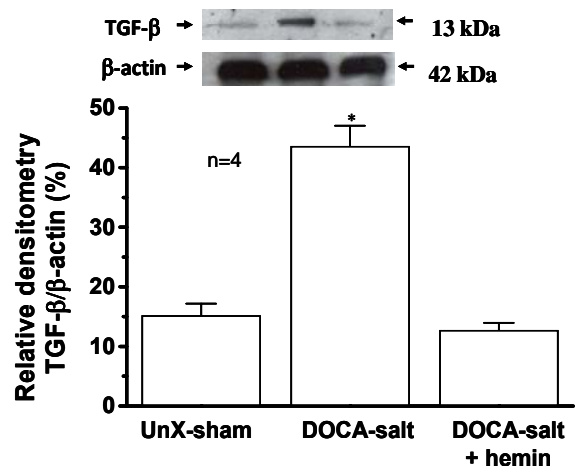
A**TGF- β expression in kidney tissue****B****C**

Figure 4.15. Hemin therapy attenuates TGF- β in the kidney. (A) Representative photomicrographs of different groups showing different intensity of reddish brown granules of TGF- β (arrow) in both proximal and distal tubular epithelium and interstitial spaces. Immunohistochemistry magnification-100X. (B) TGF- β expression was assessed semi-quantitatively using 0 to 3 scale (0- no staining, 1- very little stained area, 2- moderately stained area, 3- severely / all stained area). Fifty different fields in high power (per section) were scored and averaged per group. Kidney tissue from DOCA-salt rat shows increased immunostaining expression of TGF- β (ii) as compared to UnX-sham (i), while hemin downregulated the TGF- β expression (iii). (C) Representative western blot for all groups, and densitometry analysis of TGF- β expression against β -actin revealed significant upregulation of TGF- β expression in DOCA-salt hypertensive rats. Hemin therapy, significantly abated TGF- β expression in the DOCA-salt rats. (* $p < 0.01$; † $p < 0.01$ vs. all other groups).

proximal and distal tubules were stained abundantly with TGF- β especially in DOCA-salt hypertensive rats. TGF- β staining was abundant within tubules showing vacuolar degeneration compared to normal appearing tubules. The combined semi-quantitative score of TGF- β staining for three experimental groups are shown in **Figure 4.15.B**. The localization of TGF- β was higher in DOCA-salt hypertensive rats as compared to both the UnX-sham and hemin-treated [**Fig. 4.15.A&B**]. Renal TGF- β intensity from the DOCA-salt hypertensive rats was significantly abrogated after hemin therapy [**Fig. 4.15.B**].

The localization of TGF- β was further quantified by Western immunoblot method. The expression of TGF- β was assessed by utilizing relative densitometry against β -actin in the kidney. Interesting, the expression of TGF- β was increased by 3-fold in the kidney of DOCA-salt hypertensive rats with respect to UnX-sham control. This indicates abundant activity of TGF- β in the renal tissue of DOCA-salt hypertensive rats. Hemin administration to DOCA-salt hypertensive rats significantly abated TGF- β protein expression in the kidney with respect to untreated DOCA-salt hypertensive rats ($p < 0.01$) [**Fig. 4.15.C**].

4.9. Effect of hemin treatment on ECM proteins

4.9.1. Fibronectin expression and levels in the kidney

Renal fibrosis was verified by immunostaining of kidney sections. Further quantification of fibronectin expression was done by Western immunoblot method. **Figure 16A** shows representative images of fibronectin immunostaining. Positive staining was found in connective tissue of blood vessels. Very scanty staining was found

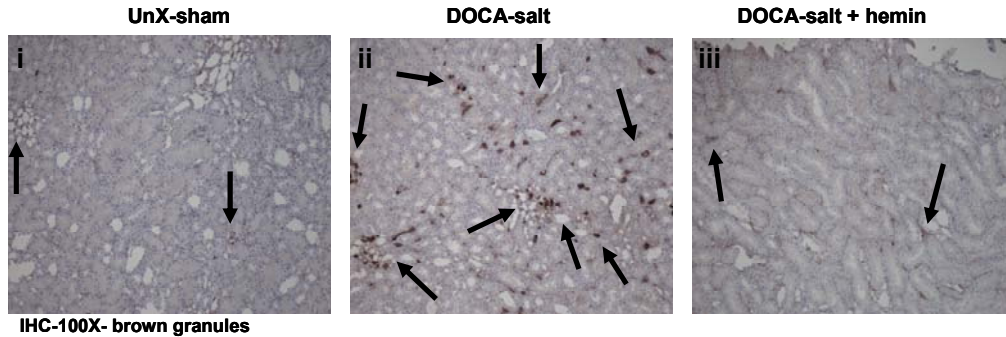
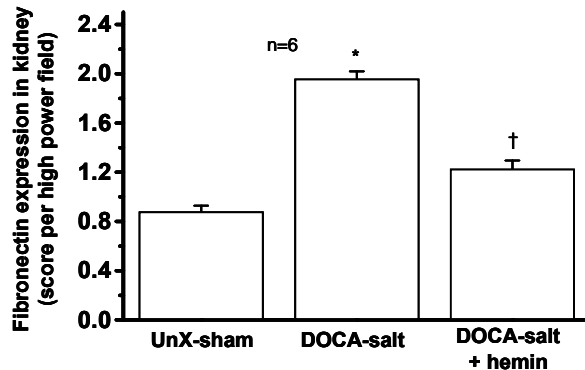
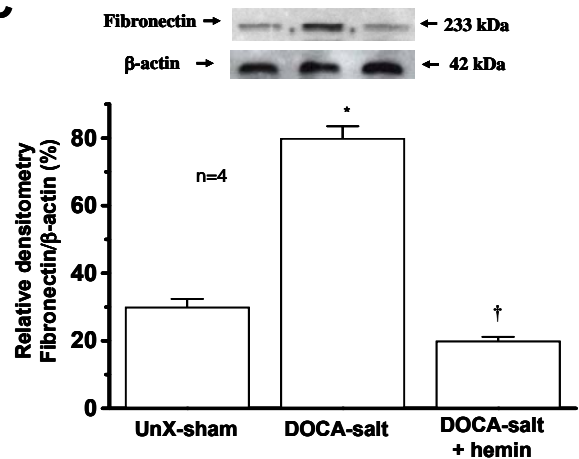
A**Fibronectin expression in kidney tissue****B****C**

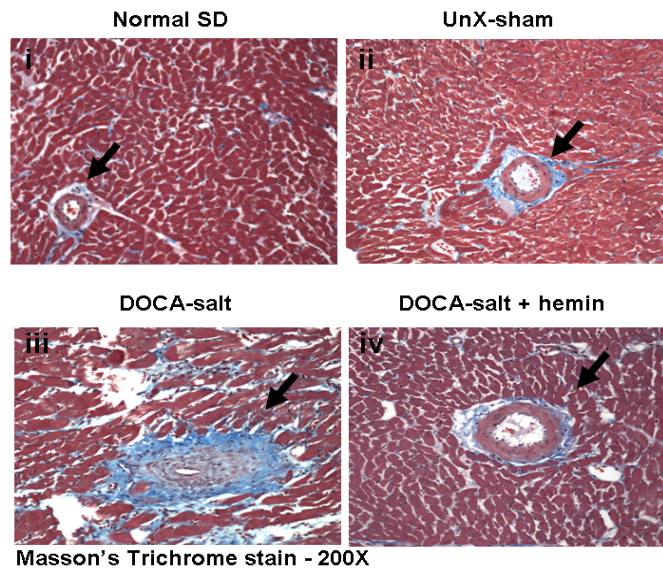
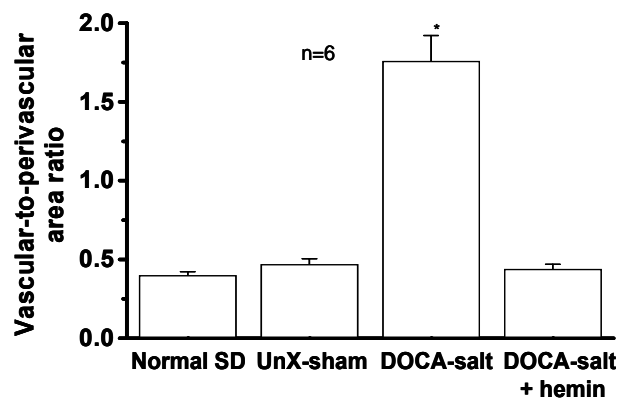
Figure 4.16. Hemin therapy prevents mobilization of fibronectin in the kidney. (A) Representative photomicrographs showing brown staining (arrow) of fibronectin in the interstitial spaces, having different intensity for different groups. Immunohistochemistry magnification-100X. (B) Fibronectin expression was assessed semi-quantitatively using a 0 to 3 scale (0- no staining, 1- very little stained area, 2- moderately stained area, 3- severely /all stained area). Fifty different areas per high power field per section were scored and averaged per group. Kidney tissue from DOCA-salt rat showed increased immunostaining of fibronectin (ii) as compared to UnX-sham (i), while hemin downregulated the fibronectin expression (iii). (C) Representative western blot and densitometry analysis of fibronectin expression against β -actin. In DOCA-salt hypertensive rat significantly higher levels of fibronectin was noted, however hemin therapy abrogated fibronectin expression. (* $p < 0.01$; † $p < 0.01$ vs. all other groups).

in the interstitium in the UnX-sham control [Fig. 4.16.A(i)]. DOCA-salt hypertensive rats showed enhanced renal interstitial fibrosis leading to increased staining intensity of fibronectin in the interstitial spaces. The fibronectin was detected in the form of brown granules forming patches in the tubular interstitial spaces [Fig. 4.16A(ii)].

Hemin therapy significantly reduced fibronectin accumulation in the DOCA-salt hypertensive rats ($p < 0.01$) [Fig. 4.16.B], however, fibronectin expression remained significantly higher than controls, when observed by semi-quantitative method [Fig. 4.16.B]. Western immunoblot analysis showed that hemin therapy significantly reduced relative fibronectin levels normalized by β -actin in the kidney of DOCA-salt hypertensive rats compared with untreated rats (80 ± 3.5 to 20 ± 1.2 , fibronectin/ β -actin %, $n=4$, $p < 0.01$) [Fig. 4.16.C].

4.9.2. Perivascular collagen depositions in the left ventricle

Left ventricular fibrosis was evaluated by using Masson's Trichrome collagen blue stain. Cardiomyocytes stained dark reddish, and ECM, such as collagen, stained blue. UnX-sham rat sections appeared morphologically normal with scanty ECM in the intermuscular spaces. DOCA-salt rats showed areas of focal patchy fibrosis as well as fibrosis around the perivascular regions, while hemin therapy attenuated the deposition of fibrosis, as observed by reduced focal extracellular and perivascular blue staining [Fig. 4.17.A]. Assessments of perivascular fibrosis were done by calculating the ratio of the fibrotic area surrounding the vessel to the total vessel area. In the DOCA-salt hypertensive rats extensive increased perivascular fibrosis indicative of reactive fibrosis in the cardiac tissue was observed compared to control rats [1.76 ± 0.162 vs. (normal SD, 0.40 ± 0.022 and UnX-sham, 0.47 ± 0.035), $n=6$, $p < 0.01$]. Interestingly, hemin

A**Perivascular fibrosis in cardiac tissue****B****Figure 4.17. Effect of hemin on perivascular fibrosis in the cardiac tissue section.**

(A) Representative photomicrographs showing blue stained collagen (arrows) around vessels of left ventricle from different groups (Masson's Trichrome stain, magnification-200X). (B) Perivascular fibrosis was assessed by calculating the ratio of the fibrosis area surrounding the vessel to the total vessel area and averaged per groups. In the DOCA-salt rats, intense areas of perivascular fibrosis were observed and the hemin regimen significantly reduced perivascular fibrosis to levels comparable to controls. (* $p < 0.01$ vs. all other groups).

(All vessels from cardiac section were imaged at 200X and using NIS-element BR-Q imaging. Total areas of vessel and perivascular fibrosis were measured using an area measurement tool and area was represented with the unit μm^2).

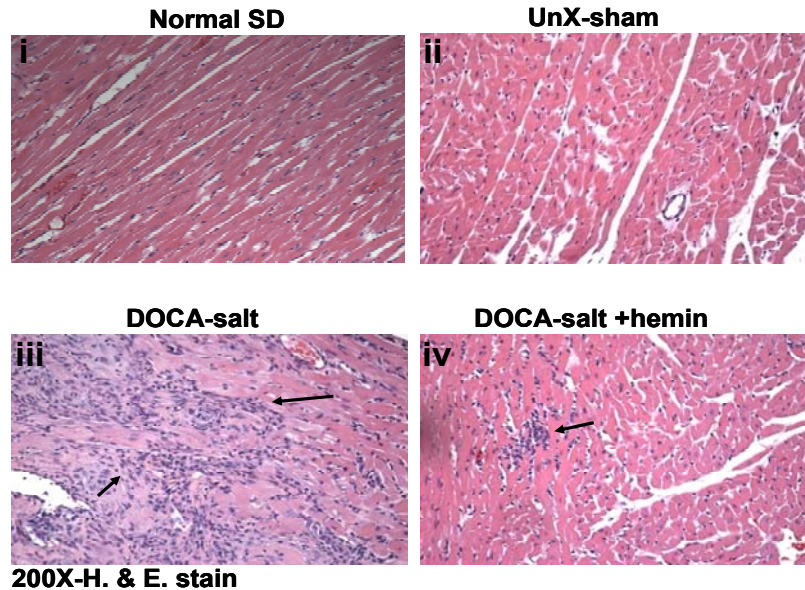
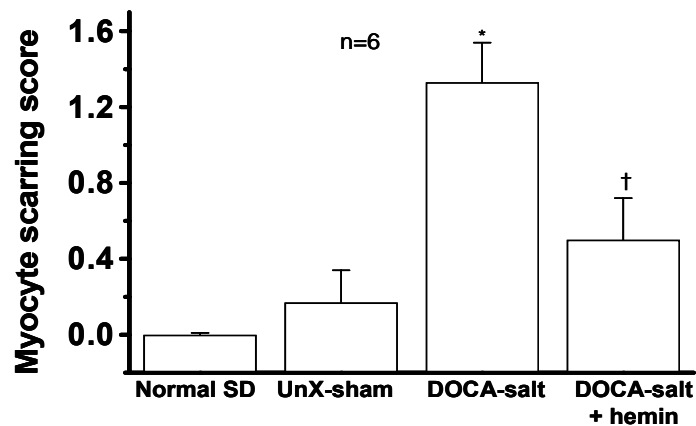
A**Myocytes scarring in cardiac tissue****B**

Figure 4.18. Hemin attenuates left ventricular myocytes scarring. (A) Representative photomicrographs (H. & E. stain, magnification-200X) from normal SD (i) and UnX-sham (ii) group showing normal cardiac myocytes, whereas cardiac myocytes from DOCA-salt rats (iii) show distortion, scarring and infiltration of inflammatory cells in the lesion (arrow). Hemin therapy significantly reduced scarring and inflammatory cell infiltration (iv) as compared to DOCA-salt rats. (B) Semi-quantitative analysis of myocyte scarring was done on 0-2 scale (0- normal myocytes, 1- mild scarred myocytes and 2- moderate to severe myocyte scarring). DOCA-salt rats showed a significantly higher myocyte scarring score as compared to control. Hemin prevented the development of lesions in the DOCA-salt rats. (* $p < 0.01$ vs. all other groups; † $p < 0.01$ vs. Normal SD and DOCA-salt groups).

therapy markedly reduced perivascular fibrosis in DOCA-salt hypertensive rats (0.44 ± 0.029 , $n=6$, $p < 0.01$) comparable to control levels [**Fig. 4.17.B**].

4.10. Assessment of hemin therapy on morphological changes in the left ventricle

4.10.1. Left ventricular myocyte scarring

The left ventricle section of DOCA-salt hypertensive rats showed reparative types of cardiac myocyte scarring. It also showed marked inflammatory cell infiltration in the scar tissue of focal patchy lesions in the interstitium [**Fig. 4.18.A(iii)**] compared with the normotensive controls. However, very few sites of scarring and inflammatory cells were noted in the interstitial spaces in the cardiac section of hemin-treated rats [**Fig. 4.18.A(iv)**]. The myocardial lesions were scored by a semi-quantitative method on a 0-2 scale. It was found that in normotensive controls the score for myocardial lesions was almost nil (normal SD, 0.0 ± 0.0 and UnX-sham, 0.17 ± 0.17 , semi-quantitative score, $n=6$) indicating that uninephrectomy did not affect cardiac tissue even after 4 weeks of surgery [**Fig. 4.18.B**]. However, uninephrectomy, DOCA and NaCl-salt caused severe myocardial lesions such as scarring, fibrosis and infiltration of inflammatory cells compared to those of controls (1.3 ± 0.22 semi-quantitative score, $n=6$, $p < 0.05$). Interestingly, hemin therapy significantly abated the myocardial scarring lesions in DOCA-salt hypertensive rats (0.5 ± 0.22 semi-quantitative score, $n=6$, $p < 0.05$) to the level seen in UnX-sham. However, it remained significantly higher level than that of the normal SD rat ($p < 0.05$) [**Fig. 4.18.B**].

4.10.2. Left ventricular myocyte hypertrophy

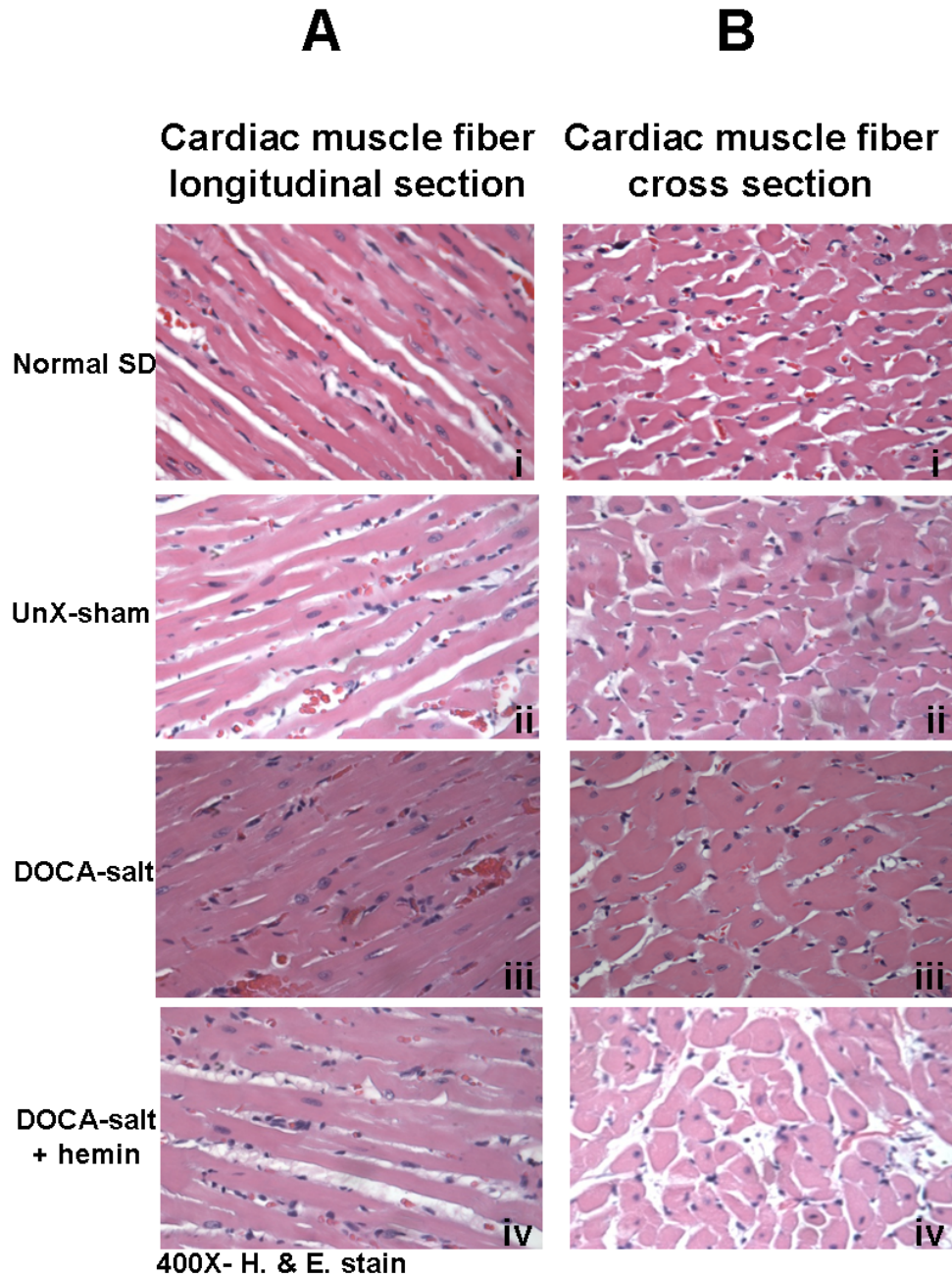


Figure 4.19. Representative photomicrographs of left ventricle myocytes from different groups with H. & E. stain, magnification-400X (A) Longitudinal and (B) Cross / transverse sections. Both Normal SD (i) and UnX-sham (ii) groups showing thin myocardial fibers with normal intermyocardial space. DOCA-salt group (iii) showed thick muscle fiber with reduced intermyocardial space. Hemin regimen in the DOCA-salt rat showed normalized muscle fiber and intermyocardial space (iv).

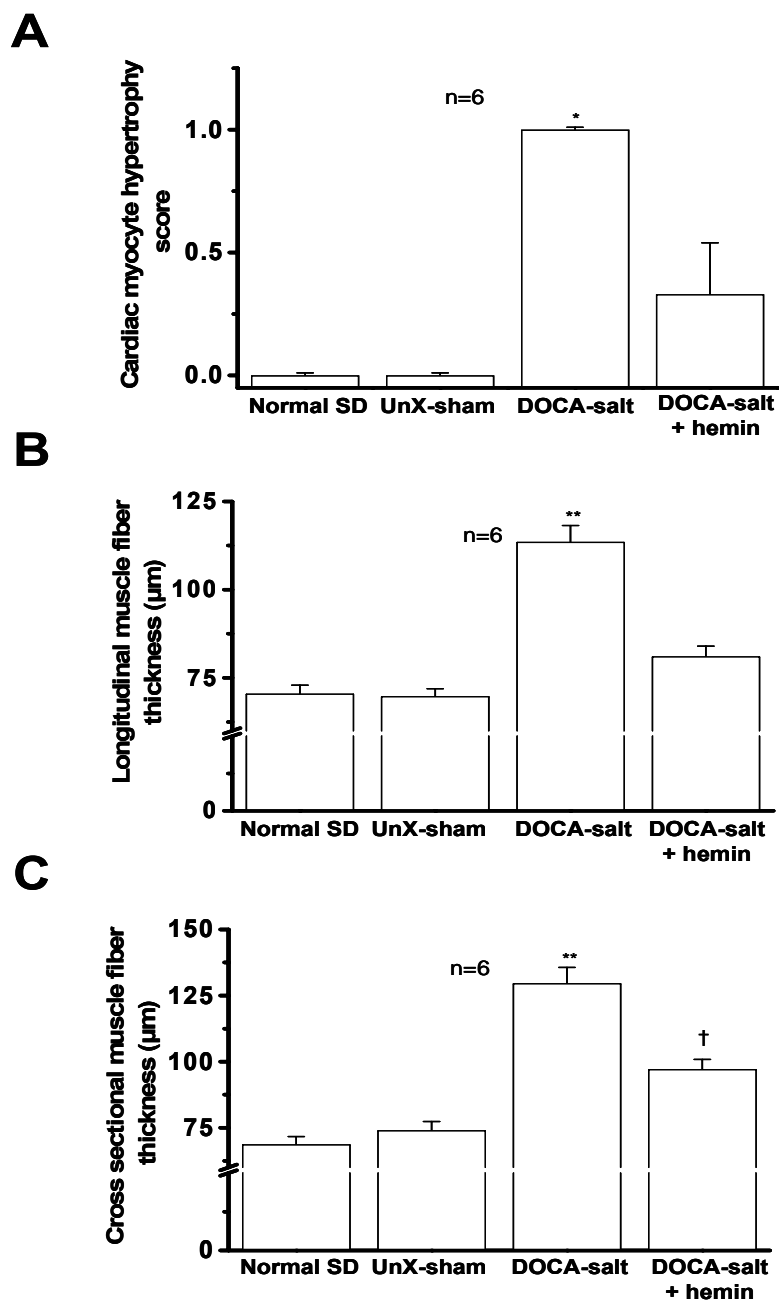


Figure 4.20. Hemin therapy attenuates cardiac myocyte hypertrophy. (A) Semi-quantitative scoring of cardiac myocyte hypertrophy (0- normal myocytes, 1- myocyte hypertrophy). The DOCA-salt rat showed significant myocyte hypertrophy, and hemin regimen prevented development of myocyte hypertrophy. (B) Longitudinal muscle fibers in DOCA-salt group were thick compared to Normal SD and UnX-sham groups. Hemin treatment reduced the muscle fiber thickness. (C) Diameter of cross / transverse sections of myocytes in DOCA-salt hypertensive rats were significantly higher as compared to normotensive controls. Hemin regimen normalized myocyte diameter. (* $p < 0.05$; ** $p < 0.01$ vs. all other groups; † $p < 0.01$ vs. normotensive controls). (Cardiac myocyte thicknesses were measured using NIS-elements BR-Q image analysis system at 400X-magnification).

Cardiac myocyte hypertrophy was assessed either by semi-quantitative scoring method or morphometric analysis of cardiomyocytes in left ventricular sections of different experimental groups by using image analysis techniques. In the DOCA-salt hypertensive rats, enlarged cardiomyocytes with increscent nuclei were evident, as compared to normal cardiomyocytes in the controls (1.0 ± 0.00 semi-quantitative score, $n=6$, $p < 0.05$) [Fig. 4.19.A&B and Fig. 4.20A]. Interesting, hemin-treated DOCA-salt hypertensive rats showed significant downregulation of cardiomyocyte thickness (0.33 ± 0.21 semi-quantitative score, $n=6$, $p < 0.05$) rats [Fig. 4.20.A].

Furthermore, consistent with whole heart and left ventricular hypertrophy data, DOCA-salt hypertensive rat myocytes were hypertrophied compared with both sham-operated and normal SD myocytes. There was a 62 and 82 % increase in the cardiomyocyte cell thickness for longitudinal and cross sections respectively, in DOCA-hypertensive as compared to the same area of the ventricle in normotensive control rats ($p < 0.01$) [Fig. 4.20.B&C]. Interestingly, the hemin regimen reduced cardiomyocyte cell thickness by 29 and 25 % for longitudinal and cross sectional measurement respectively, compared with only DOCA-salt treated rats [Fig. 4.20.B&C].

4.10.3. Morphometry of small coronary arteries in the left ventricle

Small coronary arterial wall thickness, coronary arterial media-to-lumen ratio and wall area were analyzed by measuring inner and outer diameters of all intermyocardial coronary arteries from left ventricular sections in all experimental groups [Fig. 4.21.A]. The small coronary arterial wall thickness in the control rats were, normal SD, $25.76 \pm 2.824 \mu\text{m}$ and UnX-sham, $30.59 \pm 4.515 \mu\text{m}$, ($n=6$), In the

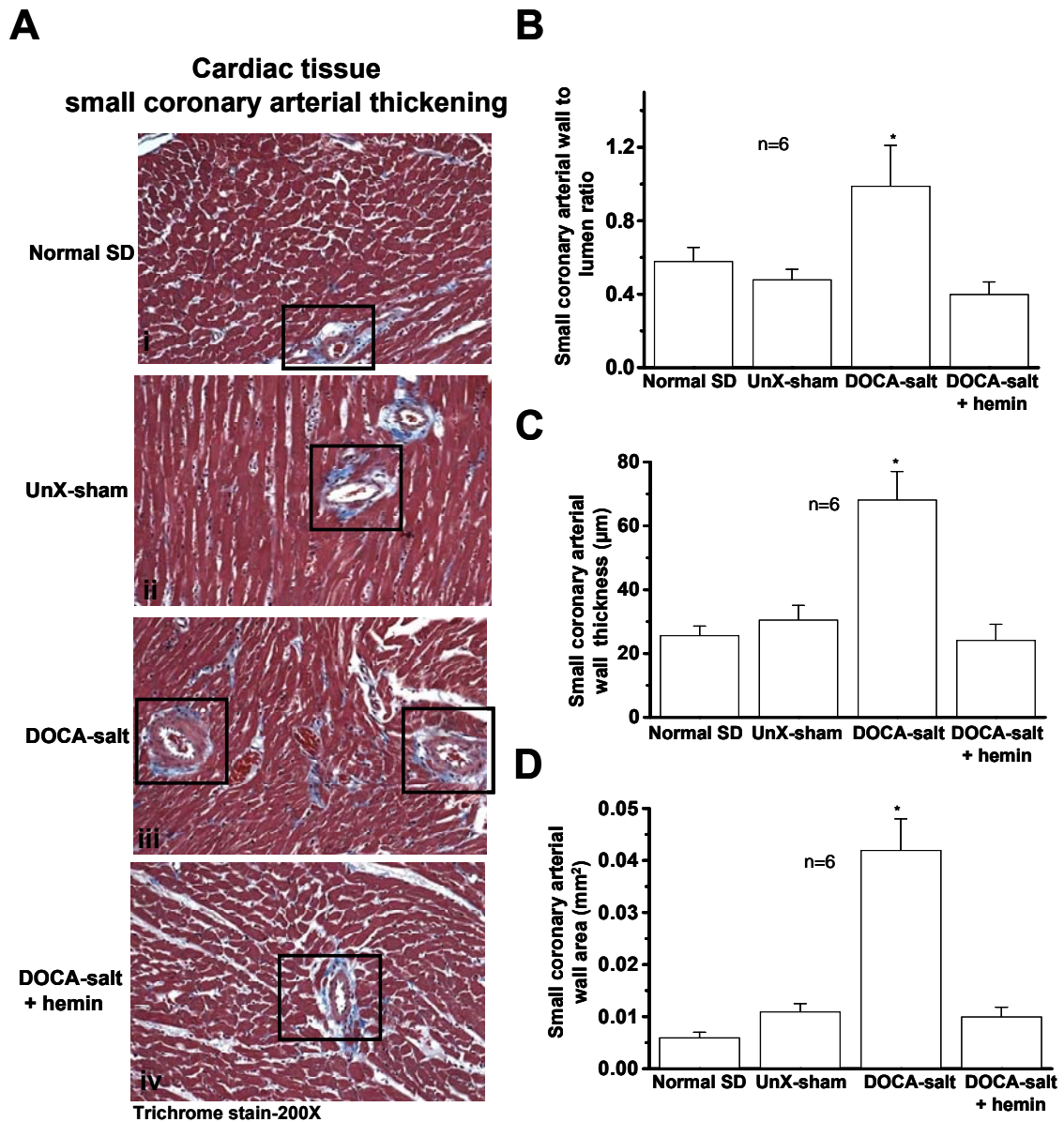


Figure 4.21. Effect of hemin on small coronary arterial remodeling in cardiac tissue. (A) Representative photomicrographs showing small coronary arteries (arrows) in cardiac tissue with H. & E. stain, magnification-200X. Small coronary arteries from DOCA-salt rat showed a significant increase in small coronary arteriolar wall-to-lumen ratio (B), small coronary arterial wall thickness (C) and small coronary arterial wall area (D). Hemin regimen downregulated all these parameters in DOCA-salt rats to levels comparable with controls. (* $p < 0.01$ vs. all other groups). (Small coronary arteries wall thickness calculated by assessing inner and outer diameter of coronary arteries using NIS-elements BR-Q image analysis system at 200X-magnification).

DOCA-salt hypertensive rat wall thickness was significantly increased to 68.23 ± 8.794 μm , $n=6$, $p < 0.01$. Interestingly, hemin-treated DOCA-salt hypertensive rats showed significant reduction of the small coronary arterial wall thickness (24.20 ± 4.981 μm , $n=6$, $p < 0.01$) compared to DOCA-salt treatment alone [Fig. 4.21.C]. Similarly, hemin-treatment normalized other indices of small coronary arterial remodeling, such as the small coronary arterial wall-to-lumen ratio (0.99 ± 0.221 to 0.4 ± 0.067 , $n=6$, $p < 0.01$) [Fig. 4.21.B] and the small coronary arterial wall area (0.042 ± 0.006 mm^2 to 0.01 ± 0.002 mm^2 , $n=6$, $p < 0.01$) [Fig. 4.21.D] to control levels.

4.11. Effect of hemin therapy on DOCA-salt-induced renal injury

4.11.1. Renal morphological lesions

In the present study, all renal pathological lesions such as glomerular hypertrophy, sclerotic and damaged glomeruli, mononuclear cell infiltration, tubular dilation, tubular cast formation and small renal arterial wall thickening were observed in the DOCA-salt hypertensive rats [Fig. 4.22, 4.24, 4.25, & 4.26] [182]. These morphological lesions were graded on a 0-3 scale using semi-quantitative method and without knowing experimental groups [182]. Interestingly, hemin therapy, significantly reduced pathological structural alteration that were noted in the DOCA-salt rats (2.09 ± 0.19 to 0.94 ± 0.08 semi-quantitative score, $n=6$, $p < 0.01$). However, score in hemin-treated rats was not reduced to control levels (normal SD, 0.15 ± 0.02 and UnX-sham, 0.38 ± 0.1 semi-quantitative score, $n=6$, $p < 0.05$) [Fig. 4.23.A]. The majority of these finding regarding morphological lesions were further confirmed by quantifying the glomerular diameter, counting damaged sclerotic glomeruli and tubular

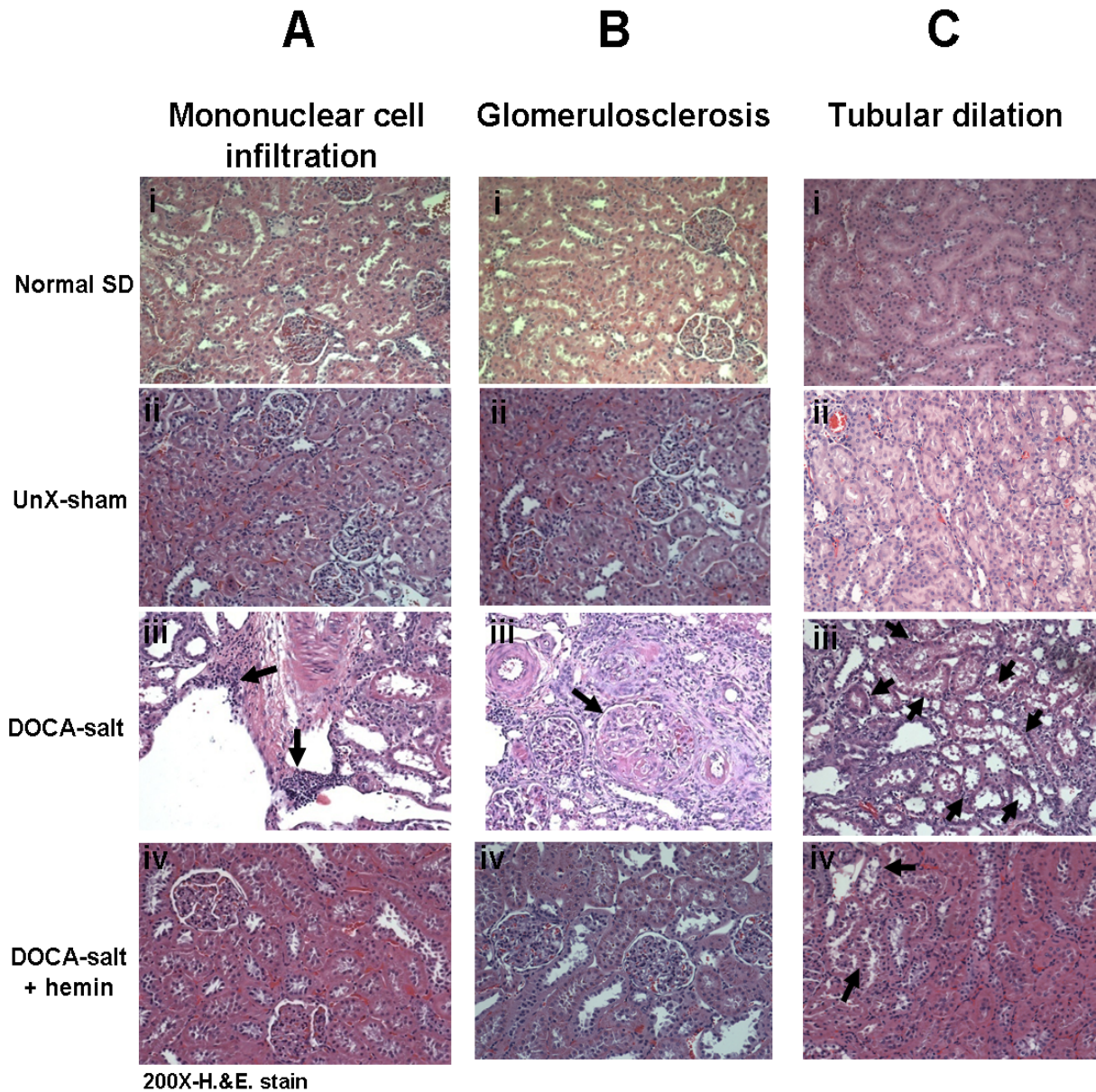


Figure 4.22. Hemin abrogates renal morphological lesions such as mononuclear cell infiltration, glomerulosclerosis and tubular dilation. Representative photomicrographs showing (A) infiltration of mononuclear cell, (B) sclerotic glomeruli and (C) tubular dilations in the kidney section of DOCA-salt rat (arrow). However, hemin-treated kidney sections of DOCA-salt rat exhibited reduction in the morphological lesions. Control kidney sections showed normal structural morphology. Magnification-200X, H. & E. stain.

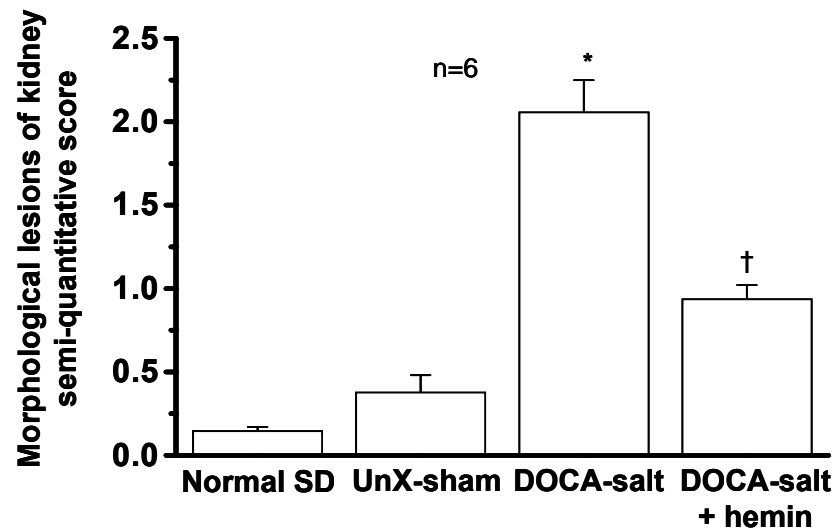
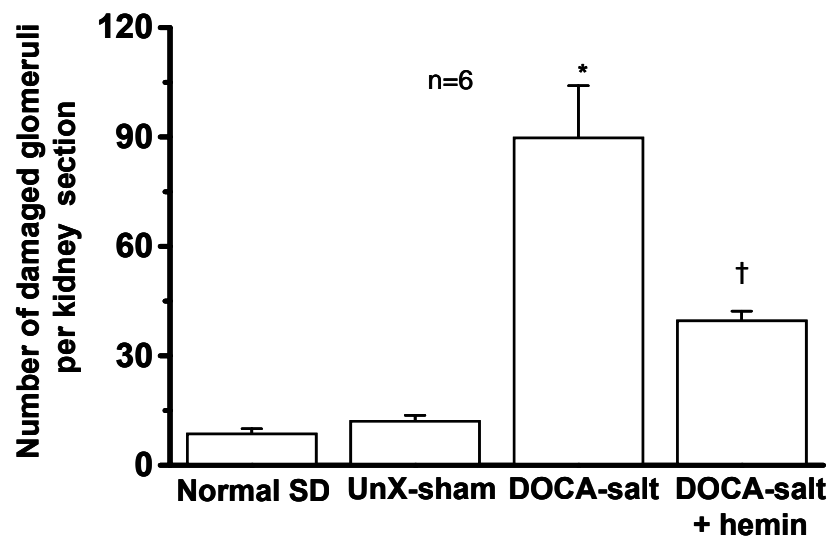
A**B**

Figure 4.23. Hemin reduces morphological lesions, and damaged and sclerotic glomeruli numbers in the kidney. (A) Semi-quantitative scoring of renal morphological lesions showed higher lesions in DOCA-salt rat, whereas in the normotensive controls renal morphology was normal. Hemin significantly reduced the lesions in the DOCA-salt rat. (B) Microscopically, quantification of damaged and sclerotic glomeruli was done in the kidney sections. DOCA-salt rats showed severe increased numbers of damaged and sclerotic glomeruli per sections. Hemin therapy significantly lowered numbers of damaged and sclerotic glomeruli. (*p < 0.01; †p < 0.01 vs. all other groups).

casts per section, and morphometric analysis of small renal arteriolar alterations in kidney tissue. These morphological lesions signify the extents of renal damages in the DOCA-salt hypertensive rats, which were present in the study. In the DOCA-salt hypertensive rat, hemin therapy attenuated pathological lesions in the kidney.

4.11.2. Glomerular hypertrophy and sclerotic/damaged glomeruli in the kidney

Renal damage was assessed by measuring glomerular hypertrophy parameter, where 30 glomeruli were randomly selected per section (180 glomeruli per group) [182]. A horizontal line measurement tool from image analysis was used to measure the diameters of glomeruli irrespective of shape. Our data demonstrated that with constant renal hypertrophy, DOCA-salt hypertensive rat glomeruli were hypertrophied compared with normotensive control glomeruli [Fig. 4.24.A]. In DOCA-salt hypertensive rat, glomerular size was significantly increased by 58.7 % as compared with the same area of renal tissue from normotensive control rats (average UnX-sham and normal SD) ($p < 0.01$) [Fig. 4.24.B]. Interestingly, hemin treatment significantly reduced glomerular hypertrophy by 22.3 % with respect to DOCA-salt rats ($p < 0.01$). The reduction of glomerular diameter did not equal control levels ($p < 0.01$) [Fig. 4.24.B].

Alongside glomerular hypertrophy, the DOCA-salt hypertensive rat showed severe glomerular injury, which was characterized as necrotic and sclerotic glomeruli having typical fibrinoid lesions in the glomerular tuft [Fig. 4.22.B]. These typical damaged and sclerotic glomeruli were counted microscopically in the kidney sections of all groups. The basal number of damaged glomeruli in controls, normal SD and UnX-sham were 9 ± 1.2 and 2 ± 1.3 , $n=6$, respectively and were not significantly different [Fig. 4.23.B]. However, in the DOCA-salt hypertensive rat numbers of damaged and sclerotic glomeruli were robustly increased to 90 ± 14.1 and were

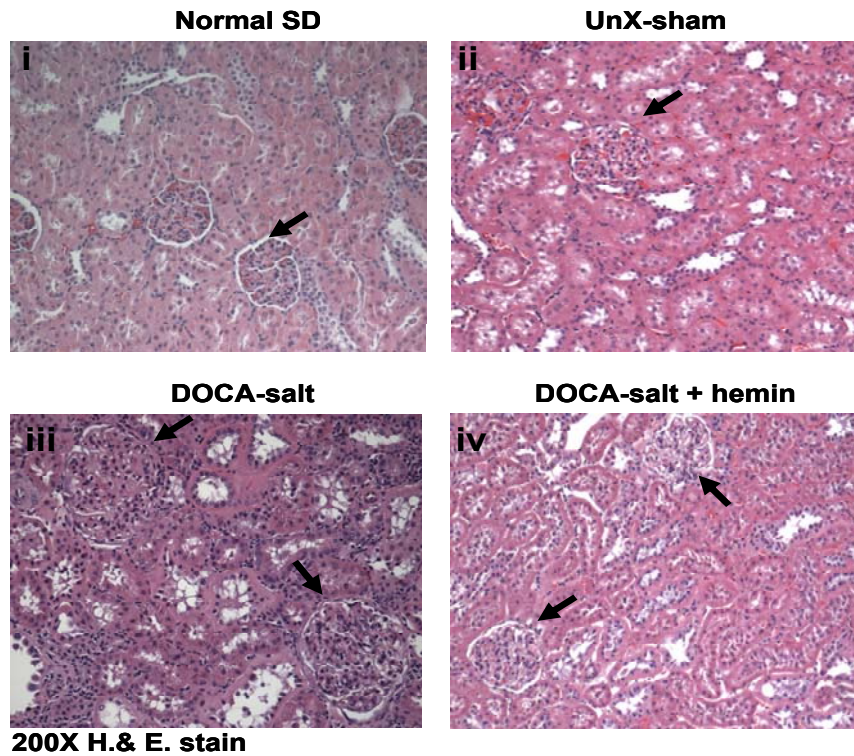
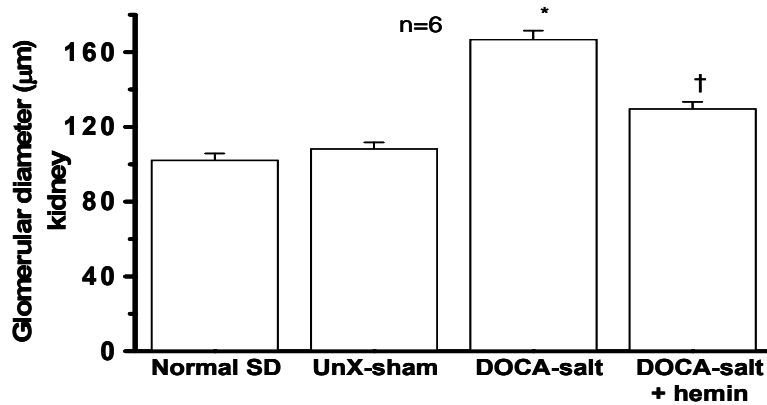
A**Glomerular hypertrophy****B**

Figure 4.24. Hemin attenuates glomerular hypertrophy. (A) Representative photomicrographs showing glomeruli per sections of kidney (arrow), H. & E. stain, magnification-200X. (B) Randomly thirty glomeruli were selected from cortex region of kidney section and measurement of glomerular diameter were done by using horizontal line scale of NIS-element BR-Q imaging system at 200X-magnification. In normotensive controls, glomerular diameters were similar to each other. In DOCA-salt hypertensive rat significant increased glomeruli diameter was noted. Hemin therapy attenuated glomerular diameter significantly. (* $p < 0.01$; † $p < 0.01$ vs. all other groups).

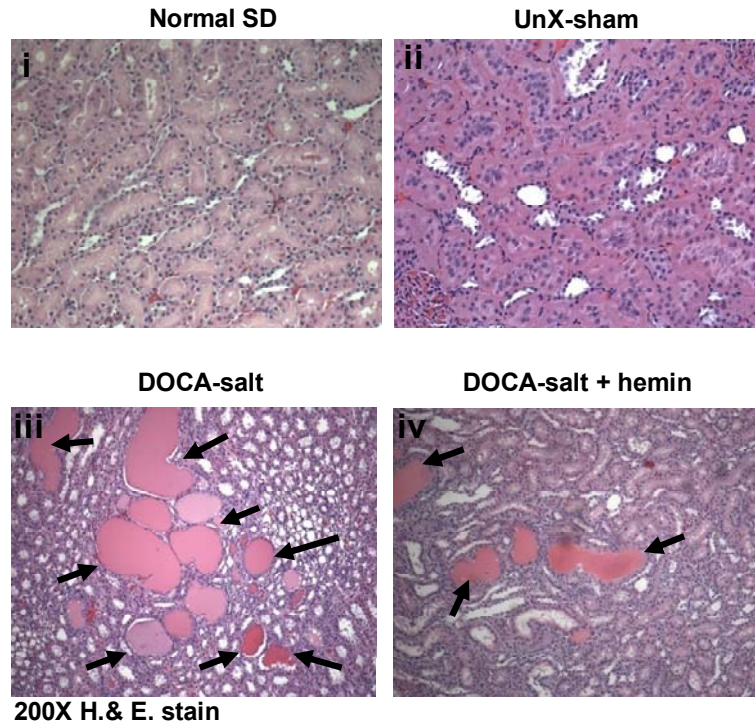
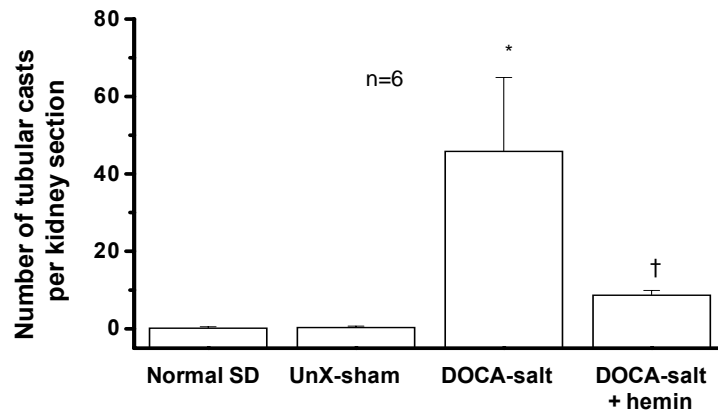
A**Tubular cast formation****B**

Figure 4.25. Hemin reduces tubular cast formation in the kidney of the DOCA-salt rat. (A) Representative photomicrographs showing pink colored tubular cast formation (arrow), H. & E. stain, magnification-200X. The normotensive controls (i&ii) showed normal tubular structure, however, the DOCA-salt rat showed severe tubular cast formation (iii). Hemin regimen significantly decreased tubular cast formation in the DOCA-salt rat (iv). (B) Microscopic quantification of tubular cast revealed that hemin therapy significantly reduced numbers of tubular cast formation as compared with untreated DOCA-salt rats. (* $p < 0.05$; † $p < 0.05$ vs. all other groups).

significantly different than controls ($p < 0.01$). The number of damaged and sclerotic glomeruli were in DOCA-salt hypertensive after hemin therapy (40 ± 2.4 vs. untreated, $n=6$, $p < 0.01$) [Fig. 4.23.B].

4.11.3. Tubular cast formation in the kidney

In the present study, tubular cast formations were counted microscopically in the kidney sections. Protein cast staining was found largely in thick ascending limbs of tubules [Fig. 4.25.A]. These cast formations were severe and clearly identified in the renal sections of the DOCA-salt hypertensive rat, which were significantly higher than that of controls [46 ± 18.9 vs controls (normal SD, 0.33 ± 0.21 and UnX-sham, 0.5 ± 0.22), $n=6$, $p < 0.01$]. In the DOCA-salt hypertensive rat hemin therapy abated the tubular cast formation (8.83 ± 1.08 , $n=6$, $p < 0.05$) significantly, which was above the levels of controls ($p < 0.05$) [Fig. 4.25.B].

4.11.4. Small renal arteries morphometry in the kidney

Small renal arterial alterations in the kidney sections were quantified using an image analysis system for the following parameters: small renal arterial wall thickness, small renal arterial wall-to-lumen ratio and small renal arterial wall area [Fig. 4.26.A]. Hemin therapy in the DOCA-salt hypertensive rat significantly attenuated all the parameters of renal arterial remodeling. Small renal arterial wall thickness was reduced from $75.2 \pm 4.08 \mu\text{m}$ to $49.0 \pm 3.54 \mu\text{m}$, $n=6$, $p < 0.01$ [Fig. 4.26.B], small renal arterial wall thickness-to-lumen ratio decreased from 0.79 ± 0.39 to 0.51 ± 0.02 , $n=6$, $p < 0.01$) [Fig. 4.26.C], and renal arterial wall area reduced from $0.048 \pm 0.007 \text{ mm}^2$ to $0.028 \pm 0.004 \text{ mm}^2$, $n=6$, $p < 0.01$ [Fig. 4.26.D] significantly as compared to DOCA-salt treatment alone. Although, small renal arterial wall thickness-to-lumen ratio did not

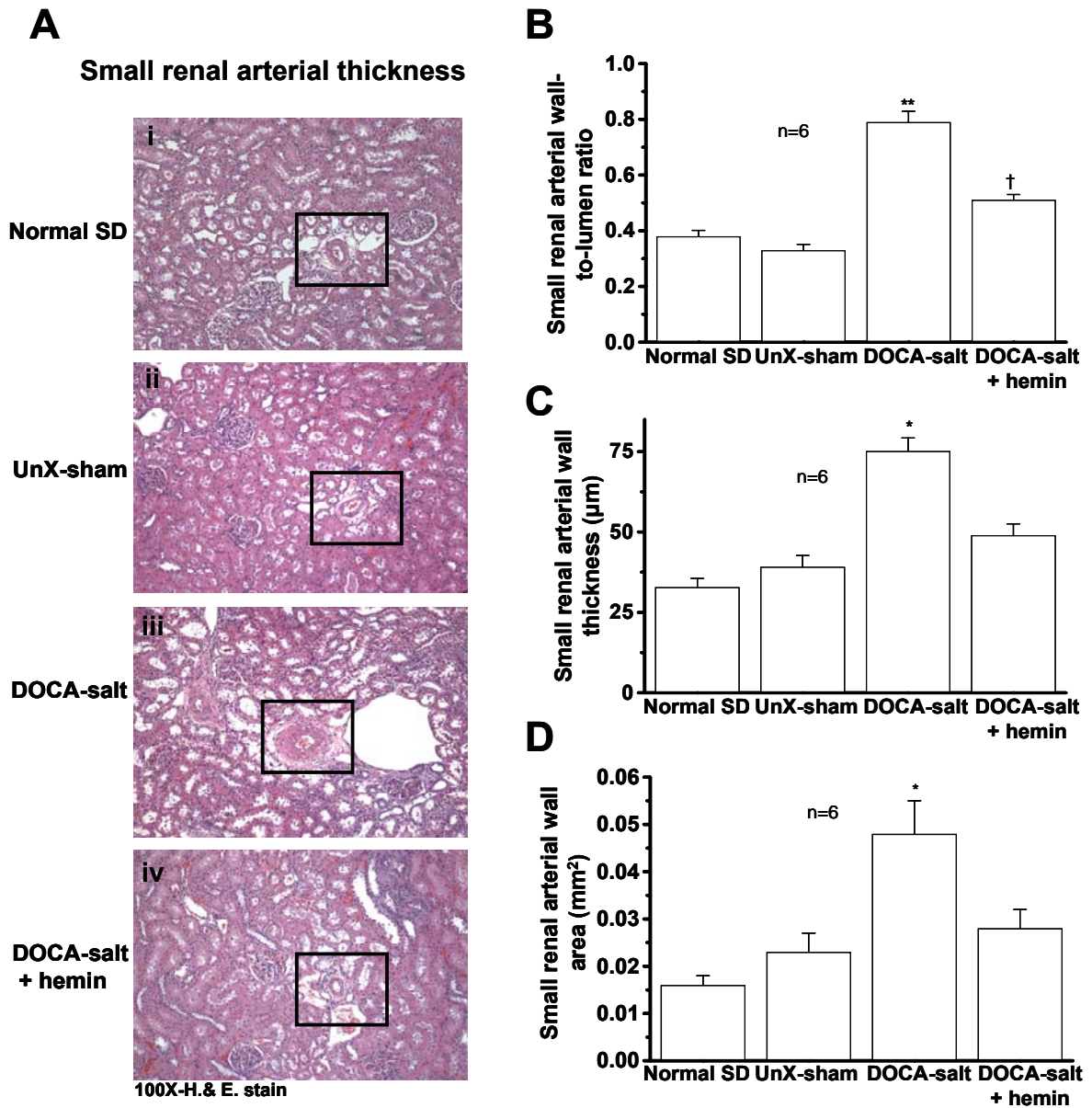


Figure 4.26. Hemin prevents small renal arterial remodeling. (A) Representative photomicrographs showing small renal arteries, magnification-100X-, H. & E. stain. Small renal arteries from DOCA-salt rats showed significant increases in small renal arterial wall-to-lumen ratio (B), small renal arterial wall thickness (C) and small renal arterial wall area (D). Hemin therapy improved small renal arterial structures as reduction of all the parameters of arterial remodeling were observed in the DOCA-salt rats. (** $p < 0.01$; * $p < 0.05$ and † $p < 0.01$ vs. all other groups). (Small renal arterial wall thickness were calculated by assessing inner and outer diameter of all small renal arteries using NIS-elements BR-Q image analysis at 200X-magnification)

restored to the control levels, small renal arterial wall thickness and renal arterial wall area were comparable with controls.

4.12. Effect of hemin regimen on functional parameters of the kidney

4.12.1. Polyurea and proteinuria

In DOCA-salt hypertensive rats, severe renal damage led to significantly higher urine excretion as compared to control rats [58.5 ± 8.61 ml/24 hrs, n=22, vs. controls (normal SD, 22.3 ± 5.17 and UnX-sham, 24.8 ± 2.89 ml/24 hrs, n=6), $p < 0.05$]. However, antihypertensive effect and improved renal lesions in the hemin-treated DOCA-salt hypertensive rat robustly reduced urine excretions comparable to control levels (33.8 ± 3.48 ml/24 hrs, n=22, $p < 0.05$) [**Fig. 4.27.A**].

Moreover, the basal urinary protein levels in the control rats were 11.7 ± 2.29 mg/24 hrs urine and 10.9 ± 2.19 mg/24 hrs urine, (n=6) for normal SD and UnX-sham, respectively. Whereas, in the DOCA-salt hypertensive rat extensive urinary protein excretion was noticed (96.3 ± 22.33 mg/24 hrs urine, n=11, $p < 0.01$). However, hemin-treated DOCA-salt rat showed significant reduction of urinary protein excretion as compared to DOCA-salt alone (18.5 ± 3.14 mg/24 hrs urine, n=11, $p < 0.01$) [**Fig. 4.27.B**].

4.12.2. Creatinine clearance rate

Plasma and urine levels of creatinine also predict the renal function and glomerular filtration rate. The plasma creatinine levels in control rats were 3.2 ± 0.50 mmol/L and 3.6 ± 0.70 mmol/L, n=6, in the normal SD and UnX-sham, respectively. In DOCA-salt hypertensive rats, the plasma creatinine level was significantly increased as compared to that of control rats (84.2 ± 4.6 mmol/L, n=6, $p < 0.01$).

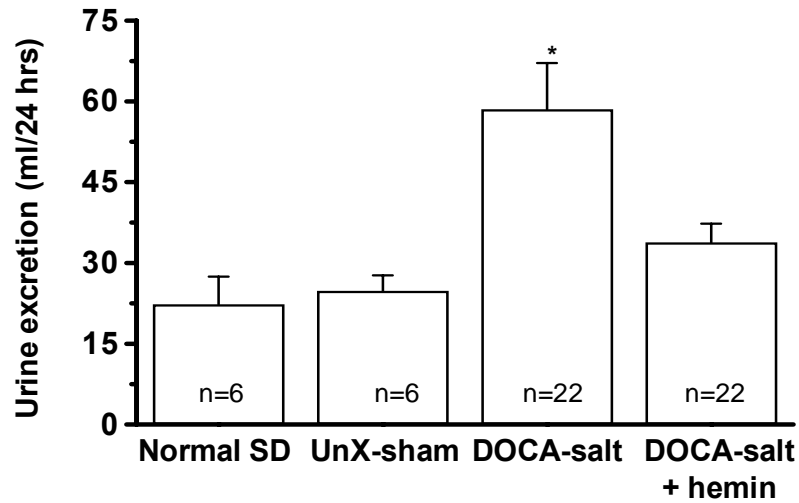
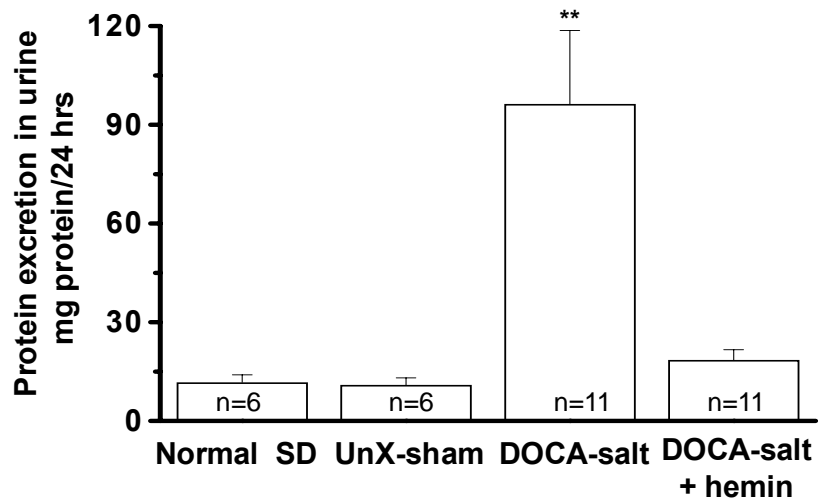
A**B**

Figure 4.27. Hemin treatment decreases urine excretion and proteinuria. In DOCA-salt rats renal damage led to severe (A) polyuria and (B) proteinuria. After hemin therapy showed reduced urine excretion and proteinuria were observed, which are functional parameters of renal damage. (* $p < 0.05$; ** $p < 0.01$ vs. all other groups).

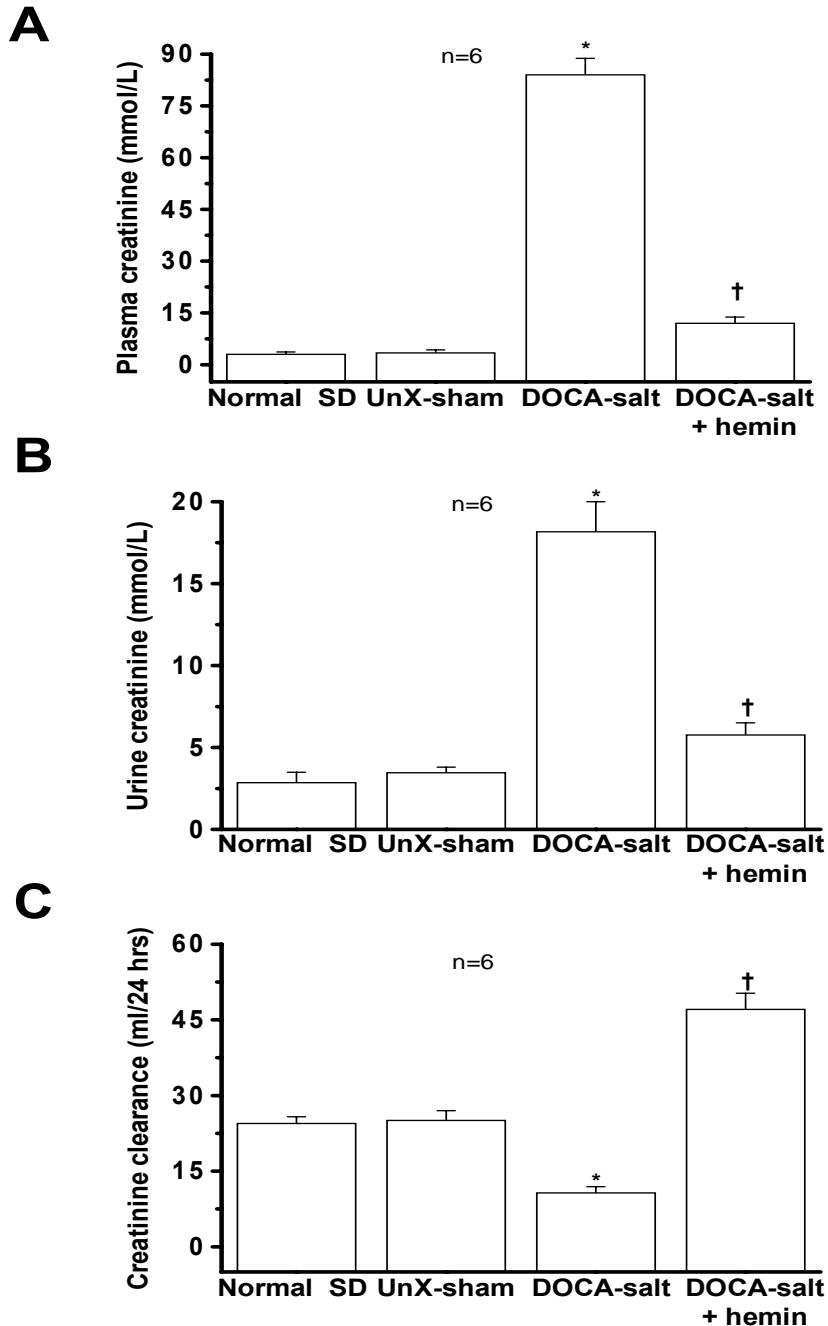


Figure 4.28. Hemin therapy reduces plasma and urine creatinine levels and creatinine clearance. DOCA-salt hypertensive rat showed increased plasma (A) and urine creatinine levels (B) and decreased creatinine clearance rate (C) as compared to normotensive controls. However, hemin regimen significantly reduced plasma and urine creatinine and improved creatinine clearance rate. (* $p < 0.01$; † $p < 0.01$ vs. all other groups).

However, hemin-treated DOCA-salt hypertensive rat showed significant attenuation of plasma creatinine levels compared to that of DOCA-salt treatment alone (12.2 ± 1.6 mmol/L, $n=6$, $p < 0.01$) [**Fig. 4.28.A**]. Similarly, urinary creatinine levels in DOCA-salt hypertensive rat were significantly higher than control rats [18.2 ± 1.8 mmol/L vs. controls (normal SD, 2.89 ± 0.60 mmol/L and UnX-sham 3.5 ± 0.30 mmol/L), $n=6$, $p < 0.01$]. However, the hemin regimen significantly reduced the urinary creatinine to a level significantly less than DOCA-salt alone but significantly higher than controls (5.8 ± 0.70 mmol/L, $n=6$, $p < 0.01$ vs. all other groups) [**Fig. 4.28.B**].

The creatinine clearance rate was calculated from plasma and urinary creatinine concentrations and total urine excretion for 24 hrs. A significant reduction in the creatinine clearance rate was observed in the DOCA-salt rat (10.8 ± 1.2 ml/24 hrs, $n=6$, $p < 0.01$) compared to control rats (normal SD 24.6 ± 1.2 ml/24 hrs and UnX-sham 25.2 ± 1.8 ml/24 hrs, $n=6$). Hemin-treated DOCA-salt rats showed an improved creatinine clearance rate (47.2 ± 3.1 ml/24 hrs, $n=6$, $p < 0.01$) [**Fig. 4.28.C**].

5. DISCUSSION

Mineralocorticoid causes retention of salt and water as it has an aldosterone mimetic property. The uninephrectomized rat, treated with DOCA and salt water, develops severe hypertension, which is also known as salt sensitive high blood pressure [201]. DOCA-salt-induced hypertension is characterized by end-stage organ damage, leading to cardiac and renal insufficiencies [201]. In the present study, the data showed that DOCA-salt treatment of uninephrectomized SD rats increased systolic blood pressure, enhanced local cardiac and renal tissue levels of angiotensin-II, and aldosterone and oxidative stress, which stimulate other signal transduction pathways leading to the development of cardiac and renal end-stage injury. Tissue angiotensin-II and aldosterone are contributing factors for cardiac and renal injury. The roles played by these hormones would be subsequent to that initiated by DOCA and NaCl-treatment. Interestingly, our study showed augmentation of HO-1 expression, HO activity and cGMP levels in cardiac and renal tissue after administration of hemin in the DOCA-salt hypertensive rat. Moreover, enhanced HO activity was associated with significant attenuation of cardiac and renal tissue angiotensin-II and aldosterone, decreased oxidative stress with subsequent downregulation of redox sensitive (oxidative/inflammatory) transcription factors such as NF- κ B and AP-1. In addition, hemin significantly decreased the profibrotic molecule TGF- β ₁ and further, reduced the mobilization of ECM proteins such as collagen and fibronectin. Hemin improved both cardiac and renal lesions shown by normalization of renal function test such as proteinuria and creatinin clearance rate.

5.1. Physiological parameters such as systolic blood pressure, body weight and hematocrit

In the present study, blood pressure was measured indirectly by incorporating the standard non-invasive tail cuff method weekly throughout the protocol on the experimental rats (except UnX-DOCA, UnX-salt and DOCA-salt + hemin + CrMP groups). In the DOCA-salt hypertensive rat model, a steadily positive sodium balance leads to continuous increase in blood pressure for the initial 3 weeks period. After this period, fluctuation of the sodium balance causes onset of malignant phase of hypertension that is associated with fibrinoid necrosis of glomeruli in the kidney [202]. Animals start showing two to three paroxysms of sodium loss with concomitant fall in body weight, fluid loss and evidence of hemoconcentration [202]. Initial high blood pressure in the DOCA-salt model is due to increase in fluid volume, in the later stage due to paroxysms sodium and fluid losses takes place, however, blood pressure is maintained at higher levels due to arterial remodeling [150], and cardiac and renal alterations.

Hemin therapy abated blood pressure in the DOCA-salt hypertensive rat over a four-week study period. Importantly, the antihypertensive effects observed in hemin-treated DOCA-salt rats are consistent with previous studies in which upregulation of HO system was shown to normalize blood pressure in SHR and DOCA-salt hypertensive model, however CrMP, a HO blocker nullified effect of hemin and enhanced systolic blood pressure [155]. The antihypertensive effect was accompanied with enhanced activity of the HO system, cGMP and total antioxidant capacity in the cardiac and renal tissue, which are some of the main blood pressure regulatory organ systems along with vasculature of the body. Products of heme catabolism by the HO

system have the properties of regulating blood pressure, especially carbon monoxide. Previously it has been showed that acute [123] or chronic [203] administration of the HO-1 inducer (stannous chloride) led to normalization of blood pressure in the SHR. In addition, HO substrates or HO-1 inducer have been shown to decrease blood pressure in the SHR [204-206]. Conversely, when the HO-1 inhibitor, zinc deuteroporphyrin 2,4 bis-glycol was administered intraperitoneally in the normotensive rat model, it led to a rapid increase in the arterial pressure and inhibited carbon monoxide production [207]. Upregulation of the HO system led to an increase in the catabolism of heme and release of different products such as ferritin, biliverdin, bilirubin and carbon monoxide. Importantly, carbon monoxide has been known as a vascular relaxant, acting through the stimulation of sGC, affecting cytochrome P450 and opening calcium-activated K^+ channels [208]. Moreover, the antihypertensive effects of hemin in the SHR model is associated with increased HO-1 expression, HO activity, sGC, and cGMP in the thoracic aorta and mesenteric arteries [153, 155]. Also, it reversed SHR-featured arterial eutrophic inward remodeling and decreased vascular endothelial growth factor expression [155]. Increased HO-1 expression and total HO activity could generate more carbon monoxide, a vasodilator and may cause vascular relaxation. Carbon monoxide plays an important role in the regulation of both renal cortical and medullary blood flow [209]. Predominantly, hemin therapy induces HO-1 in the kidney, which may increase renal cortical and medullary blood flow and would shift the pressure-natriuretic response towards the left, lowering the blood pressure in the hypertensive models [210].

Several studies have showed evidence for an enhanced production of ROS and decrease in the antioxidant defence system in plasma and tissue of hypertensive animals and humans [211]. Furthermore, in various models of hypertension such as DOCA-salt,

SHR, glucose-induced and angiotensin-induced models, a progressive increase in the production of superoxide anion have been demonstrated in vascular and cardiac tissue during the development of hypertension [212]. Oxidative stress mediated through the formation of superoxide anion is a major primary pathogenic factor in the development of hypertension, however, treatment with efficacious antioxidant therapies can prevent or markedly attenuate the development of hypertension [213]. Along with oxidative stress, growing evidence also suggests that inflammation participates in the development and pathogenesis of hypertension [214]. Therefore, for the treatment of hypertension, it is essential to counteract both oxidative stress and inflammatory cascades. Importantly, bilirubin and biliverdin, endogenous antioxidant and anti-inflammatory factors produced by the HO system [215], would suppress oxidative stress and the inflammatory cascade, known to accompany hypertension [216]. In addition, HO activity is associated with increased ferritin activity, which also possesses anti-inflammatory and antioxidant properties [217]. Interestingly, in our study, increased plasma ferritin levels were accompanied by enhanced total SOD, total antioxidant capacity and decreased NF- κ B, which indicates the suppression of oxidative stress and the inflammatory cascade in hemin treated DOCA-salt hypertensive rat. It also suggests decrease in hypertension is associated with significant reduction of both oxidative stress and inflammation in hemin treated DOCA-salt hypertensive rats.

Although, the direct effect of hemin induced molecular changes in the vasculature of the DOCA-salt rat was not incorporated in this study, previous studies showed that upregulation of the HO system led to vascular relaxation through the sGC-cGMP pathway and subsequently, normalized blood pressure in the SHR [154].

Importantly, in the present study, the heart and kidney were employed to investigate the effect of hemin to counteract DOCA-salt induced end-stage damage, as they are known to be vital organs having a role in controlling blood pressure. Improvement in these organ systems indirectly confirms the effect of hemin on blood pressure in the DOCA-salt hypertensive rat. Furthermore, decreased proteinuria and suppressed oxidative stress in the kidney, as shown by reduced urinary 8-isoprostane, also directly shows improved renal function, and in part, improved blood pressure in the DOCA-salt hypertension model. Interestingly, our study also demonstrated that upregulation of the HO system attenuated both cardiac and renal aldosterone and angiotensin-II. These hormones are known to trigger mechanisms involved in elevation of blood pressure, oxidative stress and promote inflammation by activation of NF- κ B and AP-1 [71, 218, 219]. Angiotensin-II is known as a potent vasoconstrictor, which also stimulates production of aldosterone resulting in retention of salt and water leading to increase in blood pressure. Therefore, abrogation of these hormones might have caused additive effects and led to the reduction of blood pressure in the DOCA-salt hypertensive rats.

The results from our study also showed that hemin therapy did not affect body weight since weight of treated rats were not different from the control rat. However, body weights of DOCA-salt hemin-treated DOCA-salt and both hemin and CrMP treated DOCA-salt rats were significantly lower than uninephrectomized rats. Decreased body weight in DOCA-salt group was probably due to paroxysms of sodium loss [202] and subsequently fluid loss through urinary excretion and end stage cardiac and renal damage, which was evident in the present study. Uninephrectomized rat showed increase in body weight, which was not significant with respect to normal SD control rats.

Since hemin is known to be an activator and growth promoter of early hematopoietic progenitor cells [107] blood hematocrit values were measured in the experimental rats. The hematocrit values of the hemin treated DOCA-salt rats were significantly lower than DOCA-salt alone and were within the normal range. This slight increase in the hematocrit level in the DOCA-salt hypertensive rat could be due to transient reduced plasma volume from pressure natriuresis and reduced vascular lumen, a characteristic of the DOCA-salt model [150]. Another explanation for increased hematocrit value in the DOCA-salt rat could be due to the increase in the heme content a pro-oxidant [106], and which was expressed significantly by increased oxidative stress, along which decreased total antioxidant capacity and SOD levels. Heme is a component in the synthesis of hemoglobin and increased heme content might cause increased synthesis of hemoglobin in the reticulocytes (immature RBCs). Therefore, reticulocytes could have been released into the blood circulation leading to an increased hematocrit values in the DOCA-salt rat. However, hemin treated DOCA-salt hypertensive rat could have enhanced catabolism of excessive heme content, leading to a decreased synthesis of excess hemoglobin, and reduced abnormal reticulocyte counts, which subsequently restored the hematocrit value to normal range.

5.2. Heme oxygenase and cyclic guanosine monophosphate

HO-1 is a 32 kDa protein; an inducible isoform of the HO enzyme. Different stimuli induce HO-1 expression in the various mammalian cells. The HO-1 enzyme is also sensitive to pharmacological agents. HO activity consists of the relative input by HO-1 and HO-2 proteins. However, HO-2 is the constitutive isoform and is not pharmacologically modulated [108]. Hemin is one of the most potent pharmacological

stimulators of the HO-1 enzyme [106, 107]. Accordingly, our result indicates that hemin therapy increased the HO enzyme activity in a similar way as HO-1. Importantly, our result showed that in the DOCA-salt hypertensive rat both cardiac and renal HO activity were significantly higher than the normotensive control rats. Although the basal HO activity in DOCA-salt hypertensive rat was higher than in controls, the magnitude might have been insufficient to trigger the downstream element of the HO-signal transduction pathways. This notion is consistent with inability of basal HO activity in DOCA-salt hypertensive rat to cause any detected changes in cGMP, an important signaling molecule of the HO system [Fig. 4.5.B & 4.6.B]. It is important to note that 4.5 and 2.1-fold increase of cardiac HO activity and cGMP content was demonstrated after the administration of hemin in DOCA-salt hypertensive rat [Fig. 4.5.B&C]. Similar increases of 5.6 and 2.1-fold were observed in the kidney tissue [Fig. 4.6.B&C]. Therefore, it is possible that enhanced HO activity by hemin therapy would cause a parallel increase in the production of endogenous CO that would in turn stimulate cGMP content. However, combined treatment with CrMP and hemin attenuated HO-1 expression, HO activity and cGMP levels in cardiac tissue indicative of HO blocking effect of CrMP against hemin in DOCA-salt hypertensive rat. This observation is consistent with previous finding in SHR and DOCA-salt hypertensive study [40, 153, 154].

Given that carbon monoxide, one of the products of heme catabolism, stimulates the sGC/cGMP pathway to regulate vascular tone [153], carbon monoxide may upregulate the production of cGMP in cardiac and renal tissue. In addition, cGMP has cytoprotective and antiproliferative properties [128]. Interestingly, in this study, hemin therapy enhanced the HO activity and cGMP content in both cardiac and renal tissue of

the DOCA-salt hypertensive rats. Thus, HO triggered release of carbon monoxide will stimulate cGMP, which further will activate downstream mechanisms to relax vascular tissue [122, 153] and protect cells. It needs to be clarified as to whether activation of HO directly stimulates the cGMP pathway. Although the basal HO activity in cardiac and renal tissue of DOCA-salt rats was higher than in the normotensive controls, it remains ambiguous why the higher basal HO activity in hypertensive rats did not trigger cGMP activation and attenuate damage. The possible explanation is that in the hypertensive rat, the magnitude of basal HO activity might be below the threshold necessary to stimulate cGMP, downstream mechanism of the HO system. Thus, hemin-mediated enhanced activity of the HO-1 protein was necessary to induce the downstream cGMP pathway. This is consistent with the previous finding, that increased HO activity in hypertension models did not stimulate cGMP content in SHR and DOCA-salt hypertensive models [40]. Therefore, it is necessary to investigate further interaction between HO activity and the cGMP-signaling pathway in hypertension and related end-organ diseases.

5.3. Aldosterone and angiotensin-II

In the DOCA-salt rat model, mineralocorticoid administration along with salt leads to the development of low renin, volume overload type of hypertension. In such conditions, local tissue production of angiotensin-II and aldosterone leads to tissue damage in the cardiovascular and renal systems. In end-stage organ damage synergistic interaction between aldosterone and angiotensin-II and elevated ROS activity have been shown to play a prominent role [180]. Therefore, one of the major focuses of our study was to assess the role of hemin therapy on local tissue aldosterone and angiotensin-II levels. Interestingly, increased aldosterone and angiotensin-II levels in our study were

higher than the levels reported in high salt-induced hypertension model [180]. This discrepancy might be due to the combined effects of nephrectomy, the synthetic mineralocorticoid, DOCA and NaCl-salt, which distinguishes DOCA-hypertension from the high-salt-diet-induced hypertension, a model without surgery. Our results from the present study demonstrated for the first time that hemin therapy downregulates cardiac and renal tissue levels of angiotensin-II and aldosterone in the DOCA-salt hypertensive rat. In DOCA-salt rats, suppressed systemic RAAS causes production of local tissue angiotensin-II and aldosterone, which plays a role in cardiac and renal structural remodeling. This is consistent with other types of hypertensive models such as, the aldosterone/salt [220, 221] and high salt-diet-induced hypertension in Dahl salt-sensitive rat [180]. These models are associated with cardiac and renal hypertrophy, marked collagen deposition in the left ventricle, and renal structural alterations. Importantly, aldosterone has been shown to upregulate AT₁ receptor by the synthesis of new receptor protein, which was demonstrated in cultured rat aortic vascular smooth muscle cells [222, 223]. Thus, synergistic interaction between angiotensin-II and aldosterone is envisaged in the production of end-organ damage, which involves production of ROS consistent with previous study in other types of hypertensive rat models [180].

Several studies have reported that the heart is capable of synthesizing aldosterone [180, 224]. Aldosterone acts as a prohypertensive substance by causing water retention through absorption of sodium and excretion of potassium. Recently, the role of aldosterone in mediating tissue inflammation, remodeling and fibrosis [221, 225] has been well acknowledged in non-epithelial cells in brain, vasculature, heart and glomeruli [224, 226]. These events were shown to be prominently mediated by the mineralocorticoid receptor [218, 227]. Therefore, local production of aldosterone sets a

destructive force in hypertension. Importantly, the aldosterone system in the kidney involves salt regulation. However, excessive aldosterone activity causes renal injury, fibrosis and progresses towards end-stage-renal damage [10]. It is worthwhile noting that in our study, the DOCA-salt hypertensive rat cardiac and renal aldosterone level was increased by 3.3 and 5.8-fold, respectively as compared to the controls. Interestingly, the results for cardiac aldosterone are consistent with those reported by Gomez-Sanchez et al., and Fiebeler et al., in normotensive Wistar and SD rats, respectively [224, 228]. However, some reports also showed 10-20 times higher cardiac aldosterone in the normotensive Wistar rats as compared to our results [229]. Although, Bayorh et al., used similar Caymans EIA kit for the measurement of aldosterone concentrations in both heart and kidney in the Dahl-salt sensitive rat [180] they found aldosterone levels 10-15 times lower than the concentrations found in the present study in normotensive SD rats. These discrepancies are probably due to different strains of rat used in different studies and different laboratory factors that might affect the performance of the assay. The monoclonal antibody used for the detection of aldosterone in our study might be from a different batch and/or have different specificity to the SD rats.

In the synthesis of aldosterone, the rate-limiting steps are the transport of cholesterol, mediated by the steroidogenic acute regulatory protein in the inner mitochondrial membrane. Subsequently, the reaction is controlled by P450_{scc}, and the conversion of deoxycorticosterone to aldosterone takes place by mitochondrial aldosterone synthase [224, 230]. After hemin therapy, the probable mechanism for the decrease in production of tissue aldosterone would be the regulation of CYP450 hemoprotein by the HO protein. The HO system limits the levels of heme and produces

carbon monoxide, which strongly binds to the heme moiety of CYP450 and causes enzyme inhibition [231]. Thus, it might inhibit the enzymes P450_{scc} and P450 aldosterone synthase, which are required for the synthesis of aldosterone, and may lead to decrease in production of aldosterone, thus in part favoring the improvement of cardiac and renal structural lesions. Predominantly, a previous study showed that hemin therapy reduces aldosterone synthase mRNA in SHR and plasma aldosterone levels in the DOCA-salt rat [40]. In the randomized aldosterone evaluation study (RALES) mortality trial, when patients with severe chronic heart failure were treated with spironolactone, an aldosterone antagonist, they showed improved cardiac and renal function, indicating that aldosterone plays an important role in end-organ damage [232]. Interestingly, the present data clearly shows that hemin therapy attenuated local tissue levels of aldosterone, which might be indicative of an important role of the HO system on enzyme systems involved in the synthesis of aldosterone and thus improve cardiac and renal health.

In the DOCA-salt hypertensive rat, excessive activity of local tissue aldosterone caused both cardiac and renal damage, conversely hemin therapy inhibited. Importantly, aldosterone mediates tissue injury by the activation of AT₁ receptor subtype and further production of angiotensin-II. Therefore, it is imperative to analyze local tissue levels of angiotensin-II in DOCA-salt hypertension. Moreover, an increase in local angiotensin-II has been shown to play a major role in the progression of end-organ damage in the DOCA-salt hypertension model [17]. This is consistent with our observation of cardiac and renal hypertrophy and pathological lesions seen in DOCA-salt hypertensive rats. Further, angiotensin-II causes vasoconstriction and stimulates production of ROS through AT₁ mediated mechanism, which was exhibited by increased systolic blood pressure and urinary 8-isoprostane, a marker of systemic oxidative stress. In addition, to

vasoconstrictor action, angiotensin-II is a trophic/growth factor that affects the structure of blood vessels, the heart, and the kidney. Our data shows that cardiac and renal angiotensin-II levels were 3.7 to 5.3-fold higher in DOCA-salt hypertensive rats compared to control rats. It is consistent with the notion that kidney produces more angiotensin-II levels as compared to the heart and local angiotensin-II production is tissue specific in the DOCA-salt rat, which was also seen, in the present study.

Angiotensin-II levels in both cardiac and renal tissue from normotensive SD rats are in a similar range to that observed by Mendes et al., in the Wistar rat. It indicates the consistency of angiotensin-II levels in normotensive rats [233]. However, Bayorh et al., reported 10-20 times lower angiotensin-II levels in Dahl-salt sensitive rats in both heart and kidney tissue [180]. The explanation for the discrepancy of angiotensin-II levels might be the same as given for aldosterone. Interestingly, in this study hemin-treated DOCA-salt hypertensive rats demonstrated the abrogation of both cardiac and renal angiotensin-II, which was associated with enhanced activity of HO and cGMP. It suggests a role of the HO system in modulation of angiotensin-II. Importantly, Aizawa et al., found that HO-1 was upregulated in the kidney of rats rendered hypertensive with chronic angiotensin-II-infusion, demonstrating the renoprotective effect of HO-1 against angiotensin-II induced insults [234]. Several lines of evidence also suggested that administration of the HO-1 inducer hemin ameliorates angiotensin-II induced cardiac hypertrophy [235] and renal injury induced by angiotensin-II and high salt diet [152]. However, the transient upregulation of the HO proteins would not be sufficient to prevent end-organ damage in the hypertensive rat, which was noted in our study and consistent with previous reports [149, 150], whereas, hemin-induced strong stimulation of the HO-1 may act as a feedback mechanism to decrease production of angiotensin-II

and prevent end-stage damage. Moreover, the RAS has a positive feedback loop where angiotensinogen gene activation is mediated by the rel-A NF- κ B p65 subunit, and thus stimulates the production of angiotensin-II [236], while NF- κ B can bind on the consensus binding site of HO-1 gene [67]. Downregulation of NF- κ B due to the stimulated HO system may inhibit angiotensinogen gene activation and the downstream mechanism causing a decrease in the production of angiotensin-II in the local tissue. Therefore, interaction between HO-1, angiotensin-II, and NF- κ B would be envisaged for the multifaceted peptide mediated signaling pathway.

The effects of hemin therapy on cardiac and renal aldosterone and angiotensin-II levels are novel findings in DOCA-salt hypertension. However, the precise mechanism of decrease in tissue angiotensin-II and aldosterone levels associated with enhanced HO-1 is still unknown and would be part of a future study.

5.4. Oxidative stress, inflammation, and heme oxygenase system

Hypertension is associated with increased ROS formations such as $O_2^{\cdot-}$, HO^{\cdot} or H_2O_2 . Excessive ROS production in the heart and kidney has been reported in the DOCA-salt hypertensive model [15, 46]. The elevated superoxide causes random oxidation of tissue phospholipids and generate isoprostanes [33]. Urinary 8-isoprostane has been known as a precise index of chronic and systemic non-enzymatic lipid peroxidation and overall oxidative marker of body systems [33]. It is a stable biomarker of superoxide production in vivo and in vitro [237]. The 8-isoprostane also appears in the plasma and urine under normal conditions and is elevated by oxidative stress. The isoprostane, thus released are higher than any other enzymatically derived eicosanoids

[33]. Hemin therapy leads to catabolic degradation of heme, which releases products such as bilirubin, biliverdin and ferritin. These products have the capacity to scavenge the superoxide radicals. Therefore, in hemin-treated animals the attenuation of superoxide might have prevented tissue phospholipid peroxidation and ultimately reduction of the urinary 8-isoprostane occurred. Moreover, this reduction of urinary 8-isoprostane does not mean only reduction of renal injury, but it is a sign of inhibition of oxidative stress from overall body systems [33].

NF- κ B is a transcription factor, which is expressed in a variety of pathophysiological conditions, including hypertension. NF- κ B stimulates many downstream mechanisms, which are known to play an important role in cardiac and renal injury. Mineralocorticoid-induced hypertension is associated with increased NF- κ B activity and subsequent damage by inflammation and fibrosis [94]. Increased NF- κ B activity suggested that further transcription of proinflammatory and growth factors might have occurred in DOCA-salt hypertensive rats. The transcription factor AP-1 is involved in the gene regulation of some inflammatory proteins and ECM proteins such as TGF- β in mineralocorticoid hypertension [94]. Interestingly, in hemin-treated DOCA-salt rats, 2.5 and 1.6-fold downregulation of NF- κ B and AP-1, respectively were noted equally in both cardiac and renal tissue, compared to DOCA-salt treatment alone. It means upregulation of the HO system showed more effect on NF- κ B than that of AP-1, which might downregulate proinflammatory factors to a greater degree than growth factors. Moreover, according to our data, both transcription factors levels were not restored to the basal control levels. It suggests that along with HO-1 gene [67] some other factor might be involved in the regulation of transcription factors.

Circumstantial evidence showed that increased activity of the HO system releases bilirubin, biliverdin, carbon monoxide and ferritin. These products have antihypertensive, antioxidative, cytoprotective, anti-inflammatory, and antihypertrophic properties, which have been shown in a variety of *in vivo* and *in vitro* studies. Moreover, their effects are consistent with other reports stating that hemin or HO substrate normalizes blood pressure in the SHR and DOCA-salt-induced hypertension [40, 154, 155]. Importantly, upregulation of the HO system releases free iron. Free iron rapidly converts to ferritin via ferritin synthase. It has antioxidant and anti-inflammatory properties. Thus, the enhanced activity of HO would liberate more ferritin and show its beneficial effect to prevent end-stage damage; therefore, we decided to evaluate plasma ferritin concentration. Oxidative stress is the imbalance between the production of reactive oxygen species and antioxidant capacity. The DOCA-salt hypertension model is known to exhibit an increase in oxidative stress during the development of hypertension, which subsequently leads to end-stage organ damage [15]. Importantly, liberation of biliverdin, bilirubin, ferritin and carbon monoxide, which are antioxidant products, would act as a supplementary effect on the enhancement of total antioxidant capacity in cardiac and renal tissue. Therefore, it is critical to note that compared to a single antioxidant defence system, combined antioxidant from different sources provides greater protection [104, 174-179]. Furthermore, it is worthwhile to note that the hemin-induced elevations of plasma ferritin, SOD activity and total antioxidant capacity were associated with attenuation of urinary 8-isoprostane, an index of oxidative stress. It exhibits that hemin has an antioxidant effects in DOCA-salt hypertension. Moreover, these observations are consistent with previous studies, which indicated that hemin

therapy upregulates the HO system and enhances the antioxidant effect in the tissue [104, 177, 238].

Bilirubin is a potent antioxidant which either directly scavenges superoxide or inhibits reduced NADP (NADPH) oxidase [177, 239], whereas biliverdin acts as an antioxidant via interaction with vitamin E [238]. Furthermore, the cardioprotective function of bilirubin has been shown previously. HO-1-derived bilirubin attenuates myocardial dysfunction and reduces infarct size after ischemia/reperfusion injury [101]. Additionally, higher serum bilirubin levels, related to decreased lipid peroxidation, is associated with reduced risk of coronary artery disease in humans [240]. The antioxidant mechanism of the HO-1 is also attributed to an increase in the antioxidant genes of superoxide dismutase and catalase in an experimental diabetes model [42]. Interestingly, in the present study, upregulation of HO system is accompanied by increased levels of SOD in the hemin treated DOCA-salt hypertensive rat. Furthermore, upregulation of HO-1 is associated with decreased cellular heme and increased glutathione levels that were reduced during the oxidative insult [241]. Thus, it may shift the redox state to a reduced state, decreasing superoxide formation. Therefore, an increase in SOD levels, total antioxidant capacity in this study might have inhibited oxidative injury which was confirmed by reduction of urinary 8-isoprostane. Decrease in oxidative stress might not have stimulated the upregulation of redox sensitive transcription factors NF- κ B. Previously, it was shown that prolonged administration of antioxidant decreases superoxide production, lowers systolic blood pressure, and reduces NF- κ B activation in Mineralocorticoid hypertension [46]. Angiotensin-II-induced cardiomyocyte hypertrophy was abrogated by HO-1 overexpression, and the author claims that it was

associated with suppressed ROS [235]. Interestingly, our data clearly showed that decreased urinary 8-isoprostane, a direct marker of oxidative stress, and enhanced, plasma ferritin content, total SOD level and cardiac and renal tissue total antioxidant capacity could suppress ROS and ROS-mediated downstream signaling. Thus, subsequently attenuation of cardiac and renal end-stage organ damage were exhibited after hemin therapy.

5.5. Cardiac and renal hypertrophy, transcription factors, and heme oxygenase system

In the present study, hemin treatment resulted in a significant reduction in cardiac and renal hypertrophy. The results extend the findings of a previous related study that showed that overexpression of HO-1 attenuated angiotensin-II-induced cardiac hypertrophy [235], both *in vitro* and *in vivo*. The antihypertensive effect of hemin, which significantly reduced blood pressure in the DOCA-salt hypertensive rat, could be one of the factors that prevented cardiac hypertrophy. In the hypertensive patient, an increase in cardiac after-load leads to cardiac hypertrophy, especially left ventricular hypertrophy [190, 242]. Hypertensive cardiac hypertrophy develops either by induction of mechanical stress due to elevated left ventricular after-load or neural/humoral factors [243]. Interestingly, the direct effect of HO system on cardiac tissue may contribute to antihypertrophic function *in vivo* [235]. In accordance with this notion, HO-1 induction abrogates cardiac hypertrophy in the adult stroke-prone SHR rat through a pressure-independent mechanism [244]. Alternatively, one of the important features of the development of hypertrophy or increase in cell mass is that, once external stimuli are removed, the altered growth pattern ceases and the cells reverts to their

original state [95]. Supporting this theory, suppressing external stimuli such as cardiac angiotensin-II, aldosterone, oxidative stress, transcription factor NF- κ B and TGF- β ₁ would halt the altered growth pattern of the heart, and prevent cardiac hypertrophy, as observed in the present study.

A previous study by Purcell, et al., showed that NF- κ B is required in the hypertrophic growth of primary rat neonatal ventricular cardiomyocytes, and its overexpression enhances cardiomyocyte enlargement [245]. In addition, in the double transgenic angiotensin-II dependent rat model, an inhibitor of NF- κ B suppressed the development of hypertrophy, independent of blood pressure, suggesting that NF- κ B activation is necessary for cardiac hypertrophy, and its inhibition prevents cardiac hypertrophy [246]. Recently, the importance of NF- κ B as a hypertrophic mediator in the adult heart has been shown, as reduced heart growth was observed in the gene-targeted mice lacking p50 protein after chronic angiotensin-II infusion [247]. In addition, transgenic mice expressing NF- κ B ‘super-repressor protein’ abated cardiac hypertrophy after angiotensin-II and isoproterenol infusion [248]. Importantly, oxidative stress also stimulates the activation of redox sensitive transcription factors such as NF- κ B and AP-1, leading to development of cardiac hypertrophy and injury. Therefore, signaling and activation of NF- κ B and AP-1 play important roles in the development of cardiac hypertrophy *in vivo* and prevention of signaling cascade and activation of NF- κ B and AP-1 attenuates cardiac hypertrophy. Interestingly in the present study, hemin therapy exhibited reduction of whole heart mass, left ventricular hypertrophy and cellular abrogation of cardiomyocyte thickness, which were accompanied with downregulation of NF- κ B and AP-1 expression, and subsequent attenuation of TGF- β and collagen

depositions in the cardiac tissue of DOCA-salt hypertensive rats. The blockade of the transcription factors NF- κ B and AP-1 might have caused a decrease in cardiac hypertrophy. Similarly, HO-1 induction by hemin treatment greatly improved the kidney-to-body weight ratio, suggesting amelioration of renal hypertrophy. This effect was likely linked to the enhanced activity of the HO and cGMP levels, suppression of local tissue angiotensin-II, aldosterone, oxidative/inflammatory transcription factors, TGF- β ₁ and ECM proteins. Furthermore, decrease in renal hypertrophy was probably due to the HO-1-mediated reduction of heme content in the DOCA-salt hypertensive rat. Heme, a known prooxidant, has been shown to contribute to generation of ROS [249] and renal injury [231].

Our result confirms that upregulation of the HO system abated these destructive transcription factors and attenuated cardiac and renal lesions, whereas the HO inhibitor, CrMP exacerbated damages. CrMP, selective and competitive inhibitor of HO activity, was given at dose of 4 μ mol or 2.61 mg per kg [153, 163]. Therefore, increased blood pressure, hypertrophic processes were associated with enhanced transcription factors in CrMP-treated animals [164]. Moreover, our lab had reported previously that the basal level of HO has important role in blood pressure regulation [153].

5.6. Improvement in cardiac and renal morphological lesions, and function

The central and novel finding of this study is the observation that DOCA-salt-induced pathophysiological changes in cardiac and renal tissue can be abrogated by upregulation of the HO system. Hemin therapy significantly attenuated cardiac morphological lesions such as cardiac myocyte hypertrophy, myocyte scarring,

myocardial, and perivascular fibrosis, small coronary vasculature thickening, and collagen depositions. Similarly, renal lesions such as glomerular hypertrophy, glomerular sclerosis, interstitial mononuclear cell infiltration and fibrosis, tubular dilation, small renal arterial wall thickening, and tubular cast formation in the DOCA-salt hypertensive rat were prevented by hemin therapy. The improved renal function was accompanied with decreased proteinuria, plasma and urine creatinine, and enhanced creatinine clearance rate. This attenuation of organ damage is probably linked to the direct effect of heme catabolized products and/or the interaction of different signaling pathways with the HO system, which were involved in the development of cardiac and renal injury.

NF- κ B is a heterodimer, normally present in an inactive form, bound with an inhibitory subunit protein I κ B. NF- κ B is a redox-sensitive oxidative/inflammatory transcription factor. After oxidative insults, it is activated, leading to degradation of phosphorylated I κ B and NF- κ B translocated from the cytosol into the nucleus. In the nucleus it binds to the promoter region of specific genes to initiate transcription that encodes for specific genes such as pro-inflammatory and growth factors [250]. Therefore, upregulation of NF- κ B stimulates pro-inflammatory as well as growth stimulatory factors, which causes inflammation and development of hypertrophy. Likewise, AP-1 also involved in the regulation of some proinflammatory factors, majorly modulates growth factors such as TGF- β ₁ and ECM proteins [68]. Interestingly in our study, hemin therapy attenuated oxidative/inflammatory transcription factors such as NF- κ B and AP-1 from both cardiac and renal tissue of the DOCA-salt hypertensive rat. Given that the promoter region of the HO-1 gene consists of consensus binding sites

for both NF- κ B and AP-1, suggest that the HO system probably plays important roles in the modulation of these transcription factors [67]. Moreover, these transcription factors are also triggered by enhanced activity of ROS leading to stimulation of proinflammatory and growth factors. However, upregulation of the HO system releases antioxidant products such as bilirubin, biliverdin and ferritin. Abrogation of ROS indirectly prevents upregulation of oxidative/inflammatory transcription factors such as NF- κ B and AP-1. This was consistent with the previous finding that antioxidant therapy attenuates transcription factors [46]. Importantly, DOCA-salt-induced hypertension is associated with cardiac and renal remodeling or structural changes mediated through mineralocorticoid and AT₁ receptors, [62, 201] and is associated with enhanced production of ROS and activation of NF- κ B and AP-1. In the present study, increased levels of both cardiac and renal tissue angiotensin-II and aldosterone might directly or through the oxidative mediated signaling pathway upregulate NF- κ B and AP-1 [71, 218]. Thus, it might have triggered the downstream mechanism for cardiovascular and renal remodeling, infiltration of inflammatory cells, and finally end-stage organ damage. Importantly, enhanced HO activity might downregulate oxidative/inflammatory transcriptions factors, preventing inflammatory and fibrotic cascade. Conversely, inhibition of the HO system led to an increase in NF- κ B and AP-1, and stimulated the inflammatory cascade [251]. These findings further confirm the study in HO-1 knockout mice, which showed enhanced proinflammatory activity in the mice after removal of the HO-1 gene [252]. Interestingly, the present data also showed that downregulation of NF- κ B and AP-1 were associated with decreased local tissue angiotensin-II, aldosterone and oxidative stress.

Transcription factors such as NF- κ B and AP-1 are known to stimulate the expression of TGF- β_1 , which further enhances the mobilization of ECM such as fibronectin and collagen, leading to development of fibrosis and hypertrophy. In the present study, in the DOCA-salt hypertensive rat upregulation of transcription factors were noted, which were associated with both cardiac and renal hypertrophy. The downstream mechanism for the development of hypertrophy is the activity of growth regulatory factors such as TGF- β_1 . Therefore, we performed immunohistochemical and quantitative Western immunoblot analyses of TGF- β_1 in DOCA-salt hypertensive rats and relative controls. It is interesting to note that left ventricular hypertrophy and fibrosis was associated with increased growth regulatory factors such as TGF- β_1 , in DOCA-salt hypertensive rats. Furthermore, TGF- β_1 has been linked to the development of glomerulosclerosis and interstitial fibrosis in the hypertensive kidney [86]. Interestingly, the antihypertrophic effects noted here might be due the growth modulatory action of the HO system on TGF- β_1 , which was also shown previously in human renal tubular epithelial cells in vitro [88]. In the DOCA-salt model, renal TGF- β_1 was increased which stimulated production of ECM resulting in an increase in fibronectin in the interstitium, leading to the development of fibrosis. The reduced TGF- β expression correlates with the reduction of fibronectin, and ECM protein. The protective effect of hemin on DOCA-salt-induced renal fibrosis was further verified by immunostaining of kidney sections for fibronectin and staining intensity was scored using a semi-quantitative method.

Importantly, NF- κ B and TGF- β_1 have a functional relationship with each other for the induction of inflammatory and growth modulatory actions through TGF- β_1 activated

kinase1(TAK1) [253]. Similarly, AP-1 is also involved in the regulation of the gene responsible for cell proliferation and tissue remodeling, such as TGF- β_1 [68, 72, 94]. The AP-1 binding site is also present on the promoter region of the TGF- β_1 gene [72]. Thus, activation of both NF- κ B and AP-1 led to stimulation of growth factor TGF- β_1 and deposition of ECM proteins such as collagen and fibronectin in the interstitial space, resulting in fibrosis and structural remodeling. The structural and morphological changes were associated with upregulation of NF- κ B and AP-1 transcription factors and an increase in TGF- β_1 and ECM proteins such as collagen type-1 production as well as a decrease in MMP-1 expression [254]. Hemin therapy abrogated cardiac tissue angiotensin-II, aldosterone and NF- κ B accompanied by decreased expression of TGF- β_1 and perivascular fibrosis, which gives direct evidence for the cytoprotective effects of upregulated HO system. It is worthy to note that, the HO-1 gene harbors consensus binding sites for NF- κ B and AP-1 [67]. NF- κ B is required for the transcription of the angiotensinogen gene to produce angiotensin-II [236]. Angiotensin-II and aldosterone stimulate production of oxidative cascades, which in turn trigger the transcription of NF- κ B, which also consist of the transcription binding site for AP-1, which is a growth stimulatory transcription factor. NF- κ B and TGF- β_1 are known to share a common TAK1 pathway for the modulation of inflammatory and growth signaling. AP-1 modulates TGF- β_1 activation. The production of aldosterone is regulated by the HO system through the CYP450 hemoprotein. Overviewing, the interrelationship between all these factors, we envisage the multifaceted interaction of the HO system. The novelty of this study is that it showed all these interactions from gross to the molecular level *in vivo* in the DOCA-salt animal model of hypertension.

Cardiomyocyte hypertrophy in the present study is greater than previously reported in similar type of 2Kidney1clamp hypertension model indicating additive effects of uninephrectomy, DOCA and NaCl-salt in the development of cardiac hypertrophy [187]. Cardiac intramuscular coronary arterial alterations are common findings in DOCA-salt hypertension, which includes small coronary arterial wall thickening, exaggerated media-to-lumen ratio and wall area [193, 255-257]. Interestingly, hemin therapy appreciably prevented the small coronary arterial remodeling which were confirmed by indices of arterial remodeling. This prevention of coronary arterial remodeling was accompanied with enhanced activity of cardiac cGMP levels. It confirms the notion that carbon monoxide mediated upregulation of cGMP could have caused vascular relaxation and prevented vascular smooth muscle proliferation in the small coronary arteries. Moreover, the development of cardiac or left ventricular fibrosis is one of the major complications of hypertensive cardiac disease. The increased deposition of interstitial and perivascular collagen is a hallmark of the remodeling process, which predisposes the adverse effect on cardiac events. The reduction or prevention of cardiac fibrosis would improve cardiac function in the hypertensive patients [258]. Therefore, this study has important prognostic and clinical relevance because it highlights the pathophysiological changes in a model that mimics the development and progression of fibrosis in humans. Normally ECM connects myocytes, aligns contractile elements, prevents overstretching and alterations of myocytes, and prevents rupture by transmitting force and providing tensile strength. However, non-uniform deposition of ECM changes the quality of the interstitial space, which is critical in the prediction of cardiac functional alterations. It is well known that pathological left ventricular hypertrophy is associated with ventricular remodeling

through increased mobilization of ECM proteins such as collagen and fibronectin. Ventricular remodeling eventually impacts on cardiac function and energy use, and enhances cardiac myocyte cell death by apoptotic and necrotic mechanisms, and thus forms myocyte scarring [259]. Interestingly, it is shown here for the first time that hemin attenuated left ventricular hypertrophy, perivascular fibrosis, myocyte scarring and inflammation, myocyte hypertrophy and small coronary arterial remodeling in the DOCA-salt model of end-stage damage. Abrogation of myocardial scarring and inflammation indicates that the HO might have a role in attenuation of myocardial cell death, which is triggered by pathological necrosis and apoptosis. This notion might support the previous finding that the HO-1 overexpression resulted in reduced myocardial inflammation and necrosis in response to regional ischaemia, which was accompanied with increased expression of the anti-apoptotic genes and decreased pro-apoptotic genes [260]. Moreover, carbon monoxide generated by HO-1 might protect by modulation of both Akt and P^{38MAPK} pathways [261] which are involved in mediating cellular death by apoptosis and necrosis mechanisms. In addition, the HO-1 gene transfer inhibited angiotensin-II-mediated rat cardiac myocyte apoptosis via augmented Akt (Protein kinase B gene) activation *in vitro* [262]. It is of note that Morita et al., (2005) reported that transgenic mice constitutively overexpressing HO-1 demonstrated significant reduction of oxidative radicals and levels of lipid peroxidation products in the heart as compared with wild type-mice after angiotensin-II and salt treatment [263]. Further the cytoprotective effects of hemin was associated with attenuation of cardiac remodeling, which might be due to carbon monoxide mediated increased cGMP levels in cardiac tissue. Enhanced cGMP levels might trigger downstream signaling pathways and cause relaxation of coronary vascular smooth

muscle cells, preventing the development of vascular remodeling and contraction. Improved small coronary arterial wall thickening, small coronary arterial wall-to-lumen ratio, and small coronary arterial wall area in the left ventricles of hemin-treated DOCA-salt hypertensive rats might have exhibited the effect of carbon monoxide and cGMP-signaling pathway. Improved coronary vessels may have provided a corrected blood supply to cardiac myocytes, prevent myocyte death, and thus prevent scarring. Predominantly, all pathological structural changes were accompanied with the increased expression of TGF- β in cardiac tissue, giving direct evidence of structural alterations in the heart of DOCA-salt hypertension. Furthermore, in DOCA-salt hypertension, increased production of cardiac angiotensin-II and aldosterone might have cause stimulation of cardiac fibroblasts for the remodeling process through oxidative cascades [71]. However, the direct action of angiotensin-II has been demonstrated on expression of TGF- β_1 in cardiac fibroblasts and myocytes [264]. It is of note that adeno associated virus HO-1 gene delivery markedly reduced ventricular fibrosis and remodeling, and restored left ventricular function and chamber dimension in a rat model of myocardial infarction [265].

Similarly, pathological lesions in the kidney were accompanied by increased production of tissue angiotensin-II, aldosterone and reactive oxygen species in the kidney of DOCA-salt rats and also upregulated TGF- β_1 , which subsequently increased fibronectin and renal fibrosis [86]. However, administration of antioxidants was shown to decrease the expression of TGF- β_1 and renal damage in the Dahl salt-sensitive model [266]. Consistent with this previous findings our results also showed that upregulation of the HO system was accompanied with enhanced antioxidant systems such as plasma

ferritin, renal SOD and total antioxidant capacity, which were associated with downregulation of TGF- β_1 . Alternatively, decreased aldosterone might contribute to the reduction of TGF- β_1 . Previously, it has been shown that the aldosterone blocker, eplerenone, significantly reduced TGF- β_1 and fibronectin expression with reduced glomerulosclerosis, which is independent of blood pressure [86]. Moreover, HO-1 induction has a role in protecting the kidney from noxious stimuli. In the model of acute renal failure induced by glycerol, increases in the production of heme protein lead to development of renal toxicity. This renal toxicity was attenuated by HO-1 induction and renal function was restored [267].

The DOCA-salt hypertensive rat model triggered a malignant hypertension, which gradually led to end stage renal damage. The malignant hypertensive condition leads to a severe increase in blood pressure, which causes changes in the small renal arteries by concentric thickening of the intima. This intimal layer is replaced by loose myxomatous, fibroblastic tissue; therefore, the lumen of small renal arteries is obliterated [**Fig. 4.26.A(iii)**]. Afferent glomerular arterioles often show patchy acute necrosis in the walls with the accumulation of amorphous, brightly eosinophilic proteinaceous material, called fibrinoid [95]. This damage is also termed fibrinoid necrosis and may extend from the glomerular hila into the glomerular tuft affecting segments of the glomerular capillary network leading to a hypertrophic condition of glomeruli [**Fig. 4.22.B(iii)**]. However, in essential hypertension, renal arteries and glomerular arterioles show marked thickening of walls with a combination of medial hypertrophy, elastic lamina replication, and fibrotic intimal thickening. All these changes in the renal and afferent glomerular arterioles results in smaller lumens and

thus, decreases blood supply to glomeruli. The resulting chronic ischemia leads to the development of sclerosis or hyalinization of the glomeruli, accompanied by disuse atrophy of parts of the tubules and cast formations [Fig. 4.22.B(iii) & 4.25.A.(iii)]. These changes are called hypertensive glomerulosclerosis [Fig. 4.22.B(iii)], and it further causes nephrosclerosis [95]. Therefore, chronic renal failure is caused by a slow progressive loss of functional nephrons and is morphologically known as end-organ damage [95]. The DOCA-salt hypertension shows similar types of glomerular damages leading to renal end-stage damage. In addition, prominent interstitial fibrosis and infiltration of mononuclear cells [Fig. 4.22.A(iii)] are the morphological lesions seen in the renal failure conditions. Moreover, in the hypertensive model, renal injury causes proteinuria. It depends on capillary wall damage, hemodynamic factors, and increased intracapillary pressure, which is affected by afferent and efferent arteriolar constriction. In addition, glomerular injury leads to increased transcapillary hydraulic pressure and exacerbates proteinuria [268]. Clinically, proteinuria has been considered as an index for the marked glomerular injury and severe renal damage in the patient. Damaged glomeruli are unable to restrict high molecular weight proteins such as hemoglobin, myoglobin, albumin and plasma proteins. Therefore, it passes through glomeruli and tubules giving typical cast formation and reacts with tubular epithelium causing interstitial inflammation and activation of growth factors. All these reactions lead to damage of collecting tubules and contribute to loss of proteins, since proteins are excreted in urine. Thus, analysis of protein in the urine samples was used to diagnose the intensity of renal damage, clinically. The results showed that in the DOCA-salt hypertensive rats proteinuria was associated with severe renal lesions such as glomerular

hypertrophy, glomerular sclerosis, tubular injury, and overall end-stage-renal damage. It was clinically confirmed.

In the present study, reduction of proteinuria was associated with increased HO activity, HO-1 expression, and cGMP levels. These results are consistent with a previous study in which the administration of hemin to angiotensin-II-infused rats ameliorated the glomerular filtration rate, decreased proteinuria and thus provided renoprotection [234]. A possible explanation for the reduced proteinuria is that carbon monoxide mediated upregulation of cGMP in vasculature may act as a capillary vasodilator, leading to reduced intracapillary pressure and reduced proteinuria [269]. Moreover, hemin treatment significantly reduced blood pressure to the normotensive range; therefore, the antiproteinuric effect of hemin may also be attributed to its antihypertensive effect as seen in hydralazine treatment [234]. Importantly proteinuria has a major impact on the progression of renal disease [270]. The precise mechanisms by which persistent proteinuria induces interstitial inflammation and fibrosis in renal damage are not well known, although NF- κ B activation has been involved in renal injury. Gomez-Garre et al., studied the effect of bovine serum albumin in uninephrectomized rats [271]. Tubular atrophy, dilatation and infiltration of mononuclear cells were associated with activation of NF- κ B and combined treatment with ACE inhibitor and ET₁ antagonist diminished proteinuria, renal lesions and NF- κ B activity [271]. In addition, when cultured tubular cells were exposed to bovine serum albumin, NF- κ B was activated [271]. Interestingly, proteinuria can result from renal inflammation, which is accompanied with ROS, due to increased susceptibility to proteolytic damage and inactivation of proteinase inhibitors. Furthermore, ROS can induce proteinuria either by direct degradation of glomerular

basement membranes without any direct ultrastructural abnormalities [272]. Therefore, enhanced kidney total antioxidant capacity, SOD levels in response to higher HO activity, concomitant with reduced urinary 8-isoprostane, polyurea, proteinuria and improved creatinine clearance rate in the DOCA-salt rat indicates renoprotective effects of hemin and improved kidney function.

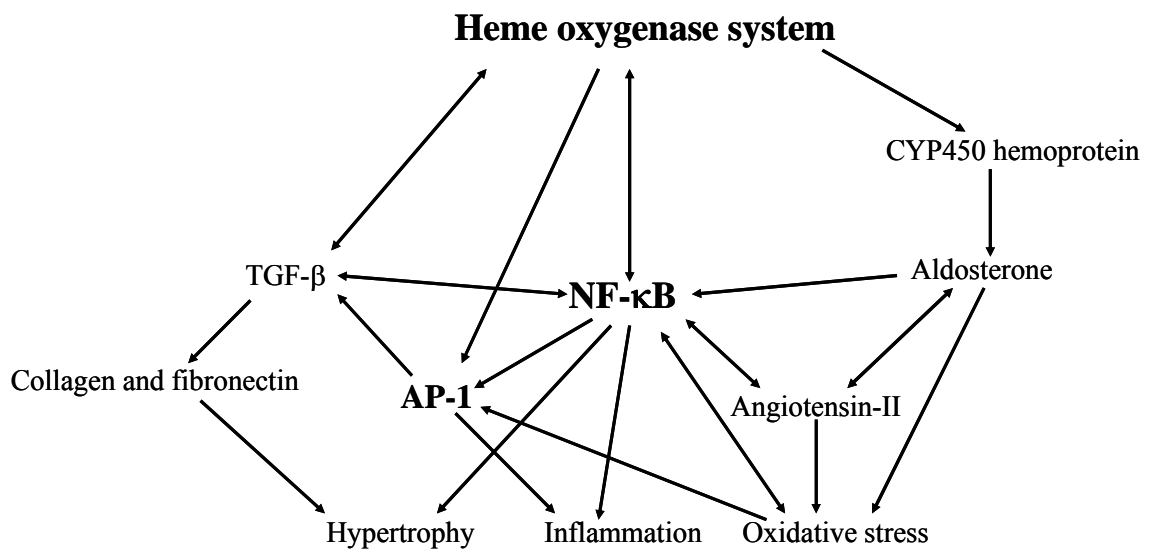


Figure 5.1. Multifaceted interaction of the HO system
(One way signaling \rightarrow and two way signaling \leftrightarrow)

Interestingly, data from our study and previously explored molecular studies of the HO system and molecular signaling involved in the end-organ damage, which were reviewed in the literature. We have discussed a novel modulatory action of the HO system and synergistic interaction between transcription factors such as NF- κ B and AP-1, growth factors such as TGF- β_1 and ECM proteins (Collagen and fibronectin) and

humoral factors like angiotensin-II and aldosterone. These interactions trigger an oxidative, inflammatory and hypertrophic cascades, which progresses to cardiac and renal end-stage damage [Figure 5.1].

Therefore, upregulation of the HO system would be envisaged for the attenuation of multifaceted diseased conditions such as hypertension, diabetes and end-organ damage. Moreover, the data provided by this study will target the future clinical relevance of the HO system by the counteracting the progression of disease conditions in humans, to improve the quality of life.

5.7. Limitation of the study

Every animal study has its limitations. In the present study, one of the limitations is indirect blood pressure measurement method. Blood pressure measurement techniques in the experimental animals are divided into two major types; one is a direct method and other indirect method. The direct blood pressure measurement method consists of a radiotelemetric device, which is surgically implanted in the animal's body, and then indwelling catheters are connected with major blood vessels to record blood pressure. The indirect blood pressure method is the non-invasive tail or limb cuff, which measures blood pressure by the cuff pressure method. In this method, the changes in blood pressure that occur during the occlusion and release of the cuff are recorded. The standard tail cuff method is commonly used to measure systolic blood pressure in laboratory rats, with some advantages [273]. It is noninvasive and relatively less expensive to operate than direct blood pressure equipment in large numbers of animals. It is of incredible worth in repeated blood pressure measurements of individual animals over a long period in the experiment. The disadvantage of the tail-cuff method is that in

order to record blood pressure physical restraint of the animal is required and warming of the animal is necessary to ensure sufficient tail blood flow. Both restraining and warming of the animal may significantly increase the core body temperature and concurrent stress, which will affect blood pressure. Therefore, the blood pressure value obtained by the tail-cuff method may not be the actual blood pressure, but instead the reaction of the animal to the stress of the underlying procedure. Recently some other limitations were noted to the indirect blood pressure method; first, this method only measures a very small sample of cardiac cycles and second, it imposes stress on animals that disturbs multiple aspects of cardiovascular system. Therefore, there are very important steps to be followed to measure blood pressure using tail-cuff methods. One should use the proper size of tail cuff depending on the age of animals [274]. In addition, animals should be daily acclimatized for the restrainer, for at least 3 days before the actual blood pressure measurement, which will reduce the effect of stress on the animals. Also, it is recommended that the same experimenter handle the animals throughout the study. Blood pressure should be measured at the same time every day when blood pressure is stable. Further, proper cleaning of the restrainer and equipment to remove foreign scents and blood odor, placement of restrainer in semi-darkened room conditions, measuring blood pressure in a quiet room, and limiting access to others during the experiments will all reduce the disturbance to animals [274, 275]. All of these important factors were considered during the blood pressure measurements.

6. SUMMARY AND CONCLUSIONS

Administration of hemin, the HO inducer, showed upregulation of HO-1 expression, total HO activity, and cGMP levels in the DOCA-salt hypertensive rats. Upregulation of the HO system accompanied with attenuation of both cardiac and renal angiotensin-II and aldosterone, and reduction of oxidative stress. In addition, abrogation of both cardiac and renal hypertrophy and inflammation were noted in the DOCA-salt hypertensive rat after hemin regimen. Importantly, upregulation of HO leads to the release of carbon monoxide, biliverdin, bilirubin and ferritin molecules. Further, carbon monoxide thus released is probably stimulated the production of cGMP in the tissue, which is a secondary messenger through which the HO system can be cytoprotective. Hemin therapy attenuated urinary 8-isoprostane and down regulated transcription factors such as AP-1, NF- κ B, TGF- β_1 and ECM proteins (fibronectin and collagen). Thus, it prevented inflammation and hypertrophy. In addition, HO-mediated heme catabolized products such as bilirubin, biliverdin and enhanced plasma ferritin levels that may be anti-inflammatory and antioxidant. Myocyte scarring and collagen deposition in the left ventricle, and severe renal damage including glomerular sclerosis, glomerular hypertrophy, tubular cast, interstitial mononuclear infiltrations and tubular dilation were noted in the DOCA-salt hypertensive rat. All these lesions were prevented by hemin therapy. Urinary protein excretion was significantly reduced and creatinine clearance rate increased in the hemin treated DOCA-salt rats, indicative of improved renal function.

Interestingly, the present study envisioned the multifaceted interaction of the HO system with NF- κ B, AP-1, TGF- β_1 and both angiotensin-II and aldosterone hormones

from the gross to cellular level and opened future doors for molecular studies of the HO system in pathophysiological events.

7. FUTURE DIRECTIONS

1. The results from the above study showed the promising effect of hemin in the DOCA-salt rat for the prevention of hypertension and hypertrophy. However, its curative effect needs to be checked for end stage-organ damage caused by hypertension and diabetes.
2. In the present study, decreases in the tissue levels of angiotensin-II and aldosterone were found, due to upregulation of the HO system. The mechanisms behind the decrease in local tissue production of angiotensin-II and aldosterone are still unclear, therefore this needs to be further explored.
3. It needs to be determined if the hemin effect is only due to a decrease in oxidative stress or some other mechanism.
4. The characterization of different molecular interactions among the HO system, extracellular matrix, fibrosis and hypertrophy needs to be investigated more precisely.
5. Antiapoptosis and antinecrosis effect of hemin need to be further clarified by employing a suitable molecular method.

8. REFERENCES

1. *Staessen, J.A., et al., Essential hypertension. Lancet, 2003. 361(9369): p. 1629-41.*
2. *Greenlund, K.J., J.B. Croft, and G.A. Mensah, Prevalence of heart disease and stroke risk factors in persons with prehypertension in the United States, 1999-2000. Arch Intern Med, 2004. 164(19): p. 2113-8.*
3. *Blaustein, M.P., et al., How does salt retention raise blood pressure? Am J Physiol Regul Integr Comp Physiol, 2006. 290(3): p. R514-23.*
4. *Weinberger, M.H., Salt sensitivity of blood pressure in humans. Hypertension, 1996. 27(3 Pt 2): p. 481-90.*
5. *Bianchi, G., et al., A renal abnormality as a possible cause of "essential" hypertension. Lancet, 1979. 1(8109): p. 173-7.*
6. *Manning, R.D., Jr., N. Tian, and S. Meng, Oxidative stress and antioxidant treatment in hypertension and the associated renal damage. Am J Nephrol, 2005. 25(4): p. 311-7.*
7. *Kearney, P.M., et al., Global burden of hypertension: analysis of worldwide data. Lancet, 2005. 365(9455): p. 217-23.*
8. *Wright, J.W., S. Mizutani, and J.W. Harding, Pathways involved in the transition from hypertension to hypertrophy to heart failure. Treatment strategies. Heart Fail Rev, 2008. 13(3): p. 367-75.*
9. *Schalekamp, M.A. and A.H. Danser, Angiotensin II production and distribution in the kidney: I. A kinetic model. Kidney Int, 2006. 69(9): p. 1543-52.*
10. *Xue, C. and H.M. Siragy, Local renal aldosterone system and its regulation by salt, diabetes, and angiotensin II type 1 receptor. Hypertension, 2005. 46(3): p. 584-90.*
11. *Mulrow, P.J., Angiotensin II and aldosterone regulation. Regul Pept, 1999. 80(1-2): p. 27-32.*
12. *Rogerson, F.M. and P.J. Fuller, Mineralocorticoid action. Steroids, 2000. 65(2): p. 61-73.*
13. *Agarwal, M.K. and M. Mirshahi, General overview of mineralocorticoid hormone action. Pharmacol Ther, 1999. 84(3): p. 273-326.*
14. *Lumbers, E.R., Angiotensin and aldosterone. Regul Pept, 1999. 80(3): p. 91-100.*

15. *Beswick, R.A., et al., NADH/NADPH oxidase and enhanced superoxide production in the mineralocorticoid hypertensive rat. Hypertension, 2001. 38(5): p. 1107-11.*
16. *Chen, X., et al., Antioxidant effects of vitamins C and E are associated with altered activation of vascular NADPH oxidase and superoxide dismutase in stroke-prone SHR. Hypertension, 2001. 38(3 Pt 2): p. 606-11.*
17. *Tian, N., et al., Interactions between oxidative stress and inflammation in salt-sensitive hypertension. Am J Physiol Heart Circ Physiol, 2007. 293(6): p. H3388-95.*
18. *Welch, W.J., A. Tojo, and C.S. Wilcox, Roles of NO and oxygen radicals in tubuloglomerular feedback in SHR. Am J Physiol Renal Physiol, 2000. 278(5): p. F769-76.*
19. *Manning, R.D., Jr., S. Meng, and N. Tian, Renal and vascular oxidative stress and salt-sensitivity of arterial pressure. Acta Physiol Scand, 2003. 179(3): p. 243-50.*
20. *Han, D., E. Williams, and E. Cadenas, Mitochondrial respiratory chain-dependent generation of superoxide anion and its release into the intermembrane space. Biochem J, 2001. 353(Pt 2): p. 411-6.*
21. *Finkel, T. and N.J. Holbrook, Oxidants, oxidative stress and the biology of ageing. Nature, 2000. 408(6809): p. 239-47.*
22. *Griendling, K.K. and G.A. FitzGerald, Oxidative stress and cardiovascular injury: Part II: animal and human studies. Circulation, 2003. 108(17): p. 2034-40.*
23. *Ozono, R., New biotechnological methods to reduce oxidative stress in the cardiovascular system: focusing on the Bach1/heme oxygenase-1 pathway. Curr Pharm Biotechnol, 2006. 7(2): p. 87-93.*
24. *Sowers, J.R., Hypertension, angiotensin II, and oxidative stress. N Engl J Med, 2002. 346(25): p. 1999-2001.*
25. *Higashi, Y., et al., Endothelial function and oxidative stress in renovascular hypertension. N Engl J Med, 2002. 346(25): p. 1954-62.*
26. *Dijkhorst-Oei, L.T., et al., Acute simultaneous stimulation of nitric oxide and oxygen radicals by angiotensin II in humans in vivo. J Cardiovasc Pharmacol, 1999. 33(3): p. 420-4.*
27. *Nagata, D., et al., Molecular mechanism of the inhibitory effect of aldosterone on endothelial NO synthase activity. Hypertension, 2006. 48(1): p. 165-71.*

28. Leopold, J.A., et al., *Aldosterone impairs vascular reactivity by decreasing glucose-6-phosphate dehydrogenase activity. Nat Med*, 2007. 13(2): p. 189-97.
29. Marney, A.M. and N.J. Brown, *Aldosterone and end-organ damage. Clin Sci (Lond)*, 2007. 113(6): p. 267-78.
30. Badr, K.F. and T.E. Abi-Antoun, *Isoprostanes and the kidney. Antioxid Redox Signal*, 2005. 7(1-2): p. 236-43.
31. Vacchiano, C.A. and G.E. Tempel, *Role of nonenzymatically generated prostanoid, 8-iso-PGF2 alpha, in pulmonary oxygen toxicity. J Appl Physiol*, 1994. 77(6): p. 2912-7.
32. Morrow, J.D., et al., *Increase in circulating products of lipid peroxidation (F2-isoprostanes) in smokers. Smoking as a cause of oxidative damage. N Engl J Med*, 1995. 332(18): p. 1198-203.
33. Morrow, J.D. and L.J. Roberts, *The isoprostanes: unique bioactive products of lipid peroxidation. Prog Lipid Res*, 1997. 36(1): p. 1-21.
34. Nourooz-Zadeh, J., et al., *Urinary 8-epi-PGF2alpha and its endogenous beta-oxidation products (2,3-dinor and 2,3-dinor-5,6-dihydro) as biomarkers of total body oxidative stress. Biochem Biophys Res Commun*, 2005. 330(3): p. 731-6.
35. Fridovich, I., *Superoxide anion radical (O₂⁻), superoxide dismutases, and related matters. J Biol Chem*, 1997. 272(30): p. 18515-7.
36. Kirkman, H.N., et al., *Mechanisms of protection of catalase by NADPH. Kinetics and stoichiometry. J Biol Chem*, 1999. 274(20): p. 13908-14.
37. Bierl, C., et al., *Determinants of human plasma glutathione peroxidase (GPx-3) expression. J Biol Chem*, 2004. 279(26): p. 26839-45.
38. Meister, A., *Glutathione-ascorbic acid antioxidant system in animals. J Biol Chem*, 1994. 269(13): p. 9397-400.
39. Yamawaki, H., J. Haendeler, and B.C. Berk, *Thioredoxin: a key regulator of cardiovascular homeostasis. Circ Res*, 2003. 93(11): p. 1029-33.
40. Ndisang, J.F., N. Lane, and A. Jadhav, *Crosstalk between the heme oxygenase system, aldosterone, and phospholipase C in hypertension. J Hypertens*, 2008. 26(6): p. 1188-99.
41. Sandstrom, J., et al., *10-fold increase in human plasma extracellular superoxide dismutase content caused by a mutation in heparin-binding domain. J Biol Chem*, 1994. 269(29): p. 19163-6.

42. *Turkseven, S., et al., Antioxidant mechanism of heme oxygenase-1 involves an increase in superoxide dismutase and catalase in experimental diabetes. Am J Physiol Heart Circ Physiol, 2005. 289(2): p. H701-7.*
43. *Droge, W., Free radicals in the physiological control of cell function. Physiol Rev, 2002. 82(1): p. 47-95.*
44. *Barnes, P.J., Nuclear factor-kappa B. Int J Biochem Cell Biol, 1997. 29(6): p. 867-70.*
45. *Serhan, C.N. and J. Savill, Resolution of inflammation: the beginning programs the end. Nat Immunol, 2005. 6(12): p. 1191-7.*
46. *Beswick, R.A., et al., Long-term antioxidant administration attenuates mineralocorticoid hypertension and renal inflammatory response. Hypertension, 2001. 37(2 Part 2): p. 781-6.*
47. *Robbins, T.L., et al., Robbins PATHOLOGIC BASIS OF DISEASE, ed. f.J. SCHOEN. 1994, Philadelphia: W.B SAUNDERS COMPANY.*
48. *Beltrami, A.P., et al., Adult cardiac stem cells are multipotent and support myocardial regeneration. Cell, 2003. 114(6): p. 763-76.*
49. *Torella, D., et al., Resident cardiac stem cells. Cell Mol Life Sci, 2007. 64(6): p. 661-73.*
50. *Nadal-Ginard, B., et al., Myocyte death, growth, and regeneration in cardiac hypertrophy and failure. Circ Res, 2003. 92(2): p. 139-50.*
51. *van Empel, V.P. and L.J. De Windt, Myocyte hypertrophy and apoptosis: a balancing act. Cardiovasc Res, 2004. 63(3): p. 487-99.*
52. *Vakili, B.A., P.M. Okin, and R.B. Devereux, Prognostic implications of left ventricular hypertrophy. Am Heart J, 2001. 141(3): p. 334-41.*
53. *Frey, N. and E.N. Olson, Cardiac hypertrophy: the good, the bad, and the ugly. Annu Rev Physiol, 2003. 65: p. 45-79.*
54. *Frey, N., et al., Hypertrophy of the heart: a new therapeutic target? Circulation, 2004. 109(13): p. 1580-9.*
55. *Krauser, D.G. and R.B. Devereux, Ventricular hypertrophy and hypertension: prognostic elements and implications for management. Herz, 2006. 31(4): p. 305-16.*
56. *Levy, D., et al., Prognostic implications of echocardiographically determined left ventricular mass in the Framingham Heart Study. N Engl J Med, 1990. 322(22): p. 1561-6.*

57. *Cooper, R.S., et al., Left ventricular hypertrophy is associated with worse survival independent of ventricular function and number of coronary arteries severely narrowed. Am J Cardiol, 1990. 65(7): p. 441-5.*
58. *Devereux, R.B., et al., Relations of left ventricular mass to demographic and hemodynamic variables in American Indians: the Strong Heart Study. Circulation, 1997. 96(5): p. 1416-23.*
59. *Benjamin, E.J. and D. Levy, Why is left ventricular hypertrophy so predictive of morbidity and mortality? Am J Med Sci, 1999. 317(3): p. 168-75.*
60. *Kahan, T. and L. Bergfeldt, Left ventricular hypertrophy in hypertension: its arrhythmogenic potential. Heart, 2005. 91(2): p. 250-6.*
61. *Schlaich, M.P., et al., Relation between cardiac sympathetic activity and hypertensive left ventricular hypertrophy. Circulation, 2003. 108(5): p. 560-5.*
62. *Weber, K.T., et al., Myocardial fibrosis: role of angiotensin II and aldosterone. Basic Res Cardiol, 1993. 88 Suppl 1: p. 107-24.*
63. *Ahn, K.S. and B.B. Aggarwal, Transcription factor NF-kappaB: a sensor for smoke and stress signals. Ann N Y Acad Sci, 2005. 1056: p. 218-33.*
64. *Hacker, H. and M. Karin, Regulation and function of IKK and IKK-related kinases. Sci STKE, 2006. 2006(357): p. re13.*
65. *Aggarwal, B.B., et al., Nuclear transcription factor NF-kappa B: role in biology and medicine. Indian J Exp Biol, 2004. 42(4): p. 341-53.*
66. *Sethi, G., B. Sung, and B.B. Aggarwal, Nuclear factor-kappaB activation: from bench to bedside. Exp Biol Med (Maywood), 2008. 233(1): p. 21-31.*
67. *Lavrovsky, Y., et al., Identification of binding sites for transcription factors NF-kappa B and AP-2 in the promoter region of the human heme oxygenase 1 gene. Proc Natl Acad Sci U S A, 1994. 91(13): p. 5987-91.*
68. *Shaulian, E. and M. Karin, AP-1 in cell proliferation and survival. Oncogene, 2001. 20(19): p. 2390-400.*
69. *Manabe, I., T. Shindo, and R. Nagai, Gene expression in fibroblasts and fibrosis: involvement in cardiac hypertrophy. Circ Res, 2002. 91(12): p. 1103-13.*
70. *van Wamel, J.E., et al., Rapid gene transcription induced by stretch in cardiac myocytes and fibroblasts and their paracrine influence on stationary myocytes and fibroblasts. Pflugers Arch, 2000. 439(6): p. 781-8.*

71. *Li, X., et al., Angiotensin II and Aldosterone stimulating NF-kappaB and AP-1 activation in hepatic fibrosis of rat. Regul Pept, 2007. 138(1): p. 15-25.*
72. *Bakiri, L., et al., Promoter specificity and biological activity of tethered AP-1 dimers. Mol Cell Biol, 2002. 22(13): p. 4952-64.*
73. *Khalil, N., TGF-beta: from latent to active. Microbes Infect, 1999. 1(15): p. 1255-63.*
74. *Herpin, A., C. Lelong, and P. Favrel, Transforming growth factor-beta-related proteins: an ancestral and widespread superfamily of cytokines in metazoans. Dev Comp Immunol, 2004. 28(5): p. 461-85.*
75. *Lijnen, P.J., V.V. Petrov, and R.H. Fagard, Association between transforming growth factor-beta and hypertension. Am J Hypertens, 2003. 16(7): p. 604-11.*
76. *Dostal, D.E., Regulation of cardiac collagen: angiotensin and cross-talk with local growth factors. Hypertension, 2001. 37(3): p. 841-4.*
77. *Noble, N.A. and W.A. Border, Angiotensin II in renal fibrosis: should TGF-beta rather than blood pressure be the therapeutic target? Semin Nephrol, 1997. 17(5): p. 455-66.*
78. *Boluyt, M.O., et al., Alterations in cardiac gene expression during the transition from stable hypertrophy to heart failure. Marked upregulation of genes encoding extracellular matrix components. Circ Res, 1994. 75(1): p. 23-32.*
79. *Villarreal, F.J. and W.H. Dillmann, Cardiac hypertrophy-induced changes in mRNA levels for TGF-beta 1, fibronectin, and collagen. Am J Physiol, 1992. 262(6 Pt 2): p. H1861-6.*
80. *Gibbons, G.H. and V.J. Dzau, The emerging concept of vascular remodeling. N Engl J Med, 1994. 330(20): p. 1431-8.*
81. *Border, W.A. and N.A. Noble, Interactions of transforming growth factor-beta and angiotensin II in renal fibrosis. Hypertension, 1998. 31(1 Pt 2): p. 181-8.*
82. *Pinto, Y.M., et al., Reduction in left ventricular messenger RNA for transforming growth factor beta(1) attenuates left ventricular fibrosis and improves survival without lowering blood pressure in the hypertensive TGR(mRen2)27 Rat. Hypertension, 2000. 36(5): p. 747-54.*
83. *Mezzano, S.A., M. Ruiz-Ortega, and J. Egido, Angiotensin II and renal fibrosis. Hypertension, 2001. 38(3 Pt 2): p. 635-8.*

84. *Tsuchiya, K., M. Naruse, and H. Nihei, Glomerular expression of endothelial nitric oxide synthase in deoxycorticosterone acetate-salt-treated rats. Clin Exp Pharmacol Physiol, 2000. 27(10): p. 818-20.*
85. *Mezzano, S.A., et al., Tubular NF-kappaB and AP-1 activation in human proteinuric renal disease. Kidney Int, 2001. 60(4): p. 1366-77.*
86. *Onozato, M.L., et al., Dual blockade of aldosterone and angiotensin II additively suppresses TGF-beta and NADPH oxidase in the hypertensive kidney. Nephrol Dial Transplant, 2007. 22(5): p. 1314-22.*
87. *Ma, L.J., et al., Transforming growth factor-beta-dependent and -independent pathways of induction of tubulointerstitial fibrosis in beta6(-/-) mice. Am J Pathol, 2003. 163(4): p. 1261-73.*
88. *Mark, A., et al., Induction of heme oxygenase-1 modulates the profibrotic effects of transforming growth factor-beta in human renal tubular epithelial cells. Cell Mol Biol (Noisy-le-grand), 2005. 51(4): p. 357-62.*
89. *Jugdutt, B.I., Remodeling of the myocardium and potential targets in the collagen degradation and synthesis pathways. Curr Drug Targets Cardiovasc Haematol Disord, 2003. 3(1): p. 1-30.*
90. *Marcey, D. and M. Ward, Fibronectin, an Extracellular Adhesion Molecule, in The Online Macromolecular Museum Exhibits. 2001.*
91. *Swynghedauw, B., Molecular mechanisms of myocardial remodeling. Physiol Rev, 1999. 79(1): p. 215-62.*
92. *Mirkovic, S., et al., Attenuation of cardiac fibrosis by pirfenidone and amiloride in DOCA-salt hypertensive rats. Br J Pharmacol, 2002. 135(4): p. 961-8.*
93. *Delcayre, C., et al., Cardiac aldosterone production and ventricular remodeling. Kidney Int, 2000. 57(4): p. 1346-51.*
94. *Fiebeler, A., et al., Mineralocorticoid receptor affects AP-1 and nuclear factor-kappab activation in angiotensin II-induced cardiac injury. Hypertension, 2001. 37(2 Part 2): p. 787-93.*
95. *Stevens A., L.J.S.a.Y.B., WHEATER'S Basic HISTOPATHOLOGY a colour atlas and text. FOURTH EDITION ed. 2002: CHURCHILL LIVINGSTONE. 285.*
96. *Abbate, M., C. Zoja, and G. Remuzzi, How does proteinuria cause progressive renal damage? J Am Soc Nephrol, 2006. 17(11): p. 2974-84.*

97. *Palmer, B.F., Proteinuria as a therapeutic target in patients with chronic kidney disease. Am J Nephrol, 2007. 27(3): p. 287-93.*
98. *Ravel, R., Clinical laboratory medicine. Sixth ed. Clinical application of laboratory data. 1995, Missouri, USA: Mosby-Year Book. Inc.,*
99. *Cheng, W., et al., Stretch-induced programmed myocyte cell death. J Clin Invest, 1995. 96(5): p. 2247-59.*
100. *Bardales, R.H., et al., In situ apoptosis assay for the detection of early acute myocardial infarction. Am J Pathol, 1996. 149(3): p. 821-9.*
101. *Clark, J.E., et al., Heme oxygenase-1-derived bilirubin ameliorates postischemic myocardial dysfunction. Am J Physiol Heart Circ Physiol, 2000. 278(2): p. H643-51.*
102. *Abraham, N.G., Heme oxygenase and the cardiovascular-renal system. Free radical biology medicine, 2005. 39(1): p. 1.*
103. *Abraham, N.G., et al., Differential effect of cobalt protoporphyrin on distributions of heme oxygenase in renal structure and on blood pressure in SHR. Cell Mol Biol (Noisy-le-grand), 2002. 48(8): p. 895-902.*
104. *Balla, G., et al., Ferritin: a cytoprotective antioxidant strategem of endothelium. J Biol Chem, 1992. 267(25): p. 18148-53.*
105. *Poss, K.D. and S. Tonegawa, Reduced stress defense in heme oxygenase 1-deficient cells. Proc Natl Acad Sci U S A, 1997. 94(20): p. 10925-30.*
106. *Abraham, N.G. and A. Kappas, Pharmacological and clinical aspects of heme oxygenase. Pharmacol Rev, 2008. 60(1): p. 79-127.*
107. *Abraham, N.G. and A. Kappas, Heme oxygenase and the cardiovascular-renal system. Free Radic Biol Med, 2005. 39(1): p. 1-25.*
108. *Cruse, I. and M.D. Maines, Evidence suggesting that the two forms of heme oxygenase are products of different genes. J Biol Chem, 1988. 263(7): p. 3348-53.*
109. *Keyse, S.M. and R.M. Tyrrell, Heme oxygenase is the major 32-kDa stress protein induced in human skin fibroblasts by UVA radiation, hydrogen peroxide, and sodium arsenite. Proc Natl Acad Sci U S A, 1989. 86(1): p. 99-103.*
110. *Tenhunen, R., H.S. Marver, and R. Schmid, Microsomal heme oxygenase. Characterization of the enzyme. J Biol Chem, 1969. 244(23): p. 6388-94.*

111. *Tenhunen, R., H.S. Marver, and R. Schmid, The enzymatic conversion of heme to bilirubin by microsomal heme oxygenase. Proc Natl Acad Sci U S A, 1968. 61(2): p. 748-55.*
112. *Kirkby, K.A. and C.A. Adin, Products of heme oxygenase and their potential therapeutic applications. Am J Physiol Renal Physiol, 2006. 290(3): p. F563-71.*
113. *Hill-Kapturczak, N., S.H. Chang, and A. Agarwal, Heme oxygenase and the kidney. DNA Cell Biol, 2002. 21(4): p. 307-21.*
114. *Vachharajani, T.J., et al., Heme oxygenase modulates selectin expression in different regional vascular beds. Am J Physiol Heart Circ Physiol, 2000. 278(5): p. H1613-7.*
115. *Ryter, S.W. and R.M. Tyrrell, The heme synthesis and degradation pathways: role in oxidant sensitivity. Heme oxygenase has both pro- and antioxidant properties. Free Radic Biol Med, 2000. 28(2): p. 289-309.*
116. *Vile, G.F., et al., Heme oxygenase 1 mediates an adaptive response to oxidative stress in human skin fibroblasts. Proc Natl Acad Sci U S A, 1994. 91(7): p. 2607-10.*
117. *Lin, F. and A.W. Girotti, Hemin-enhanced resistance of human leukemia cells to oxidative killing: antisense determination of ferritin involvement. Arch Biochem Biophys, 1998. 352(1): p. 51-8.*
118. *Balla, J., et al., Endothelial-cell heme uptake from heme proteins: induction of sensitization and desensitization to oxidant damage. Proc Natl Acad Sci U S A, 1993. 90(20): p. 9285-9.*
119. *Vogt, B.A., et al., Acquired resistance to acute oxidative stress. Possible role of heme oxygenase and ferritin. Lab Invest, 1995. 72(4): p. 474-83.*
120. *Berberat, P.O., et al., Heavy chain ferritin acts as an antiapoptotic gene that protects livers from ischemia reperfusion injury. Faseb J, 2003. 17(12): p. 1724-6.*
121. *Burg, R.V., Toxicology updates. Journal of applied toxicology, 1999. 19(5).*
122. *Piantadosi, C.A., Biological chemistry of carbon monoxide. Antioxid Redox Signal, 2002. 4(2): p. 259-70.*
123. *Sacerdoti, D., et al., Treatment with tin prevents the development of hypertension in spontaneously hypertensive rats. Science, 1989. 243(4889): p. 388-90.*

124. Zhang, X., et al., Carbon monoxide inhibition of apoptosis during ischemia-reperfusion lung injury is dependent on the p38 mitogen-activated protein kinase pathway and involves caspase 3. *J Biol Chem*, 2003. 278(2): p. 1248-58.
125. Otterbein, L.E., et al., MKK3 mitogen-activated protein kinase pathway mediates carbon monoxide-induced protection against oxidant-induced lung injury. *Am J Pathol*, 2003. 163(6): p. 2555-63.
126. Kyriakis, J.M. and J. Avruch, Protein kinase cascades activated by stress and inflammatory cytokines. *Bioessays*, 1996. 18(7): p. 567-77.
127. Kajimura, M., N. Goda, and M. Suematsu, Organ design for generation and reception of CO: lessons from the liver. *Antioxid Redox Signal*, 2002. 4(4): p. 633-7.
128. Ramos, K.S., H. Lin, and J.J. McGrath, Modulation of cyclic guanosine monophosphate levels in cultured aortic smooth muscle cells by carbon monoxide. *Biochem Pharmacol*, 1989. 38(8): p. 1368-70.
129. Yu, L., et al., Nitric oxide: a mediator in rat tubular hypoxia/reoxygenation injury. *Proc Natl Acad Sci U S A*, 1994. 91(5): p. 1691-5.
130. Morita, T. and S. Kourembanas, Endothelial cell expression of vasoconstrictors and growth factors is regulated by smooth muscle cell-derived carbon monoxide. *J Clin Invest*, 1995. 96(6): p. 2676-82.
131. Morita, T., et al., Carbon monoxide controls the proliferation of hypoxic vascular smooth muscle cells. *J Biol Chem*, 1997. 272(52): p. 32804-9.
132. Brune, B. and V. Ullrich, Inhibition of platelet aggregation by carbon monoxide is mediated by activation of guanylate cyclase. *Mol Pharmacol*, 1987. 32(4): p. 497-504.
133. Gunther, L., et al., Carbon monoxide protects pancreatic beta-cells from apoptosis and improves islet function/survival after transplantation. *Diabetes*, 2002. 51(4): p. 994-9.
134. Snyder, S.H., S.R. Jaffrey, and R. Zakhary, Nitric oxide and carbon monoxide: parallel roles as neural messengers. *Brain Res Brain Res Rev*, 1998. 26(2-3): p. 167-75.
135. Verma, A., et al., Carbon monoxide: a putative neural messenger. *Science*, 1993. 259(5093): p. 381-4.
136. Fujita, T., et al., Paradoxical rescue from ischemic lung injury by inhaled carbon monoxide driven by derepression of fibrinolysis. *Nat Med*, 2001. 7(5): p. 598-604.

137. *Wedel, B.J. and D.L. Garbers, New insights on the functions of the guanylyl cyclase receptors. FEBS Lett, 1997. 410(1): p. 29-33.*
138. *Schmidt, H.H., S.M. Lohmann, and U. Walter, The nitric oxide and cGMP signal transduction system: regulation and mechanism of action. Biochim Biophys Acta, 1993. 1178(2): p. 153-75.*
139. *Stone, J.R. and M.A. Marletta, Soluble guanylate cyclase from bovine lung: activation with nitric oxide and carbon monoxide and spectral characterization of the ferrous and ferric states. Biochemistry, 1994. 33(18): p. 5636-40.*
140. *Stone, J.R. and M.A. Marletta, Spectral and kinetic studies on the activation of soluble guanylate cyclase by nitric oxide. Biochemistry, 1996. 35(4): p. 1093-9.*
141. *Tsiftoglou, A.S., A.I. Tsamadou, and L.C. Papadopoulou, Heme as key regulator of major mammalian cellular functions: molecular, cellular, and pharmacological aspects. Pharmacol Ther, 2006. 111(2): p. 327-45.*
142. *Kappas, A., A method for interdicting the development of severe jaundice in newborns by inhibiting the production of bilirubin. Pediatrics, 2004. 113(1 Pt 1): p. 119-23.*
143. *Sun, Z.J. and Z.E. Zhang, Historic perspectives and recent advances in major animal models of hypertension. Acta Pharmacol Sin, 2005. 26(3): p. 295-301.*
144. *Pinto, Y.M., M. Paul, and D. Ganten, Lessons from rat models of hypertension: from Goldblatt to genetic engineering. Cardiovasc Res, 1998. 39(1): p. 77-88.*
145. *Moreau, P. and E.L. Schiffrin, Role of endothelins in animal models of hypertension: focus on cardiovascular protection. Can J Physiol Pharmacol, 2003. 81(6): p. 511-21.*
146. *van den Meiracker, A.H., Endothelins and venous tone in DOCA-salt hypertension. J Hypertens, 2002. 20(4): p. 587-9.*
147. *French, J.F., et al., Dual inhibition of angiotensin-converting enzyme and neutral endopeptidase in rats with hypertension. J Cardiovasc Pharmacol, 1995. 26(1): p. 107-13.*
148. *Wong, P.C., et al., In vivo pharmacology of DuP 753. Am J Hypertens, 1991. 4(4 Pt 2): p. 288S-298S.*
149. *Van den Berg, D.T., E.R. de Kloet, and W. de Jong, Central effects of mineralocorticoid antagonist RU-28318 on blood pressure of DOCA-salt hypertensive rats. Am J Physiol, 1994. 267(6 Pt 1): p. E927-33.*

150. Gavras, H., H.R. Brunner, and J.H. Laragh, *Renin and aldosterone and the pathogenesis of hypertensive vascular damage. Prog Cardiovasc Dis, 1974. 17(1): p. 39-49.*
151. Cowley, A.W., Jr., *Long-term control of arterial blood pressure. Physiol Rev, 1992. 72(1): p. 231-300.*
152. Pradhan, A., M. Umezu, and M. Fukagawa, *Heme-oxygenase upregulation ameliorates angiotensin II-induced tubulointerstitial injury and salt-sensitive hypertension. Am J Nephrol, 2006. 26(6): p. 552-61.*
153. Ndisang, J.F., W. Zhao, and R. Wang, *Selective regulation of blood pressure by heme oxygenase-1 in hypertension. Hypertension, 2002. 40(3): p. 315-21.*
154. Ndisang, J.F., et al., *Induction of heme oxygenase-1 and stimulation of cGMP production by hemin in aortic tissues from hypertensive rats. Blood, 2003. 101(10): p. 3893-900.*
155. Wang, R., et al., *Sustained normalization of high blood pressure in spontaneously hypertensive rats by implanted hemin pump. Hypertension, 2006. 48(4): p. 685-92.*
156. da Silva, J.L., et al., *Dual role of heme oxygenase in epithelial cell injury: contrasting effects of short-term and long-term exposure to oxidant stress. J Lab Clin Med, 1996. 128(3): p. 290-6.*
157. Yu, M., et al., *Endothelin antagonist reduces hemodynamic responses to vasopressin in DOCA-salt hypertension. Am J Physiol Heart Circ Physiol, 2001. 281(6): p. H2511-7.*
158. Yu, M., V. Gopalakrishnan, and J.R. McNeill, *Role of endothelin and vasopressin in DOCA-salt hypertension. Br J Pharmacol, 2001. 132(7): p. 1447-54.*
159. Ruzicka, M., et al., *The renin-angiotensin system and volume overload-induced cardiac hypertrophy in rats. Effects of angiotensin converting enzyme inhibitor versus angiotensin II receptor blocker. Circulation, 1993. 87(3): p. 921-30.*
160. Ammarguella, F.Z., et al., *Fibrosis, matrix metalloproteinases, and inflammation in the heart of DOCA-salt hypertensive rats: role of ET(A) receptors. Hypertension, 2002. 39(2 Pt 2): p. 679-84.*
161. Assayag, P., et al., *Compensated cardiac hypertrophy: arrhythmogenicity and the new myocardial phenotype. I. Fibrosis. Cardiovasc Res, 1997. 34(3): p. 439-44.*

162. Katz, S.A., et al., Myocardial renin is neither necessary nor sufficient to initiate or maintain ventricular hypertrophy. *Am J Physiol Regul Integr Comp Physiol*, 2000. 278(3): p. R578-86.
163. Ndisang, J.F. and R. Wang, Alterations in heme oxygenase/carbon monoxide system in pulmonary arteries in hypertension. *Exp Biol Med (Maywood)*, 2003. 228(5): p. 557-63.
164. Jadhav, A., E. Torlakovic, and J.F. Ndisang, Interaction Among Heme Oxygenase, Nuclear Factor- κ B, and Transcription Activating Factors in Cardiac Hypertrophy in Hypertension. *Hypertension*, 2008.
165. Stiene-Martin E.A., Lotspeich-Steininger, and K.J. A., CLINICAL HEMATOLOGY, PRINCIPLE, PROCEDURES CORRELATIONS. Second Edition ed. 1998, New York: Lippincott, philadelphia, New York. 817.
166. Nishikawa, K., Angiotensin AT1 receptor antagonism and protection against cardiovascular end-organ damage. *J Hum Hypertens*, 1998. 12(5): p. 301-9.
167. Bledsoe, G., L. Chao, and J. Chao, Kallikrein gene delivery attenuates cardiac remodeling and promotes neovascularization in spontaneously hypertensive rats. *Am J Physiol Heart Circ Physiol*, 2003. 285(4): p. H1479-88.
168. Maina, C.I. and M. Ogunde, Reversal of left ventricular hypertrophy by propranolol in hypertensive rats. *Afr Health Sci*, 2005. 5(1): p. 29-32.
169. Guo, D.F., et al., Development of hypertension and kidney hypertrophy in transgenic mice overexpressing ARAP1 gene in the kidney. *Hypertension*, 2006. 48(3): p. 453-9.
170. Llesuy, S.F. and M.L. Tomaro, Heme oxygenase and oxidative stress. Evidence of involvement of bilirubin as physiological protector against oxidative damage. *Biochim Biophys Acta*, 1994. 1223(1): p. 9-14.
171. Bradford, M.M., A rapid and sensitive method for the quantitation of microgram quantities of protein utilizing the principle of protein-dye binding. *Anal Biochem*, 1976. 72: p. 248-54.
172. Chen, L., M.N. Salafranca, and J.L. Mehta, Cyclooxygenase inhibition decreases nitric oxide synthase activity in human platelets. *Am J Physiol*, 1997. 273(4 Pt 2): p. H1854-9.
173. Koracevic, D., et al., Method for the measurement of antioxidant activity in human fluids. *J Clin Pathol*, 2001. 54(5): p. 356-61.
174. Apak, R., et al., Total antioxidant capacity assay of human serum using copper(II)-neocuproine as chromogenic oxidant: the CUPRAC method. *Free Radic Res*, 2005. 39(9): p. 949-61.

175. Baranano, D.E., et al., *Biliverdin reductase: a major physiologic cytoprotectant. Proc Natl Acad Sci U S A*, 2002. 99(25): p. 16093-8.
176. Stocker, R., A.N. Glazer, and B.N. Ames, *Antioxidant activity of albumin-bound bilirubin. Proc Natl Acad Sci U S A*, 1987. 84(16): p. 5918-22.
177. Stocker, R., et al., *Bilirubin is an antioxidant of possible physiological importance. Science*, 1987. 235(4792): p. 1043-6.
178. Hintze, K.J. and E.C. Theil, *DNA and mRNA elements with complementary responses to hemin, antioxidant inducers, and iron control ferritin-L expression. Proc Natl Acad Sci U S A*, 2005. 102(42): p. 15048-52.
179. Jeney, V., et al., *Pro-oxidant and cytotoxic effects of circulating heme. Blood*, 2002. 100(3): p. 879-87.
180. Bayorh, M.A., et al., *Alterations in aldosterone and angiotensin II levels in salt-induced hypertension. Clin Exp Hypertens*, 2005. 27(4): p. 355-67.
181. Volland, H., et al., *A solid-phase immobilized epitope immunoassay (SPIE-IA) permitting very sensitive and specific measurement of angiotensin II in plasma. J Immunol Methods*, 1999. 228(1-2): p. 37-47.
182. Jadhav, A., E. Torlakovic, and J.F. Ndisang, *Hemin therapy attenuates kidney injury in deoxycorticosterone acetate-salt hypertensive rats. Am J Physiol Renal Physiol*, 2008.
183. Baeuerle, P.A. and D. Baltimore, *Activation of DNA-binding activity in an apparently cytoplasmic precursor of the NF-kappa B transcription factor. Cell*, 1988. 53(2): p. 211-7.
184. Katavetin, P., et al., *High glucose blunts vascular endothelial growth factor response to hypoxia via the oxidative stress-regulated hypoxia-inducible factor/hypoxia-responsible element pathway. J Am Soc Nephrol*, 2006. 17(5): p. 1405-13.
185. Smith, S.H., et al., *Regional myocyte size in two-kidney, one clip renal hypertension. J Mol Cell Cardiol*, 1988. 20(11): p. 1035-42.
186. Conrad, C.H., et al., *Myocardial fibrosis and stiffness with hypertrophy and heart failure in the spontaneously hypertensive rat. Circulation*, 1995. 91(1): p. 161-70.
187. Lee, T.M., et al., *Effect of pravastatin on left ventricular mass in the two-kidney, one-clip hypertensive rats. Am J Physiol Heart Circ Physiol*, 2006. 291(6): p. H2705-13.

188. *Armstrong, A.T., et al., Quantitative investigation of cardiomyocyte hypertrophy and myocardial fibrosis over 6 years after cardiac transplantation. J Am Coll Cardiol, 1998. 32(3): p. 704-10.*
189. *Conrad, C.H., et al., Myocardial fibrosis and stiffness with hypertrophy and heart failure in the spontaneously hypertensive rat, in Circulation. 1995. p. 161-70.*
190. *Jin, X., et al., Differential protein expression in hypertrophic heart with and without hypertension in spontaneously hypertensive rats. Proteomics, 2006. 6(6): p. 1948-56.*
191. *Rahman, A., et al., Heart extracellular matrix gene expression profile in the vitamin D receptor knockout mice. J Steroid Biochem Mol Biol, 2007. 103(3-5): p. 416-9.*
192. *Rikitake, Y., et al., Decreased perivascular fibrosis but not cardiac hypertrophy in ROCK1+/- haploinsufficient mice. Circulation, 2005. 112(19): p. 2959-65.*
193. *Millette, E., et al., Comparison of the cardiovascular protection by omapatrilat and lisinopril treatments in DOCA-salt hypertension. J Hypertens, 2003. 21(1): p. 125-35.*
194. *Zimlichman, R., et al., Insulin induces medial hypertrophy of myocardial arterioles in rats. Am J Hypertens, 1995. 8(9): p. 915-20.*
195. *Brand, M., et al., Angiotensinogen modulates renal vasculature growth. Hypertension, 2006. 47(6): p. 1067-74.*
196. *Pillebout, E., et al., JunD protects against chronic kidney disease by regulating paracrine mitogens. J Clin Invest, 2003. 112(6): p. 843-52.*
197. *Xia, C.F., et al., Kallikrein gene transfer reduces renal fibrosis, hypertrophy, and proliferation in DOCA-salt hypertensive rats. Am J Physiol Renal Physiol, 2005. 289(3): p. F622-31.*
198. *Dundar, M., I. Kocak, and N. Culhaci, Effects of long-term passive smoking on the diameter of glomeruli in rats: Histopathological evaluation. Nephrology (Carlton), 2004. 9(2): p. 53-7.*
199. *Gallego, B., et al., Effect of chronic and progressive aortic constriction on renal function and structure in rats. Can J Physiol Pharmacol, 2001. 79(7): p. 601-7.*
200. <http://www.ahc.umn.edu/rar/blood.html>, *Research Animal Resources., in Guidelines for Collection of Blood from Experimental Animals.*
- . 2006, *University of Minnesota Board of Regents.USA.*

201. Rocha, R. and C.T. Stier, Jr., *Pathophysiological effects of aldosterone in cardiovascular tissues. Trends Endocrinol Metab*, 2001. 12(7): p. 308-14.
202. Gavras, H., et al., *Malignant hypertension resulting from deoxycorticosterone acetate and salt excess: role of renin and sodium in vascular changes. Circ Res*, 1975. 36(2): p. 300-9.
203. Escalante, B., et al., *Chronic treatment with tin normalizes blood pressure in spontaneously hypertensive rats. Hypertension*, 1991. 17(6 Pt 1): p. 776-9.
204. Johnson, R.A., et al., *Heme oxygenase substrates acutely lower blood pressure in hypertensive rats. Am J Physiol*, 1996. 271(3 Pt 2): p. H1132-8.
205. Martasek, P., et al., *Hemin and L-arginine regulation of blood pressure in spontaneous hypertensive rats. J Am Soc Nephrol*, 1991. 2(6): p. 1078-84.
206. Levere, R.D., et al., *Effect of heme arginate administration on blood pressure in spontaneously hypertensive rats. J Clin Invest*, 1990. 86(1): p. 213-9.
207. Johnson, R.A., et al., *A heme oxygenase product, presumably carbon monoxide, mediates a vasodepressor function in rats. Hypertension*, 1995. 25(2): p. 166-9.
208. Wang, R., *Resurgence of carbon monoxide: an endogenous gaseous vasorelaxing factor. Can J Physiol Pharmacol*, 1998. 76(1): p. 1-15.
209. Arregui, B., et al., *Acute renal hemodynamic effects of dimanganese decacarbonyl and cobalt protoporphyrin. Kidney Int*, 2004. 65(2): p. 564-74.
210. Vera, T., et al., *HO-1 induction lowers blood pressure and superoxide production in the renal medulla of angiotensin II hypertensive mice. Am J Physiol Regul Integr Comp Physiol*, 2007. 292(4): p. R1472-8.
211. Dhalla, N.S., R.M. Temsah, and T. Netticadan, *Role of oxidative stress in cardiovascular diseases. J Hypertens*, 2000. 18(6): p. 655-73.
212. Wu, R., et al., *Enhanced superoxide anion formation in vascular tissues from spontaneously hypertensive and desoxycorticosterone acetate-salt hypertensive rats. J Hypertens*, 2001. 19(4): p. 741-8.
213. de Champlain, J., et al., *Oxidative stress in hypertension. Clin Exp Hypertens*, 2004. 26(7-8): p. 593-601.
214. Savoia, C. and E.L. Schiffrin, *Inflammation in hypertension. Curr Opin Nephrol Hypertens*, 2006. 15(2): p. 152-8.
215. Kaur, H., et al., *Interaction of bilirubin and biliverdin with reactive nitrogen species. FEBS Lett*, 2003. 543(1-3): p. 113-9.

216. Wu, L. and B.H. Juurlink, *Increased methylglyoxal and oxidative stress in hypertensive rat vascular smooth muscle cells. Hypertension, 2002. 39(3): p. 809-14.*
217. Ferris, C.D., et al., *Haem oxygenase-1 prevents cell death by regulating cellular iron. Nat Cell Biol, 1999. 1(3): p. 152-7.*
218. Sun, Y., et al., *Aldosterone-induced inflammation in the rat heart : role of oxidative stress. Am J Pathol, 2002. 161(5): p. 1773-81.*
219. Arima, S., et al., *Nongenomic vascular action of aldosterone in the glomerular microcirculation. J Am Soc Nephrol, 2003. 14(9): p. 2255-63.*
220. Peng, H., et al., *Antifibrotic effects of N-acetyl-seryl-aspartyl-Lysyl-proline on the heart and kidney in aldosterone-salt hypertensive rats. Hypertension, 2001. 37(2 Part 2): p. 794-800.*
221. Blasi, E.R., et al., *Aldosterone/salt induces renal inflammation and fibrosis in hypertensive rats. Kidney Int, 2003. 63(5): p. 1791-800.*
222. Ullian, M.E., L.G. Walsh, and T.A. Morinelli, *Potentiation of angiotensin II action by corticosteroids in vascular tissue. Cardiovasc Res, 1996. 32(2): p. 266-73.*
223. Ullian, M.E., J.R. Schelling, and S.L. Linas, *Aldosterone enhances angiotensin II receptor binding and inositol phosphate responses. Hypertension, 1992. 20(1): p. 67-73.*
224. Gomez-Sanchez, E.P., et al., *Origin of aldosterone in the rat heart. Endocrinology, 2004. 145(11): p. 4796-802.*
225. Ambroisine, M.L., et al., *Aldosterone and anti-aldosterone effects in cardiovascular diseases and diabetic nephropathy. Diabetes Metab, 2004. 30(4): p. 311-8.*
226. Gomez-Sanchez, E.P., et al., *Is aldosterone synthesized within the rat brain? Am J Physiol Endocrinol Metab, 2005. 288(2): p. E342-6.*
227. Iglarz, M., et al., *Involvement of oxidative stress in the profibrotic action of aldosterone. Interaction with the renin-angiotensin system. Am J Hypertens, 2004. 17(7): p. 597-603.*
228. Fiebeler, A., et al., *Aldosterone synthase inhibitor ameliorates angiotensin II-induced organ damage. Circulation, 2005. 111(23): p. 3087-94.*
229. Silvestre, J.S., et al., *Myocardial production of aldosterone and corticosterone in the rat. Physiological regulation. J Biol Chem, 1998. 273(9): p. 4883-91.*

230. Capponi, A.M., *Regulation of cholesterol supply for mineralocorticoid biosynthesis. Trends Endocrinol Metab*, 2002. 13(3): p. 118-21.
231. Botros, F.T., et al., *Increase in heme oxygenase-1 levels ameliorates renovascular hypertension. Kidney Int*, 2005. 68(6): p. 2745-55.
232. Pitt, B., et al., *The effect of spironolactone on morbidity and mortality in patients with severe heart failure. Randomized Aldactone Evaluation Study Investigators. N Engl J Med*, 1999. 341(10): p. 709-17.
233. Mendes, A.C., et al., *Chronic infusion of angiotensin-(1-7) reduces heart angiotensin II levels in rats. Regul Pept*, 2005. 125(1-3): p. 29-34.
234. Aizawa, T., et al., *Heme oxygenase-1 is upregulated in the kidney of angiotensin II-induced hypertensive rats : possible role in renoprotection. Hypertension*, 2000. 35(3): p. 800-6.
235. Hu, C.M., et al., *Heme oxygenase-1 inhibits angiotensin II-induced cardiac hypertrophy in vitro and in vivo. Circulation*, 2004. 110(3): p. 309-16.
236. Li, J. and A.R. Brasier, *Angiotensinogen gene activation by angiotensin II is mediated by the rel A (nuclear factor-kappaB p65) transcription factor: one mechanism for the renin angiotensin system positive feedback loop in hepatocytes. Mol Endocrinol*, 1996. 10(3): p. 252-64.
237. Roberts, L.J., 2nd and J.D. Morrow, *The generation and actions of isoprostanes. Biochim Biophys Acta*, 1997. 1345(2): p. 121-35.
238. Stocker, R. and E. Peterhans, *Antioxidant properties of conjugated bilirubin and biliverdin: biologically relevant scavenging of hypochlorous acid. Free Radic Res Commun*, 1989. 6(1): p. 57-66.
239. Lanone, S., et al., *Bilirubin decreases nos2 expression via inhibition of NAD(P)H oxidase: implications for protection against endotoxic shock in rats. Faseb J*, 2005. 19(13): p. 1890-2.
240. Sano, K., H. Nakamura, and T. Matsuo, *Mode of inhibitory action of bilirubin on protein kinase C. Pediatr Res*, 1985. 19(6): p. 587-90.
241. Quan, S., et al., *Expression of human heme oxygenase-1 in the thick ascending limb attenuates angiotensin II-mediated increase in oxidative injury. Kidney Int*, 2004. 65(5): p. 1628-39.
242. Mosterd, A., et al., *Trends in the prevalence of hypertension, antihypertensive therapy, and left ventricular hypertrophy from 1950 to 1989. N Engl J Med*, 1999. 340(16): p. 1221-7.

243. Yamazaki, T., I. Komuro, and Y. Yazaki, *Role of the renin-angiotensin system in cardiac hypertrophy. Am J Cardiol*, 1999. 83(12A): p. 53H-57H.
244. Seki, T., et al., *Induction of heme oxygenase produces load-independent cardioprotective effects in hypertensive rats. Life Sci*, 1999. 65(10): p. 1077-86.
245. Purcell, N.H., et al., *Activation of NF-kappa B is required for hypertrophic growth of primary rat neonatal ventricular cardiomyocytes. Proc Natl Acad Sci U S A*, 2001. 98(12): p. 6668-73.
246. Muller, D.N., et al., *NF-kappaB inhibition ameliorates angiotensin II-induced inflammatory damage in rats. Hypertension*, 2000. 35(1 Pt 2): p. 193-201.
247. Kawano, S., et al., *Blockade of NF-kappaB ameliorates myocardial hypertrophy in response to chronic infusion of angiotensin II. Cardiovasc Res*, 2005. 67(4): p. 689-98.
248. Freund, C., et al., *Requirement of nuclear factor-kappaB in angiotensin II- and isoproterenol-induced cardiac hypertrophy in vivo. Circulation*, 2005. 111(18): p. 2319-25.
249. Zager, R.A., et al., *Iron, heme oxygenase, and glutathione: effects on myohemoglobinuric proximal tubular injury. Kidney Int*, 1995. 48(5): p. 1624-34.
250. May, M.J. and S. Ghosh, *Signal transduction through NF-kappa B. Immunol Today*, 1998. 19(2): p. 80-8.
251. Sasaki, T., et al., *Heme arginate pretreatment attenuates pulmonary NF-kappaB and AP-1 activation induced by hemorrhagic shock via heme oxygenase-1 induction. Med Chem*, 2006. 2(3): p. 271-4.
252. Kapturczak, M.H., et al., *Heme oxygenase-1 modulates early inflammatory responses: evidence from the heme oxygenase-1-deficient mouse. Am J Pathol*, 2004. 165(3): p. 1045-53.
253. Sakurai, H., et al., *TGF-beta-activated kinase 1 stimulates NF-kappa B activation by an NF-kappa B-inducing kinase-independent mechanism. Biochem Biophys Res Commun*, 1998. 243(2): p. 545-9.
254. Chen, J. and J.L. Mehta, *Angiotensin II-mediated oxidative stress and procollagen-1 expression in cardiac fibroblasts: blockade by pravastatin and pioglitazone. Am J Physiol Heart Circ Physiol*, 2006. 291(4): p. H1738-45.
255. Brilla, C.G. and K.T. Weber, *Mineralocorticoid excess, dietary sodium, and myocardial fibrosis. J Lab Clin Med*, 1992. 120(6): p. 893-901.

256. Lee, R.M., M. Richardson, and R. McKenzie, *Vascular changes associated with deoxycorticosterone-NaCl-induced hypertension. Blood Vessels*, 1989. 26(3): p. 137-56.
257. Anderson, P.G., S.P. Bishop, and S.B. Digerness, *Coronary vascular function and morphology in hydralazine treated DOCA salt rats. J Mol Cell Cardiol*, 1988. 20(10): p. 955-67.
258. Grobe, J.L., et al., *Chronic angiotensin-(1-7) prevents cardiac fibrosis in DOCA-salt model of hypertension. Am J Physiol Heart Circ Physiol*, 2006. 290(6): p. H2417-23.
259. Deschamps, A.M. and F.G. Spinale, *Pathways of matrix metalloproteinase induction in heart failure: bioactive molecules and transcriptional regulation. Cardiovasc Res*, 2006. 69(3): p. 666-76.
260. Melo, L.G., et al., *Gene therapy strategy for long-term myocardial protection using adeno-associated virus-mediated delivery of heme oxygenase gene. Circulation*, 2002. 105(5): p. 602-7.
261. Akamatsu, Y., et al., *Heme oxygenase-1-derived carbon monoxide protects hearts from transplant associated ischemia reperfusion injury. Faseb J*, 2004. 18(6): p. 771-2.
262. Foo, R.S., et al., *Heme oxygenase-1 gene transfer inhibits angiotensin II-mediated rat cardiac myocyte apoptosis but not hypertrophy. J Cell Physiol*, 2006. 209(1): p. 1-7.
263. Morita, T., et al., *Heme oxygenase-1 in vascular smooth muscle cells counteracts cardiovascular damage induced by angiotensin II. Curr Neurovasc Res*, 2005. 2(2): p. 113-20.
264. Rosenkranz, S., *TGF-beta1 and angiotensin networking in cardiac remodeling. Cardiovasc Res*, 2004. 63(3): p. 423-32.
265. Liu, X., et al., *Heme oxygenase-1 (HO-1) inhibits postmyocardial infarct remodeling and restores ventricular function. Faseb J*, 2006. 20(2): p. 207-16.
266. Hisaki, R., et al., *Tempol attenuates the development of hypertensive renal injury in Dahl salt-sensitive rats. Am J Hypertens*, 2005. 18(5 Pt 1): p. 707-13.
267. Nath, K.A., et al., *Induction of heme oxygenase is a rapid, protective response in rhabdomyolysis in the rat. J Clin Invest*, 1992. 90(1): p. 267-70.
268. Yoshioka, T., et al., *Role for angiotensin II in an overt functional proteinuria. Kidney Int*, 1986. 30(4): p. 538-45.

269. *Mosley, K., et al., Heme oxygenase is induced in nephrotoxic nephritis and heme, a stimulator of heme oxygenase synthesis, ameliorates disease. Kidney Int, 1998. 53(3): p. 672-8.*
270. *Ruggenti, P., A. Schieppati, and G. Remuzzi, Progression, remission, regression of chronic renal diseases. Lancet, 2001. 357(9268): p. 1601-8.*
271. *Gomez-Garre, D., et al., Activation of NF-kappaB in tubular epithelial cells of rats with intense proteinuria: role of angiotensin II and endothelin-1. Hypertension, 2001. 37(4): p. 1171-8.*
272. *Razzaque, M.S., Fibrogenesis: Cellular and Molecular Basis. 2005, Germany: Springer US. 27-37.*
273. *Van Vliet, B.N., et al., Direct and indirect methods used to study arterial blood pressure. J Pharmacol Toxicol Methods, 2000. 44(2): p. 361-73.*
274. *Bunag, R.D., Facts and fallacies about measuring blood pressure in rats. Clin Exp Hypertens A, 1983. 5(10): p. 1659-81.*
275. *Meneton, P., et al., Renal physiology of the mouse. Am J Physiol Renal Physiol, 2000. 278(3): p. F339-51.*

9. APPENDIX

Significant parts of thesis have been published in the following journals and some additional published papers:

Publications:

1. **JADHAV A, TORLAKOVIC E AND NDISANG JF.** Hemin therapy attenuates kidney injury in deoxycorticosterone acetate-salt hypertensive rats. **AJP: Renal Physiology, 2008, Dec 30** [Epub ahead of print].
2. NDISANG JF, LANE N AND **JADHAV A.** The heme oxygenase system abates hyperglycaemia in Zucker Diabetic Fatty rats by potentiating insulin-sensitizing pathways. **Endocrinology, 2008, Dec 23** [Epub ahead of print].
3. **JADHAV A, TORLAKOVIC E AND NDISANG JF.** Interaction among heme oxygenase, nuclear factor-kappa B, and transcription activating factors in cardiac hypertrophy in hypertension. **Hypertension, 2008, Nov;52(5):910-17.**
4. NDISANG JF, LANE N AND **JADHAV A.** Cross-talk between the heme oxygenase system, aldosterone and phospholipase C in hypertension, **J. Hypertension, 2008, Jun:26(6):1188-99.**
5. NDISANG JF, **JADHAV A.** AND LANE N Interaction between the heme oxygenase system and aldosterone in hypertension, **Int J Angiol, 2007;16(3):92-97.**